UNIVERSITA' DEGLI STUDI DI PADOVA

FACOLTA' DI SCIENZE MM.FF.NN.
Corso di Laurea Specialistica in Biologia Molecolare

IRON STRESS IN CYANOBACTERIA: ASSOCIATION OF CP43' WITH PHOTOSYSTEM II

Supervisor : Prof. James Barber
(Division of Molecular Biosciences,   Imperial College London)

Relatore : Prof. Giorgio Mario Giacometti
(Dipartimento di Biologia, Università degli Studi di Padova)

Laureanda:Elisa Corteggiani Carpinelli

ANNO ACCADEMICO 2005-2006

Abstract

Photosynthesis is the amazing process capable of transform sun light into energy of chemical compounds, therefore allowing all the forms of life on our planet to exist. In oxygenic photosynthetic organisms a special machine, Photosystem II, has the unique property of oxidising water and realising O_2 in to the atmosphere as a consequence. PS II has been shown to have a close homology with purple bacteria reaction centre, although this latter complex doesn't evolve oxygen. PS II uses light energy to transfer electrons from water to the plastoquinone pool and this represent the first part of a linear electron flow, described by the Z scheme, that is one of the tenet of photosynthesis research.

An additional Chla-binding protein, CP43', is highly expressed in cyanobacteria grown in iron stress conditions, whose amino acid sequence shows a significant similarity with CP43 subunit of PS II. The major difference is the lack of approximately 130 amino acids in the lumenal loop, while the main structural and functional features seem to be preserved in the two protein. It has been previously hypothesized that CP43' could partially replace CP43 in the assembly of PSII reaction center complexes, although, at the moment there are no evidences of a functional association of CP43' with PS II. If a CP43'-conjugated PS II like complex did assemble and was stable and capable to perform the primary charge separation, this photosystem is likely to release the steric inhibition around the donor side of the reaction center and thus to allow a possible electron flow around PSII. This hypothetical photosystem could be imagined as an essential complex, whose structure and function is really close to that of purple bacteria photosystem and to that of the ancestor photosystem from whom probably both this latter and PS II come from.

Table of Contents

3   Results and Discussion

4   Conclusions

Chapter 1 – Introduction

1.1 Photosynthesis

Life on earth ultimately depends on energy derived from the sun. Photosynthesis, the only process of biological importance that can harvest this energy, is the physico-chemical process by which plants, algae and photosynthetic bacteria use light energy to drive the synthesis of organic compounds. In plants, algae and certain types of bacteria, the photosynthetic process results in the release of molecular oxygen and the removal of carbon dioxide from the atmosphere that is used to synthesize carbohydrates (oxygenic photosynthesis). Other types of bacteria use light energy to create organic compounds but do not produce oxygen. Photosynthesis provides the energy and reduced carbon required for the survival of virtually all life on our planet, as well as the molecular oxygen necessary for the survival of oxygen consuming organisms . In addition, a large fraction of the planet's energy resources results from photosynthetic activity in either recent or ancient times (fossil fuels currently being burned to provide energy for human activity).

The overall process of photosynthesis is a redox chemical reaction that can be synthetically expressed by this net reaction:

$$CO_2 + 2H_2A + \text{Light Energy} \longrightarrow [CH_2O] + 2A + H_2O$$
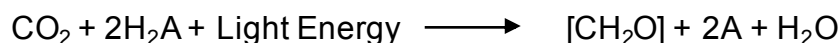
In oxygenic photosynthesis, 2A is O_2, whereas in anoxygenic photosynthesis, which occurs in some photosynthetic bacteria, the electron donor can be an inorganic hydrogen donor, such as H_2S (in which case A is elemental sulfur) or an organic hydrogen donor such as succinate (in which case, A is fumarate). Because glucose, a six carbon sugar, is often an intermediate product, the empirical equation representing the balanced overall chemical reaction of photosynthesis for oxygen evolving organisms is frequently written as follows:

$$6CO_2 + 12H_2O + \text{Light Energy} \longrightarrow C_6H_{12}O_6 + 6O_2 + 6H_2O$$
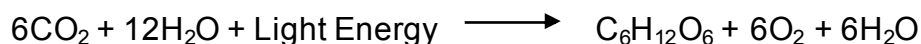
Although somewhat arbitrary, a conceptually useful description of the complex series of reactions that culminate in the reduction of CO_2 can be divided into "light" reactions and carbon fixation or "dark" reactions. The light reactions take place in the specialized thylakoid membranes and release, as end products, the high-energy compounds ATP and NADPH, which are used for the synthesis of sugars in the carbon fixation reactions, that take place in the surrounding aqueous region. In the work that I present we focus on the "light reactions" of oxygenic photosynthetic organisms.

1.2   Photosynthetic Organisms

The photosynthetic prokaryotes have been classified into two separate urkingdoms. The halobacteria, that use bacteriorhodopsin as the photosynthetic pigment, are grouped within the archeabacteria. All the other prokaryotic phototrophic species are widely distributed amongst the phyla of the (eu)bacterial domain (Woese, 1987; Woese et al., 1990) including the cyanobacteria (and prochlorophytes), the green sulfur bacteria, the green phylamentous bacteria, the purple bacteria and the heliobacteria. Of these, only the cyanobacteria and prochlorophytes are capable of oxygenic photosynthesis, while all remaining photosynthetic bacteria are anoxygenic. The striking difference in the mechanism of photosynthesis between the halobacteria and the eubacteria has been interpreted in the past to speculate that photosynthesis was invented twice during the course of evolution. Despite this observation the scientific community generally agrees now that all extant photosynthetic cells are descended from a single common ancestor that possessed a primeval photosynthetic mechanism. This interpretation is supported by the analysis of Lake and colleagues (1985), based on the three-dimensional structure of ribosomes, of Tzukihara et al (1982) and, more recently, of Schubert et al (1998), based on the structural model of PSI and Rhee et al. (1998) based on the structure of PSII.

According to the endosymbiotic theory, cyanobacteria-like cells were incorporated into the eukaryotic systems and developed into the plastids of algae and higher plants (Margulis, 1981, 1996; Stiller & Hall, 1997) thereby extending oxygenic photosynthesis into the eukarya. It's well established that there exist a close similarity in the molecular mechanism of photosynthetic electron transfer between the anoxygenic prokaryotes and the chloroplast of higher plants. The photosynthetic eubacteria are thus a favourite model experimental material since their growth can be controlled in terms of light and nutrient conditions and their fast generation time makes them suitable for genetic manipulation studies.

Considering the functional-distinct and spatially-separate multienzyme complexes that constitute the photosynthetic electron transfer path, we find again that all the photosynthetic organisms share important far-reaching analogies:

- *light-harvesting complexes*
  These are pigment-proteins with no photochemical activity, that act as light gathering antennae for the photochemical reaction centres.
  Anoxygenic photobacteria contain two spectrally different forms of light harvesting chlorophyll complexes, indicated as B890 and B800-850 in organisms that contain bacteriochlorophyll a. A similar antenna system belongs to the bacterichlorophyll b organisms, but it is characterized by an absorption capacity further in the near infra-red.

Much of the light harvesting capacity of red algae and cyanobacteria resides in phycobiliproteins. Different phycobilins bind to the αβ-monomers of phycobiliproteins, that aggregate in the macromolecular complexes called phycobilisomes. This antennae serve as accessory pigments for PSII and are normally attached to the surface or the photosynthetic membrane.

Light harvesting complexes (LHC) of higher plants associate to Photosystem II (PSII) and Photosystem I (PSI) reaction centres contain chlorophyll a and b and in addition the carotenoids xanthophylls, neoxanthin and lutein. The extensive LHC2 and LHC1 complexes are largely buried within the lipid bilayer, although it has been proved that they protrude from both surfaces of the lipid bilayer.

- *photochemical reaction centres*

  The reaction centres accept singlet excited energy from the light harvesting systems and convert it into electrochemical potential free energy. This is comprised of an electric potential gradient across the membrane and a chemical potential difference between the oxidant and the reductant, that drives a series of consequential electron transfer reactions. This early electron transfer steps are incredibly similar in all the reaction centres.

  All bacterial photosynthetic systems identified to date belong to two distinct groups, conveniently classified by the respective terminal electron acceptors of the electron transfer systems. Type-I (alternatively iron-sulfur type) RC-complexes possess high-potential Fe_4S_4-clusters as their terminal electron acceptors and include the photosystems of anoxygenic heliobacteria and green sulfur bacteria as well as photosystem I (PSI) of oxygenic photosynthesis (Prince et al., 1985; Nitschke et al., 1987; Trost & Blankenship, 1989; Trost et al., 1992). Photosynthetic systems of type-II (quinone-type) are characterised by a quinone-type terminal electron acceptor. This group is constituted by the RC complexes of green filamentous bacteria, purple bacteria and photosystem II (PSII) of oxygenic photosynthesis (Barber, 1988; Rutherford, 1988; Mathis, 1990; Nitschke & Rutherford, 1991; Blankenship, 1992). Whereas anoxygenic bacteria posses a single RC-complex, either of type-I or of type-II, oxygenic cyanobacteria, plants and algae have two photosynthetic systems (one of each type: PSII and PSI) electrochemically linked in series. As a result they are able to oxidise water and reduce $NADP^+$ at the two extremes of the electrochemical range accessible in vivo..

- *oxidoreductases*

  These are haem-containing enzymes which couple the dissipation of the light-induced redox potential to the translocation of protons across the photosynthetic membrane.

The anoxygenic photosynthetic eubacteria also contain dehydrogenases which can feed reducing equivalents into the photosynthetic electron

transfer chain upon oxidation of substrates, such as succinate. In oxygenic photosynthetic organism the corresponding enzyme would be that involved in the oxidation of water.

We focus our attention in this work on the photosynthetic membrane complexes responsible for the light reactions in cyanobacteria.

Figure 1.1 The Evolution of Photoautothrophes. When photosynthesis first appeared on Earth, it was most probably based around hydrogen sulphide. The supply of H_2S is rather limited on Earth, being found only around areas of volcanic activity. Therefore some autotrophs (the Cyanobacteria) subsequently made the leap to using water instead, which is of course in great abundance. Photosynthesis based on water produces a significant by-product: oxygen. In the picture colonies of different species of Cyanobacteria.
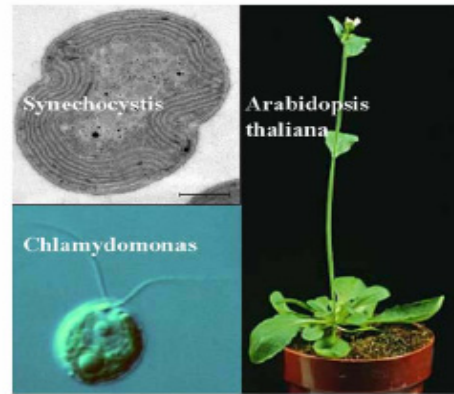
Figure 1.2 The Evolution of Oxygenic Organisms. Cyanobacteria, pumping oxygen into the Earth's atmosphere, produced a dramatic change in its gas composition. When atmospheric O_2 reached a crytical concentration a new type of heterotrophic life evolved to take advantage of the oxygen as an energy source: the aerobic respirators. In the picture the three most popular pohotosynthetic oxygenic organisms used in photosynthesis research are shown: the eubacterium Synechocystis (procariota); the unicellular algae *Clamidomonas* (euchariota) and the higher plant *Arabidopsis*.
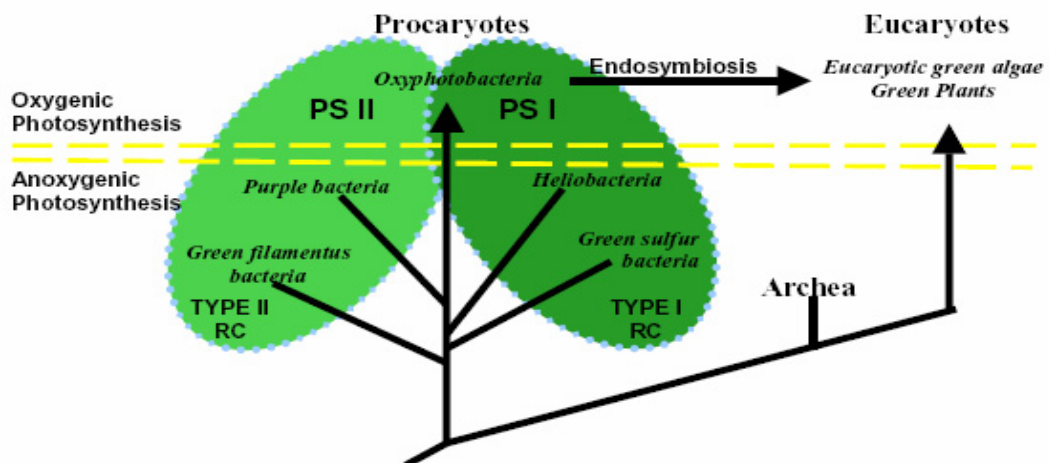
Figure 1.3 The evolution of Photosynthetic Organisms. Overview of the known distribution of photosynthetic reaction centre complexes amongst the prokaryotes and eukaryotes. Anoxygenic photosynthetic organisms contain one type of reaction center, either Type-I (PSI like) or Type-II (PSII like). Oxygenic organisms contain both types of RC-complexes. Eukaryotes are thought to have acquired their photosynthetic ability by endosymbiotically incorporating oxygenic bacteria as their chloroplasts (adapted from Scubert et al., 1998)

1.3 The thylakoid reactions in oxygenic organism: the electron transfer path

The electron transfer pathway in all the oxygen-evolving organism involves the co-operation of three integral membrane protein complexes: two photosystems, Photosystem II (PSII) and Photosystem I (PSI), site of primary charge separation, in which light energy is transformed in redox-free energy; and $Cytb_6f$ complex, that bridges the electron transport between the two spatially separated photosystems. It is generally accepted that they function in series in a non-cyclic electron transport, named "Z scheme", by which electrons released from water by PSII pass through $Cytb_6f$ and on to PSI, which generates the strong reductant necessary for $NADP^+$ reduction. In addition, the electron transfer reactions concentrate protons inside the membrane veside and create an electric field across the photosynthetic membrane. In this process the electron transfer reactions convert redox free energy into an electrochemical gradient of protons. The energy stored in the proton electrochemical gradient is used by a membrane bound protein complex (ATP-Synthase) to covalently attach a phosphate group to adenosine diphosphate (ADP), forming adenosine triphosphate (ATP). The NADPH and ATP formed by the light reactions provide the energy for the photosynthetic carbon reduction cycle.
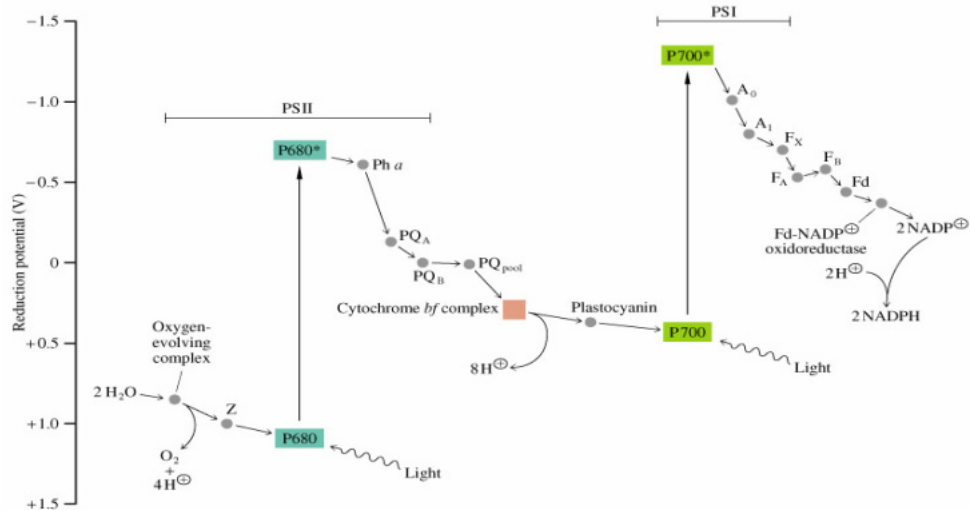
Fig.1.4 Schematic representation of the Z schaem with redox potentials

Each photosystem can be resolved into a photoactive core complex, where light energy is converted into stable chemical products, and a light harvesting antenna system. Cyanobacteria depend on chlorophyll *a* and phycobilisomes to gather light energy.

Photosystem II is the molecular machine in which the first event of the complete electron transfer pathway takes place. It is a homodimeric multisubunit protein, directionally embedded in the thylakoid membranes and it's the only known protein complex that can oxidize water, resulting in the release of O_2 into the atmosphere. Photochemistry in photosystem II is initiated by charge separation between P680 and pheophytin, creating P680+/Pheo-. Primary charge separation takes about a few picoseconds. Subsequent electron transfer steps have been designed through evolution to prevent the primary charge separation from recombining. This is accomplished by transferring the electron within 200 picoseconds from pheophytin to a plastoquinone molecule (Q_A) that is permanently bound to photosystem II. While this first quinone works as a one-electron acceptor at the Q_A-site, a second plastoquinone molecule, that is loosely bound at the Q_B-site, can accept two electrons from Q_A, becoming fully reduced and protonated after two photochemical turnovers of the reaction centre. The reduced plastoquinone then dissociates from the reaction centre and diffuses into the hydrophobic core of the thylakoid membrane. After which, an oxidized plastoquinone molecule finds its way to the Q_B-binding site and the process is repeated. Because the Q_B-site is near the outer aqueous phase, the protons added to plastoquinone during its reduction are taken from the outside of the membrane. Plastoquinone serves thence two key functions: transfers electrons from the photosystem II reaction centre to the cytochrome b_6f complex and carries protons across the photosynthetic membrane. The cytochrome b_6f complex removes the electrons from reduced plastoquinone and facilitates the release of the protons into the inner aqueous space. The electrons are eventually transferred to the photosystem I reaction centre. Electron transfer from the cytochrome b_6f complex to photosystem I is mediated by a small Cu-protein, plastocyanin (PC), or by a haem protein, cytochrome c_6 (cyt c_6). Plastocyanin is water soluble and operate in the inner lumenal space of the photosynthetic membrane. Electron transfer from photosystem I to NADP+ requires again a small FeS protein, ferredoxin, and ferredoxin-NADP oxidoreductase, a peripheral flavoprotein that operates on the outer surface of the photosynthetic membrane. Ferredoxin and NADP+ are water soluble and are found in the outer stromal phase. As is evident electrons are transferred between large protein complexes by small mobile molecules that play a unique important role in photosynthetic energy conversion, carrying electrons (or hydrogen ions) over relatively long distances.

PSI captures light energy by a large internal antenna system and guides it to the core of the reaction centre with high efficiency. After primary charge separation initiated by excitation of the chlorophyll dimer P700, the electron passes along the electron transfer chain (ETC) consisting of the spectroscopically identified cofactors A_0 (Chla), A_1 (phylloquinone) and the Fe_4S_4 clusters F_X, F_A and F_B. At the stromal (cytoplasmic) side, the

electron is donated by F_B to ferredoxin (or flavodoxin) and thence transferred to $NADP^+$ reductase. The reaction cycle is completed by re-reduction of P700+ by plastocyanin or cytochrome c_6 at the inner (lumenal) side of the membrane. In so far as it is known, photosystem I linear electron transfer is not coupled to proton translocation, whereas the cyclic one probably is.
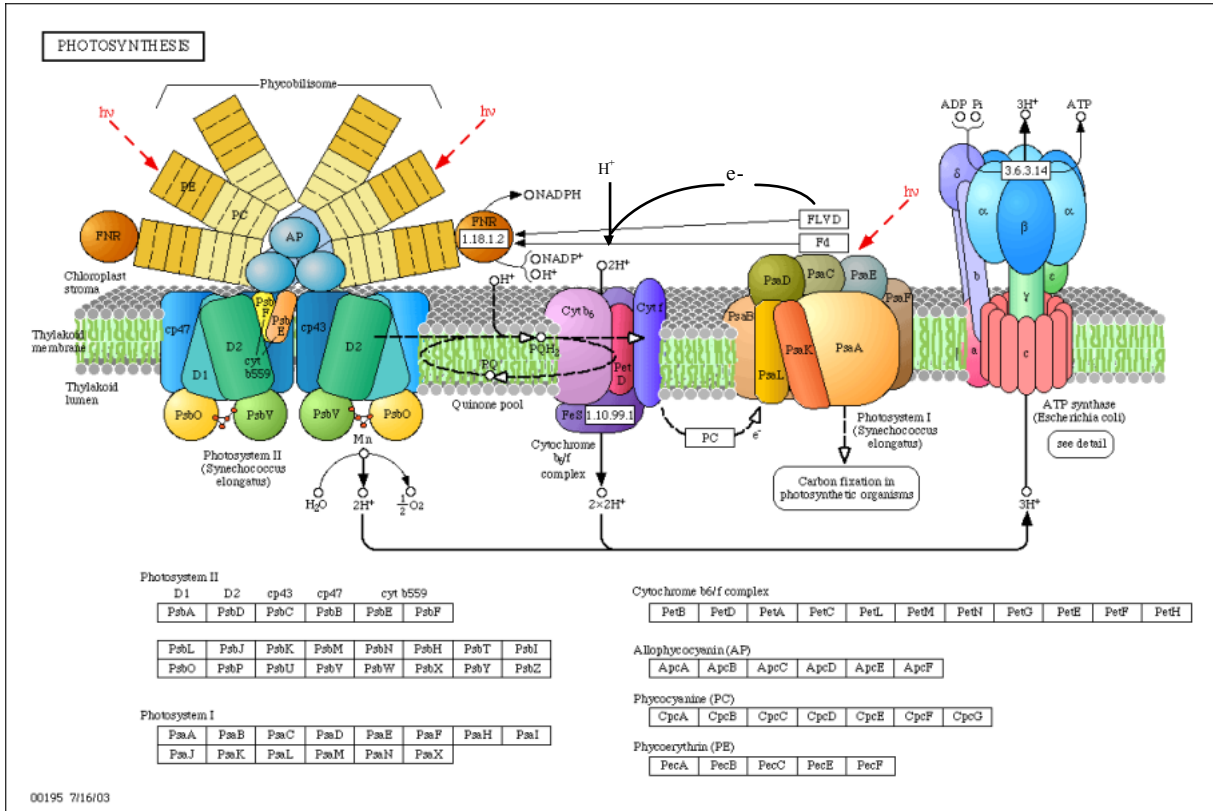

Fig.1.5 Overview of the photosynthetic apparatus in *Synechocystis* (taken from KEGG Pathway database)

1.4 The big protein complexes responsible for photosynthetic electron transfer:

1.4.1 Phycobilisomes

Cyanobacteria, red algae and cryptophytan algae have, in addition to the antennae complexes of PS I and PS II within the thylakoid membrane, accessory extra-membrane light-harvesting antennae, the phycobilisomes (PBS). PBSs serve as a harvester of light energy in the spectral gap between the major chlorophyll absorbing bands (500–660 nm), allowing the species bearing them to utilize the entire visible range of sunlight. Attached primarily to reaction centres of Photosystem II, the PBS can functionally link more than 600 energy absorbing pigments to a single PS II dimer (Glazer 1989). In addition to the chlorophyll a molecules attached to the PS II internal antenna subunits (CP43 and CP47), this brings the total antenna cross section to more than 350 cofactors per reaction centre. This can be compared to about 100 chlorophylls per cyanobacterial PS I monomer (Jordan et al. 2001). This enlarged PS II antenna base allows many cyanobacterial species to increase the ratio of PS I/ PS II to between 3 and 6 (Shen et al. 1993). In green algae and plants, which contain only membrane bound light harvesting complexes, the ratio of PS I to PS II is close to 1 (Danielsson et al. 2004). Many reports exist showing the ability of the PBS to transfer energy to PS I *in vitro* (Kirilovsky and Ohad 1986) and *in vivo* (Rakhimberdieva et al. 2001); however, whether binding to PS I is mediated by specific interactions or by transient association is unclear (Aspinwall et al. 2004).

Electron microscopic studies have shown PBS as large granules attached to the thylakoid membrane in a regular pattern. All PBS complexes have been shown to contain two substructures: a core structure found closest to the membrane surface, and a series of rods emanating out from the core (Glazer 1985; Glazer 1989; Huber 1989; MacColl 1998). This antennae are coupled by their core with PS II and the efficiency of the transfer of the light energy is >95%. Both core and rod structure contain subunits which covalently bind the light harvesting linear tetrapyrolle bilin pigments, and additional subunits lacking pigments called linker proteins.

The exciting variation in colour and the different types of absorption spectra of the phycobiliproteins originate from five bile pigments related to biliverdin, which is their biosynthetic precursor. Biliverdin is an oxidative degradation product of haem. The different absorption proprieties of the phycobilins are caused by subtle structural differences in the tetrapyrrole prosthetic group. The most frequently occurring pigments are the blue phycocyanobilin (PCB, λ_{max} 600-670nm), the red phycoerithrobilin (PEB, λ_{max} 540-570nm) and the red phycourobilin (PUB, λ_{max} 490-500nm). Phycobilin chromophores are generally singly bound to the polipeptide chain by thioether linkages. Each cofactor contains two propionic acids

jutting out from rings II and III. These potentially negatively charged groups are usually found in electrostatic contact with positively charges residues such as arginine. Thus, the extension of the cofactor must be a closely controlled balance between the natural tendency of the cofactor to close in to a ring like or helical structure, and the linearizing power of the protein. Slight changes within this balance are utilized to tune each cofactor to the appropriate absorption wavelength, thus maximizing the spectral cross-section, and allowing for efficient energy transfer.

Phycobiliproteins are hydrophilic polypeptides. Through a process of gene duplication and evolutionary optimization, four major subgroups of phybiliproteins (PBPs) can be found: allophycocyanin in the cores (APC, λ_{max} = 652 nm), phycocyanin in rods, closest to the core (PC, λ_{max} = 620 nm), phycorerythrin (PE, λ_{max} = 560 nm) and phycoerythrocyanin (PEC, λ_{max} = 575 nm) in the rods, distal to the cores. The physical arrangement of the different PBPs creates a clear energy gradient from PE (or PEC) through PC to APC and down into the chlorophyll bed of the reaction centre (λ_{max} = 670–680 nm). The structure of the core subcomplex was found to be variable according to organism, and to contain 2–5 cylinders. High-resolution transmission electron microscopy (TEM) indicated so far that the thickness of each cylinder was due to multiple rings of a thickness of about 30 Å. These thin rings are comprised of $(\alpha\beta)_3$ trimers of APC. Components which make up the rods are comparable to those of the core, but the basic unit is a disk of 60 Å in width. Phycocyanin hexamers $(\alpha\beta)_6$, together with one of the linker polypeptides from the 30KDa family, form these discs. In several cyanobacteria the type of C-PC and the number of discs is regulated by light intensity and/or light quality as well as iron availability. Phycoerithrins, which facultatively occur in the outer disc of the rods, are found in various spectral forms: a form containing only PEB chromophores is frequent in fresh water and soil cyanobacteria; a second one that binds PUB chromophores in varying number and ratio is rather found in marine cyanobacteria and red algae.

SDS-PAGE of physobilisome samples from different species of cyanobacteria and red algae resolved up to nine colourless polypeptides, which act as linker polypeptides. Reconstitution experiments with this linker polypeptides and with dissociated phycobiliproteins showed that the former were essential for the correct arrangement of the latter into functional PBS, e.g. the formation of the core and the rods, the attachment of the rods to the core and the exact positioning of the hexameric discs within them. In the PBS rods, one linker binds to a phycobiliprotein hexamer and in the PBS core, between one and four linkers form a complex with APC. The complexes are probably formed by electrostatic interactions between the basic linker polypeptides and the acidic biliproteins. By sticking to the end of the PBS rods they probably also restrict the disc stacking. Moreover, the various linker polypeptides bound to the trimers or hexamers are able to modulate their spectral properties,

therefore acting as bridging and directing elements for energy transfer from the different rods to the cores and finally to PS II.
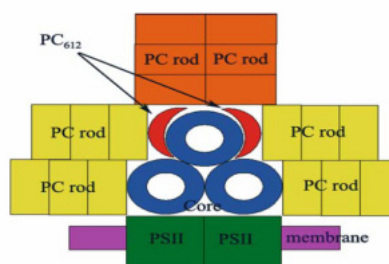

Figure 1.6 Model of the PBS. The three blue rings represent the APC core. The four yellow rectangles represent four PC rods running parallel to both the membrane and themselves. The two orange rectangles represent the additional two PC rods, perpendicular to the membrane. The two green boxes are the approximate dimensions of two PSII monomers, which bind a single PSB. The two red crescents represent the putative positions of the linker between PC rods and the core. There may be additional linker PCs connecting the other rods (Adir, 2005).

1.4.2 Reaction centres

1.4.2.1 Photosystem II

Photosystem II is the homodimeric multisubunit protein–cofactor complex that performs the first step of the photosynthetic pathway in the thylakoid membranes. A number of medium resolution X-Ray structure of the Cyanobacterial complex have been published in the last decade (Zouni et al. 2001, Kamira and Shen 2003, Ferreira et al. 2004, Loll et al. 2005), which provided a description of the general arrangement of the protein matrix and cofactors. A precious improvement has been done with the data presented by Ferriera et al. in 2004, refined at 3.5 Å, because many of their features coincide with predictions derived from biochemical and spectroscopic probing experiments and because they also provided, for the first time, enhanced structural details regarding placement of the individual subunits, including the extrinsic ones, and an accurate description of the protein environment of the various redox-active cofactors and pigments within the RC and its antenna system. That model included also the first hypothetical structure of the OEC. The resolution of the structural arrangement of the Manganese cluster it's the actual challenge and could provide solid structural basis for the unravelling of the 'water-splitting' mechanism. After the elaboration of this first model, a different interpretation of the electron density map around the Manganese cluster has been proposed by Loll et al. (2005) who refined the crystal structure at 3.0 Å resolution. Both the data are still not close enough to the atomic detail needed for the accurate description of the oxygen evolving centre, and moreover high X-ray energies and exposure times used to obtain diffraction data might have resulted in radiation damage that reduced the Mn atoms, probably to all Mn^{2+}, in contrast to the native

Mn^{3+} and Mn^{4+} oxidation states (Klein et al., 1993). Nevertheless the X-Ray models provided the framework to which data obtained using different approaches can be compared as well as encouraging the implementation new biophysical investigations.
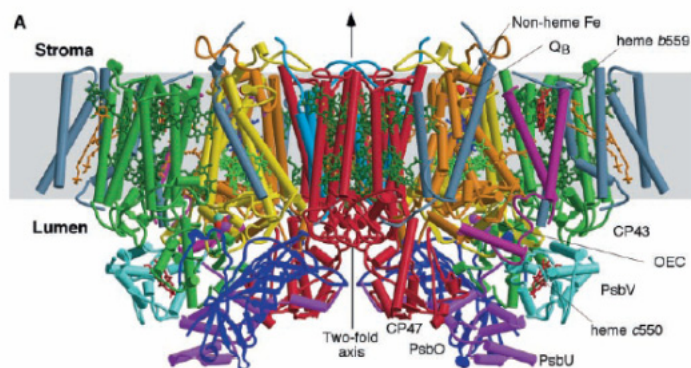
Figure 1.7 PSII dimer: subunits and cofactors at 3.5 Å resolution (from Ferreira et al., 2004)

In the structure released in 2004 by Ferreira et al., each monomer contains 19 protein subunits, 53 cofactors including 36 chlorophyll a (Chl) and 7 all-trans carotenoids assumed to be β-carotene. The more recent 3.0 Å structure includes 20 subunits and 77 cofactors per monomer. 11 β–carotenes have been assigned and 14 integrally bound lipids have been seen in the crystal for the first time.

In all of the structures now available, it can be seen that membrane-spanning helices of the PsbA and PsbD RC subunits form the centre of each PSII monomer complex. RC chromophores (comprising six Chl, two Pheoa, the plastoquinones Q_A and Q_B, and the redox-active tyrosines Y_Z and YD) are bound to these subunits, as expected. D1 and D2 subunits comprise five transmembrane helices organized in a manner almost identical to that of the L and M subunits of the reaction centre of photosynthetic purple bacteria (bRC) (Deisenhofer et al.,1985, Allen et al., 1988). However, the C-terminal domains and the loops joining the transmembrane helices are more extended in the case of the D1 and D2 subunits compared with bRC, especially on the lumenal side close to the OEC. Flanking the opposite sides of the D1/ D2 heterodimer are the CP43 (PsbC) and CP47 (PsbB) polypeptides. Each of this subunit has a large lumenal domain between transmembrane helices V and VI. The disposition of Chl molecules in PsbB and C are now resolved in detail: 16 Chl a are bound to PsbB, and 14 are bound to PsbC.

Of the 11 β-carotenes resolved in the structure, two carotenoids are bound to the D1 and D2 subunits, three are at CP43 and five at CP47. In the reaction centre one of these carotenoids is position such as to facilitate electron flow from cyt b_{559} and Chlz$_{D2}$ to P680, the RC chlorophyll of Photosystem II. In contrast its counterpart Car$_{D1}$ is oriented roughly perpendicular to the membrane plane and does not bridge between Chlz$_{D1}$ and other cofactors of the electron transfer chain. It is unlikely that Car$_{D1}$

participates in electron transfer reactions. Its position is rather optimised for transfer and/or quenching of $Chlz_{D1}$ triplet states and quenching of singlet oxygen that could be produced by 3P680 (Diner et al., 2001). By contrast, the position of Car_{D2} seems to be less efficient for quenching of triplet states, but is in keeping with a role as a 'molecular wire' in putative secondary electron transfer when the Mn_4Ca cluster is not functional or is absent (Diner et al., 2001). This idea is supported by calculations of maximal electron transfer rates, showing that secondary electron transfer reactions will predominantly occur on the D2 side.

A belt of 11 lipids surrounds the reaction centre, separating it from the antenna and smaller subunits. Three remaining lipids and the detergent molecules are located at the monomer–monomer interface. The unusually high lipid content in the PSII complex provides a structural flexibility that might be required for local mobility of subunits and promotes subunit–subunit recognition. A similar 'lubricant' role may be fulfilled by lipid molecules located at the dimerization interface. This is particularly important for PSII that at high light intensities, when D1 is specially prone to photodamage, undergoes monomerization to favour a rapid turnover of D1 subunit (Barbato et al., 1992).

Accessory subunits (i.e., PsbH, I, J, K, L, M, N, T, X, and Z) have been modelled into the structures; L, M, and T are suggested to be involved in formation of PSII dimers, whereas I and X are proposed to stabilize binding of the fifth and sixth Chl molecules, Chl_{ZD1} and Chl_{ZD2}, that are bound to PsbA and D, respectively. The PsbJ, K, N, and Z subunits are clustered near PsbC, and are hypothesized to be involved in carotenoid binding (Ferreira et al., 2004).

On the stromal side of the structure, the Q_A binding site is composed of amino acid residues belonging to PsaD; for the Q_B site, the ligands form a part of PsbA. A non haem iron is positioned between these sites and ligated by four His residues and a bicarbonate.

As predicted from biochemical and mutagenesis experiments (Bricker and Frankel, 2002), the large extrinsic loops of PsbB and C provide binding sites for attachment of PsbO, which is visible on the lumenal side of the complex as an elongated structure containing β-sheets, consistent with predictions from physical characterizations of the soluble protein (Shutova et al., 1997). Although PsbO stabilizes the inorganic ion cluster, neither the 3.5 Å model nor the more recent 3.0 Å predict that PsbO ligands bind to the Mn atoms. However, a loop in PsbO extends in the direction of the Mn cluster, and this loop has been proposed by Ferreira et al. to function as a hydrophilic pathway between the lumen and the inorganic ion cluster.

The major issue concerns the structure of the inorganic ion cluster itself. All models to date propose a monomer-trimer arrangement of the Mn atoms in the cluster, in agreement with spectroscopic experiments (Peloquin et al., 2000). In the model of Ferreira et al., three Mn atoms and an atom of Ca^{2+} form a distorted cube like structure. In the interpretation

proposed by Loll at al., three of the Mn atoms plus a Ca^{2+} cation form the vertexes of a trygonal pyramid.

The pathway of electron transfer in PSII is generally agreed to be as follows: $H_2O \rightarrow [Mn4CaCl] \rightarrow Yz/YZ \bullet \rightarrow P680/ P680+ \rightarrow$ Pheoa/Pheoa$- \rightarrow$ QA/QA$- \rightarrow$ QB/QB$-$. It is now clear from mutagenesis of the haem-binding pocket of cyt b$_{559}$ that it is not required for O_2-evolution activity (Morais et al., 2001), although cyt b$_{559}$ is necessary for assembly of stable PSII complexes and may function in a cyclic reaction around PSII (Stewart and Brudvig, 1998). The crystal structures of PSII have revealed more exact details of the organization of electron transfer cofactors. The model obtained from the more recent X-Ray structure is presented in Figure 1.8.
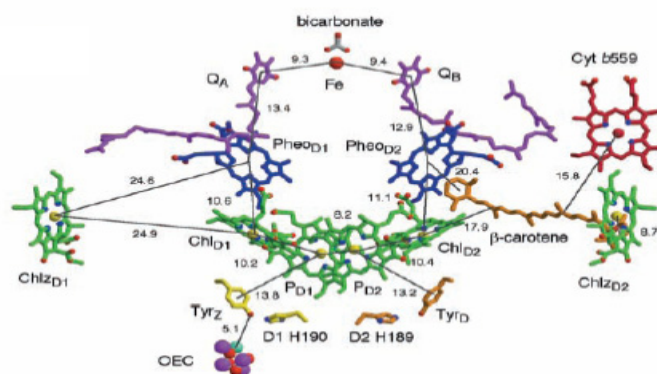
Figure 1.8 Redox-active cofactors and electron transfer chain. View along the membrane plane of the cofactors involved in the electron transfer chain (from Ferreira et al. 2004). Fe^{2+} (red), Mn (purple) and Ca^{2+} (green) ions are shown as spheres, distance are indicated in Å in the figure. In the more recent structure released by Loll et al. (2005) the cofactors arrangement was substantially confirmed a part form the positioning of a new carotenoid in electronic transfer contact with Chl_{ZD1} and $Chl_{D1.}$ Interatomic distances were also consistent with those of the previous structure, although in same cases slightly shorter distances have been calculated in the new structure.

The bifurcated electron transfer pathway comprised of Chl a, Pheo a, and plastoquinones is similar to the arrangement of cofactors of the RC of purple photosynthetic bacteria (Deisenhofer and Michel, 1989). A notable difference is the spacing of the two Chl molecules that are presumed to make up P680. In PSII this distance is estimated to be 8.3 Å rather than the 7.6 Å in bacteria. This slightly longer distance observed , together with the difference in the head-group orientation, may explain why P680 shows more monomeric character and weaker electronic coupling than its bacterial counterpart (Barter et al., 2003).

P_{D1} and P_{D2} are located close to Chl_{D1} and Chl_{D2} (Fig. 2B), which are equivalent to the accessory BChls of the bRC. The P680 excited state is delocalized over the four chlorophylls (Durrant et al., 1995, Dekker and van Grondelle, 2000), and Chl_{D1}, which is the chlorophyll closest to the active $Pheo_{D1}$, is involved in the initial primary charge separation (Barber and Archer, 2001, Diner et al., 2001).

The structural model shows that the cofactors are separated by relatively short distances: 10.6 Å for P680-Chl a [PsbA(D1)] and for Chl a [PsbA (D1)]-Pheo a, and 14 Å for Pheo a-Q_A. These distances are consistent with the rapid rates of electron transfer that have been measured. The Y_Z-Mn cluster complex is shown in figure 1.8. The distance between the tyrosine and the metal centre is approximately 7 Å; this observation is in agreement with the distance derived from magnetic resonance experiments (Lakshmi et al., 1999, Britt et al., 2000).

1.4.2.2   Photosystem I

PSI is an integral membrane protein complex that normally functions to transfer electrons from the soluble electron carrier plastocyanin (Pc) to the soluble electron carrier ferredoxin (Fd). Under certain environmental conditions in some cyanobacteria and algae, alternative electron donors and acceptors, such as cytochrome c_6 and flavodoxin, can function in place of PC and Fd. In terms of functional activity PSI is unique in generating highly reducing species that are capable of reducing $NADP^+$ in an energetically favourable reaction. The PSI reductants are the strongest produced in any biological system.

In prokaryotic PSI at least 11 polypeptides have been identified by SDS-PAGE, while in higher plants 3 additional subunits are found when the isolated reaction centre complex is analysed. Two relatively high molecular mass subunits of approximately 83kDa, PsaA and PbaB, are present as single copies to form an heterodimer which binds P700, A_0, A_1 and F_X as well as the majority of the chlorophylls. The terminal electron acceptors in PSI, F_A and F_B, are bound by a low molecular mass subunit of approximately 9kDa, known as PsaC. PsaC protein is relatively hydrophobic and is tightly associated with the PsaA-PsaB heterodimer. Reconstitution experiments and site specific mutagenesis have confirmed that all the electron carriers are present in the three subunits PsaA, PsaB and PsaC and that those are sufficient for stable charge separation. The function of the additional non-prosthetic group binding subunits of PSI is less well defined. PsaL is required for trimer formation, as proved using cyanobacterial PSI mutants, in which the protein had been knocked out. Concerning the other peripheral subunits, deletion analysis in cyanobacteria has shown that many of these subunits are not required for the functioning or assembly of the PSI complex (Chitnis et al. 1995). However these analysis have been done under optimal growth conditions, and it may be that the requirement for this subunits can only be observed under less optimal conditions.

The crystal structure of PSI from the thermophilic cyanobacterium *S. elongatus* (Jordan et al. 2001), resolved at 2.5 Å, has provided decisive

insights on the structure and on the role of the major core protein as well as of the peripheral subunits and has provided the framework for the already identified components of the electron transfer chain.

PSI has been crystallised from *S. elongatus* as a trimer and this form is also present *in vivo*. The 11 biochemically characterised and sequenced protein subunit have been assigned in the electron density map derived by X-Ray crystallography, as well as 127 cofactors. Trimeric PSI resembles a clover leaf. Its threefold rotation axis coincides with the crystallographic C3 axis, which is perpendicular to the membrane plane.

At the `trimerization domain' close to the C3 axis, PsaL forms most of the contacts between the monomers. PSI contains nine protein subunits featuring transmembrane α-helices (PsaA, PsaB, PsaF, PsaI, PsaJ, PsaK, PsaL, PsaM and PsaX) and three stromal subunits (PsaC, PsaD and PsaE). The large (Mr 83K) subunits PsaA and PsaB are related by a pseudo-C2 axis located at the centre of the PSI monomer and oriented parallel to the C3 axis. The organic cofactors of the electron transfer chain are arranged in two branches along the pseudo-C2 axis. The other membrane-instrinsic subunits are peripheral to the PsaA/PsaB core and contribute to the coordination of antenna cofactors. The `flat but rugged' lumenal surface of PSI is mainly formed by loop regions connecting transmembrane α-helices of subunits PsaA and PsaB. The amino-acid sequences of the loops contain segments not conserved between PsaA and PsaB. The loops, forming several short α-helices and β-sheets, shield the cofactors from the aqueous phase. A hollow close to the pseudo-C2 axis has been suggested to be the binding site for the electron carriers cytochrome c_6 or plastocyanin. The base of the hollow is formed by α-helices A/B-ij of loops A/B-ij in which two conserved Trp residues A655 and B631 are located. As they point into the putative binding site, they may be engaged in interaction with and/or electron transfer from cytochrome c_6 or plastocyanin to the oxidized primary electron donor $P700^+$. This view is supported by mutagenesis studies on cyanobacterial PSI where substitution of some of the amino acids of A/B-ij including Trp affects electron transfer to P700 (Lancaster at al., 2000 and Sun et al., 1999). PsaC, which harbours the two Fe_4S_4 clusters F_A and F_B, contains a large loop extruding on the aqueous phase that may be engaged in docking of ferredoxin or flavodoxin. The complete binding pocket for ferredoxin or flavodoxin is formed by subunits PsaC, PsaD and PsaE. The long C terminus of PsaC interacts with PsaA/B/D and appears to be important for the proper assembly of PsaC into the PSI complex. PsaD has a loop segment close to the C terminus which is attached by numerous hydrogen bonds to the stromally exposed sides of PsaC and E, and seems to help in the positioning of these subunits, as suggested by the importance of PsaD for electron transfer from F_X to F_A/F_B.
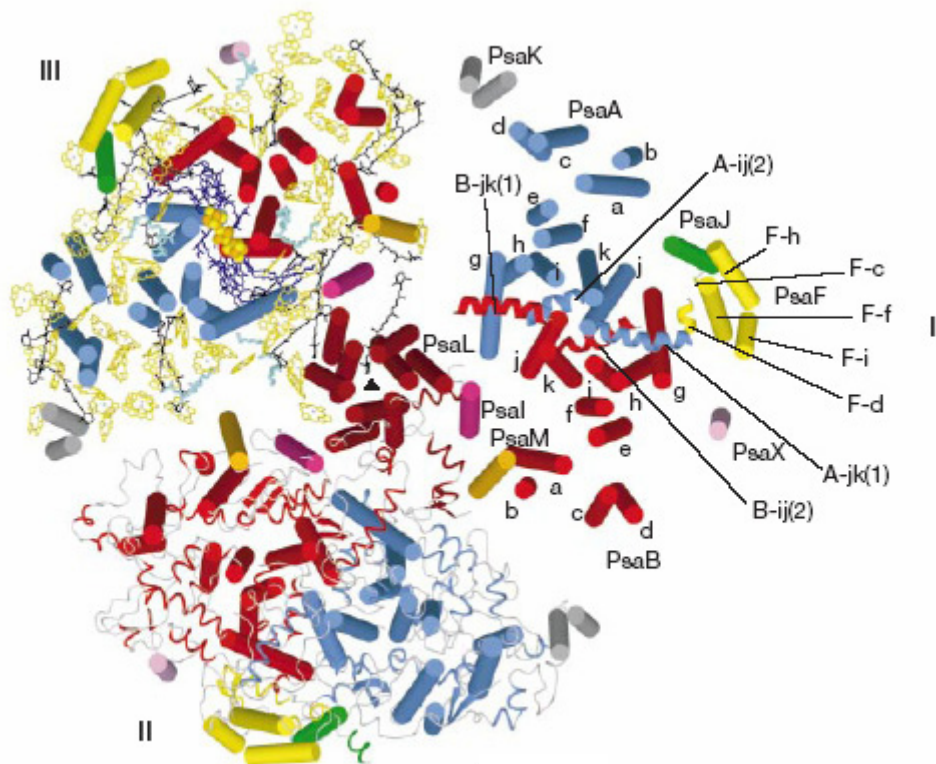
Figure 1.9 Structural model of PS I trimer at 2.5 AÊ resolution. View along the membrane normal from the stromal side. For clarity, stromal subunits have been omitted. Different structural elements are shown in each of the three monomers (I, II and III). I, arrangement of the transmembrane a-helices (cylinders). Subunits are labelled. II, membrane-intrinsic subunits. In addition to the transmembrane α-helices of the stromal and lumenal loop regions are shown in ribbon representation. III, complete set of cofactors shown with the transmembrane α-helices (the side chains of the antenna Chla molecules have been omitted). ETC: quinones and chlorophylls in blue, iron and sulphur atoms of the three Fe_4S_4 clusters as orange and yellow spheres, respectively. Antenna system: chlorophylls in yellow, carotenoids in black, lipids in turquoise (form Jordan et al., 2001).

The small subunits featuring transmembrane α-helices bind and stabilize the cofactors of the core antenna system. PSI features a core antenna system formed by 90 Chla molecules, 79 of which are bound to PsaA and PsaB, while the rest is harboured by the small subunits, coordinated to His imidazoles, or to oxygen atoms of Gln, Asp, Glu and Tyr side chains, to peptides or to water oxygens. Almost all of the Chla molecules are at Mg^{2+}-Mg^{2+} distances between 7 and 16 Å, a range facilitating fast excitation energy transfer of the Förster type.
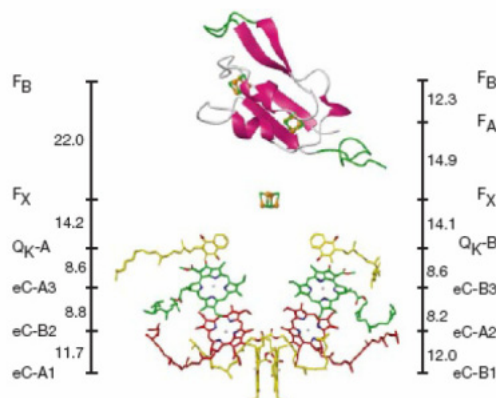
Figure 1.10 Cofactors of the electron transfer chain (ETC) and of PsaC. View parallel to the membrane plane. The pairs of chlorophylls of the ETC are arranged in two branches A and B. They are labelled eC, followed by the letter A or B indicating whether PsaA or PsaB, respectively, coordinates Mg2+, and by numbers 1 to 3 starting from the lumenal side. Phylloquinones are QK-A and QK-B. The Fe_4S_4 clusters are labelled FX, FA and FB according to their spectroscopic terms. The centre-to-centre distances between the cofactors (black lines) are given in AÊ . respectively. Antenna system: chlorophylls in yellow, carotenoids in black, lipids in turquoise (form Jordan et al., 2001).

The electron transfer chain of PSI is formed by six chlorophylls, two phylloquinones and three Fe_4S_4 cluster. The chlorophylls and phylloquinones are arranged in two branches A and B as pairs of molecules related by the pseudo-C2 axis and coordinated to PsaA and PsaB. The cofactors forming one branch are not bound exclusively to one subunit of PSI. Charge separation is initiated at the primary electron donor P700 formed by a chlorophyll pair identify in the structure. The chlorin planes of these chlorophylls are parallel at 3.6Å interplanar distance and oriented perpendicular to the membrane plane. Rings I and II overlap partially with the Mg^{2+} ions separated by 6.3Å. P700+ formation is characterised by absorbance changes in the red and blue spectral regions and by the generation of an EPR free-radical signal indicative of an oxidized chlorophyll species. The E_m for the P700/P700+ couple is approximately +500mV. Time resolved kinetic measurements on A_0 have been done under conditions where the PSI electron acceptors are in the oxidized state prior to light activation. On the base of this studies Hastings et al. (1994) supported so far the hypothesis of a Chl dimer being oxidised and a Chla monomer being reduced in the light.

The Chl dimer has been identify in the structure as an heterodimer of chlorophyll a and a', in agreement with previous chlorophyll extraction experiments from purified PSI particles (Watanabe et al., 1985). One or both of the Chl a molecules of the third pair of chlorophylls next to the P700 probably represents the electron acceptor A_0. Electron transfer in PSI proceeds from A_0 to A_1, the next bound electron acceptor. Measurements of the spin-polarized EPR signal of the primary reactant have provided strong evidence for a phylloquinone in the role of A_1. One or both of the phylloquinones localized in each of the two branch of cofactors might correspond to the electron acceptor A_1. A controversial issue in PSI is whether one or both branches of the ETC are active. Spectroscopic data on P700+ and the radical pair P700+/A_1- suggest an asymmetry of electron transfer along the electron transport chain (ETC) in PSI. P700 is the only site where a significant structural difference between the two branches is obvious. According to kinetic investigations, electron transfer in PSI involves both branches of the ETC with different rate constants (Joliot and Joliot, 1999; Guergova et al. 2001) of 35×10^{-6} s^{-1} and 4.4×10^{-6} s^{-1} for the electron transfer steps from each phylloquinone to F_X. Mutation of Trp A697 in the QK-A binding site decreases the slower rate, indicating that the A branch is the slower one. Electron transfer from A_1 proceeds then to the series of membrane bound Fe-S centres. The first acceptor in this series is F_X, which is a rare example of an inter-polypeptide iron sulphur cluster. F_X is coordinated to both PsaA and PsaB in strictly conserved loop segments. The terminal bound electron acceptors is PSI are the two Fe_4S_4 clusters in PsaC. F_A and F_B have been definitely assigned in the structure, in perfect agreement with previous evidences collected by specific mutagenesis in cysteine residues of PsaC (Zhao et al., 1992). The arrangement of the clusters, defined by the X-Ray data, with F_A being closer to F_X than F_B suggests a sequence $F_X \rightarrow F_A \rightarrow F_B$ in electron transfer, in agreement with spectroscopic data (Golbeck, 1999).

1.4.3 Cyt b_6f

Cytochrome b_6f complex provides the electronic connection between photosystem I and photosystem II reaction centres by oxidizing lipophilic plastoquinol and reducing plastocyanin or cytochrome c_6. One electron is transferred from the doubly reduced dihydroplastoquinone PQH_2 to a high-potential electron transfer chain, consisting of the Rieske iron-sulfur protein and cytochrome f on the electropositive side of the membrane. The process result in the release of two proton towards the lumenal side of the membrane. Electron transfer and proton translocation functions are performed in a similar way by the respiratory cytochrome bc1 complex, but using one high-potential c haem, cytochrome c1, instead of the functionally analogous cytochrome f, and dihydroubiquinol as electron

donor. The lipophilic quinones move in both case through the membrane bilayer phase between a site for oxidation and proton release on the electropositive, or lumenal side and a site for reduction and proton uptake on the electronegative side. The b_6f and $bc1$ complexes share the basic elements of this process, which is explained by a the so called Q–cycle mechanism. QH_2 gives up one electron to the Rieske iron-sulfur centre, which is in turn reoxidized by transfer the electron to either cytochrome f or c_1 in the two respective complexes. Through the latter then the electron is passed out of the complex to the soluble acceptors in the aqueous lumenal phase, respectively plastoyanin/cyt c_6 or cytochrome c. The loss of one electron from QH_2 and the release of the two protons in the lumenal space, generates a semiquinone radical, $Q^-\bullet$. The second electron is transferred from the semiquinone to the haem b_p (also indicated as haem b_L), which passes it across the membrane via haem b_n (or haem b_H) to another quinone bound at a site on the electron negative side of the membrane. The process is accompanied by the uptake of a proton from the adjacent aqueous phase (stroma). The fully oxidised quinone, generated as the second electron is passed to the b cytochromes, may then dissociate from is binding site adjacent to the intermembrane space.
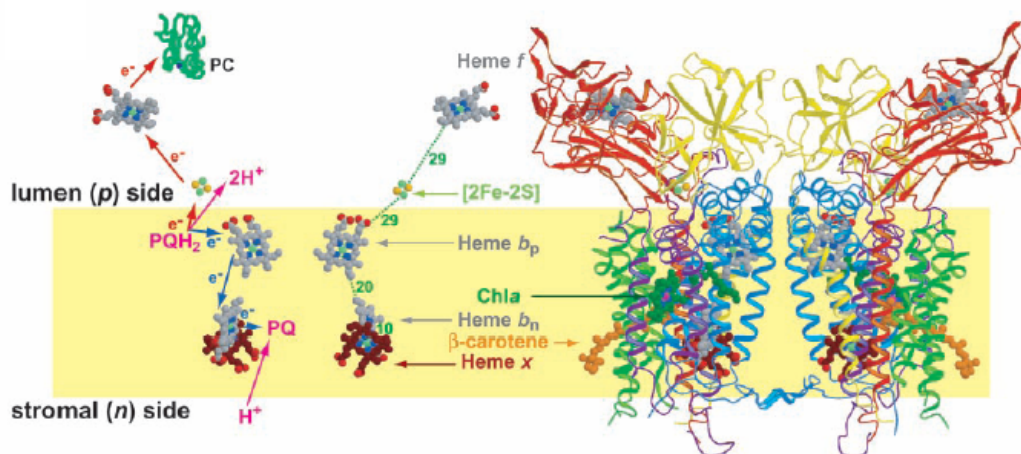
Figure 1.11 Cytochrome b_6f complex. On the left the electron and proton transfer pathway through the b_6f complex is represented and distances between redox cofactors are in scale with the adjacent representation of he crystal structure. On the right a side view showing bound cofactors and protein subunits is reported. The colour code is as follows: Cytochrome b6 is in blue; subunit IV in purple; cytochrome f is red; ISP is in yellow; PetG, -L, -M, and -N are in green; and the yellow band represents the membrane bilayer (from Kurisu et al., 2003).

A structural framework for the Q cycle is provided by crystal structures of dimeric cytochrome b_6f and cytochrome $bc1$. The localization of the redox active groups (the four haem cofactors and the [2Fe-2S] cluster) has allowed to trace the pathway of electron transfer. Moreover the two monomers form two protein-free central cavities, one on each side of the transmembrane interface. A small portal (11 x 12 Å) in the wall of each cavity leads to a p-side antechamber, or "Q_p pocket", which is bounded by

the [2Fe-2S] Cluster and haem b_p. Two p-side quinone-analog inhibitors, TDS and 2,5-dibromo-5-methyl-6-isopropyl-benzoquinone (DBMIB), were separately cocrystallized with the b_6f complex. In the 3.0 Å structure of a co-crystal with TDS, the head group of TDS binds at the roof of the central cavity on the p side of the complex, and its 13-carbon tail extends through a portal into the Q_p pocket. An endogenous plastoquinone molecule was found bound at the n side of each central cavity, identifying this as the "Q_n pocket", that serve as quinone exchange site. The quinone is reduced on the open n or stromal side of the complex and oxidized in the Q_p niche on the p side. To reach this Q_p pocket, the quinone must pass through the 11 x 12 Å portal.

Within the b_6f complex, in addition to this linear mode of electron flow, the system can switch to a cyclic mode, in which photosystem I returns some of its electrons to the b_6f complex rather than feeding them into biosynthesis. This is necessary to balance the activities of the two photosystems, which depend on the variable amounts of solar energy absorbed by each. The cyclic mode of electron flow is still poorly understood, although the recent X-ray structures of the cyanobacterial and algal complex have provided important insights for the elaboration of a plausible mechanism. In particular the surprise of the crystal structures has been the identification of a unique haem, assigned as haem x, seen for the first time in *C. reinhardtii's b$_6$f complex*, and localized at a position between haem b_n and the central cavity, where proton uptake and reduction of plastoquinone take place. The nearly perpendicular planes of haem x and haem b_n are in contact through the propionate-H_2O linkage, which implies efficient electron transfer between the two haems and an electron transfer function for haem x that includes haem b_n. Haem x does not appear to be required for Q-cycle function, since the other elements of the Q cycle (haems b_p and b_n) are identically oriented in the b_6f and bc1 complexes, have identical interhaem distances, and have similar hydrophobic environments between haems. The accessibility of haem x from the stroma, makes it a good candidate for the hitherto elusive ferredoxin-plastoquinone reductase inferred to be essential for the cyclic pathway. In addition the positive stromal-side surface potential of cytochrome b_6f would facilitate an hypothetical docking of anionic ferredoxin to the stromal (n) side of the complex near haem x.

Concerning the main structural characteristics, cytochrome b_6f complex from *Mastigocladus laminosus*, a thermophilic cyanobacterium, has been crystallize in dimeric form. Each monomer contains four large subunits (18 to 32 kD), including cytochrome f, cytochrome b6, the Rieske iron-sulfur protein (ISP), and subunit IV; as well as four small hydrophobic subunits, PetG, PetL, PetM, and PetN, whose function has not been completely unravelled yet. The monomer includes also, as already mentioned, four haems and one [2Fe-2S] cluster, beside one chlorophyll a, one β-carotene and one plastoquinone. The presence of the chlorophyll crates a

constriction at the entry of the Q_p pocket in the photosynthetic cytochrome complex, that results therefore less accessible than the analogous pocket in cytochrome bc1. In contrast the Q_n site is more accessible in cytochrome b_6f.

The most characteristic feature of cytochrome b_6f, if compared to bc1, it's the extrinsic lumenal subunit, cyt f. Cytochrome f is not related to the analogous cyt c1 and presents some unique features even among the c type cytochromes: it is mostly β-strand, an elongate 75 Å structure consisting of a small and a large domain, that host the haem group; it has a buried chain of 5 water molecules spanning 11 Å ; finally one of the axial haem ligands is the alpha-amino group of the N-terminal amino acid residue. What is also deducible from structural studies is that cytochrome f subunit is highly specialized to optimise the interaction with his electron acceptor, plastocyanin. Complementary surface charges indeed face on the two protein near the redox centres, where the docking of plastocyanin takes place.
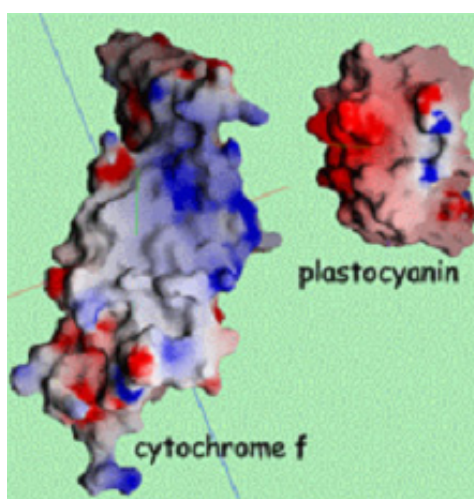
Figure 1.12 Interaction of cytochrome f with it's electron acceptor, plastocyanin. In the figure protein surfaces have been coloured according their electrostatic potential (from negative, blue, to positive, red. Neutral residues are represented in grey). The docking site between the cytochrome subunit and plastocyanin is characterized by complementary surface charges. Ionic-strength dependence of rates of oxidation of cytochrome f by plastocyanin in solution is an ulterior indication of the presence of electrostatic interactions between the redox partners.

1.4.4 Photosynthetic phosphorilation and ATP synthase

1.4.4.1 Photophosphorilation

Mitchell's chemiosmotic theory (Mitchell, P. 1961,1966) proposed that an electrochemical proton gradient across the membrane (which is only slightly permeable to many ionized species and particularly to H^+) is formed by the vectorial transport of H^+ into the thylakoid lumen coupled to electron transport, as a consequence of the alternate disposition across the membrane of electron carriers which can bind protons and other that cannot be protonated.

The experimental use of artificial electron acceptors and donors has demonstrated, in agreement with Mitchell's theory, that electron transport can be coupled with ATP synthesis only when the chemical structure and the lipophilicity of the electron carriers added is such as to allow vectorial proton transport across the membrane (Trebst, 1974).

In this way, the loss of redox free energy available during "downhill" electron transfer is partially conserved as electrochemical potential energy of the proton gradient. The synthesis of ATP occurs when the protons accumulated inside the thylakoid lumen are transported out into the external water phase by an anisotropic, proton-translocating ATP synthase- ATPase (the complex F_1-F_0), which catalyses the reaction:

$$ADP + P_i + nH^+_{in} \rightarrow ATP + H_2O + nH^+_{out}$$
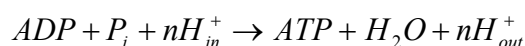
The free energy change of ATP synthesis is given by

$$\Delta G_P = \Delta G_0^P + RT \ln \frac{[ATP]}{[ADP][P_i]}$$

and the free energy change for H^+ efflux is

$$\Delta G_H = RT \ln \frac{[H^+_{out}]}{[H^+_{in}]} + F\left(\Psi_{out} - \Psi_{in}\right)$$

Synthesis of ATP can only occur when $\Delta G_P + \Delta G_H < 0$, while ATP hydrolysis occurs when the reverse it's true, provided that the ATPase is activated.

All the available evidence indicates that the synthesis of ATP is not directly coupled to electron transport, but is only dependent on the protonmotive force. If an uncoupler is added in continuous light, ATP synthesis is abolished or decreased, while electron transport is accelerated (Rasing and Slater, 1972).

The introduction of permeating buffers (Hangarter and Ort, 1985) into the inner phase of the thylakoids does not alter the number of single turnover flashes required to produce the threshold value of protonmotive force necessary to initiate ATP synthesis. This would indicate that the pooled protons utilized by the ATP synthase are not located in the internal water phase, nor are they rapidly equilibrated with it: the only alternative would be that he proton pool is located within the membrane, and a proton-conducting system must then exist capable of transferring protons from where they are generated to the ATP synthase complex, without allowing equilibration with the buffered internal phase. The intramembrane proton conduction could be imaged as being due to intrinsic proteins (Williams, R. 1961, 1978). However, there is a body of evidences that protons are released into the aqueous phase where they diffuse to the ATP synthase (reviewed by Mulkidjanian et al., 2005).

1.4.4.2 ATP synthase

ATP synthesis by both photophosphorylation and oxidative phosphorylation occurs on the F_1F_0-ATP synthase enzyme. Functionally, ATP synthase is tripartite, consisting of: a motor in the membrane that converts the energy of an electrochemical ion gradient into subunit rotation; a rotating transmission device, the `rotor stalk', which transmits the energy over a distance of greater than 100 Å to the catalytic sites; and the catalytic sites, three in number, where the mechanical energy of rotation is converted into the chemical bond between the ADP-O and Pi. F_1F_0-ATP synthases are basically similar whatever the source. In their simplest form in prokaryotes they contain eight different subunits, with stoichiometry $\alpha_3\beta_3\gamma\delta\epsilon ab_2c_{10-14}$ (Senior 1988 and Fillingame 1990). The catalytic core of the enzyme is $\alpha_3\beta_3\gamma$, consisting of a hexagon of alternating α and β subunits with helices of γ in the centre. ATP synthesis and hydrolysis reactions occur at three catalytic sites (Leslie and Walker 2000). Proton transport is effected by the a and c subunits. The `rotor stalk' is composed of γε, connected firmly to the c-ring at the base, and interacting with α and β at the top [Nakamoto et al. 1999, Stock et al. 1999, Capaldi et al. 2000]. The `stator stalk' is composed of $b_2\delta$, with δ binding to α-subunit at the top of the molecule [Wilkens et al. 2000, Ogilvie et al. 1997], and β2, anchored in the membrane by the N-terminal transmembrane helices, interacting there with the a subunit.

To fulfil the major objective of elucidating the mechanism of energy coupling between the transmembrane proton gradient and the catalytic sites of F_1F_0-ATP synthase and the molecular events required to accomplish the chemical synthesis of ATP, a number of different approaches has been used to establish a structural model for the complex enzyme and therefore reveal its mechanism. Progressively more accurate low-resolution models, obtained from Electron Microscopy and Single

Particle analysis techniques, have been used as a framework for building a molecular model from higher resolution X-Ray structures of subcomplexes and individual subunits. Additional information from protein cross-linking experiments and equilibrium nucleotide binding studies have given an important contribute to assign a coherent model starting from the heterogeneous structural data available. Of great importance have been also the recent NMR structures of the most flexible regions: a model for ε was done (Capaldi et al 2000), found to be in good agreement with the previous X-Ray one; NMR unravelled the structure of the C-term portion of δ (Wilkens et al 1997), spotted by mutagenesis as a functionally important region and located spatially close to b and α; further NMR studies of E. coli ATP synthase have identified two distinct conformations of c-subunit, dependent on pH, and differing drastically in orientation of the C-terminal helix (Girvin et al 1998); finally a model for the transmembrane arrangement of the two N-terminal helices of b-subunit has been presented (Dmitriev et al 1999) leading closer to the highly desirable completion of this structure. Figure 1.13 represent a summary of the current knowledge of the structure of ATP synthase from mitochondria. The model is based on EM studies of single particles (Karrash and Walker 1999), it incorporates the structure of bovine F1-ATPase (Abrhams et al 1994) and information from the electron density map of the F1–c10 complex from *S. cerevCP43'e* (Stock et al 1999). The composition, stoichiometry and arrangement of the subunits in the peripheral stalk (subunits OSCP, F6, b and d) come from biochemical and reconstitution studies [20,33]. The position of subunit a relative to the c10 ring was deduced from studies of the bacterial enzyme (Jiang and Fillingame 1998). The bacterial and chloroplastic models are largely based on this same framework and filled with X-Ray structures of *E.coli* subunits and hypothetical models based on the homology with the eucariotic ones (Stock et al 2000).

Concerning the catalytic mechanism of F_1F_0-ATP synthase, an old and still interesting theory is the one proposed by Boyer. Boyer predicted (Boyer 1989, 1993) that catalysis requires sequential involvement of the three catalytic sites, each of which changes its binding affinity for substrates and products as it proceeds through a cyclical mechanism, the `binding change mechanism'. In the ATP synthesis thereby each site first acts to bind ADP and Pi, then acts to chemically synthesize ATP, then opens to release the ATP, and all three activities are ongoing simultaneously at the three different sites. This model, however, has not yet been framed in molecular terms, which will present a true test of its viability. As a consequence the different uniside, biside and triside model for the catalytic mechanism are still worthy of further consideration as potentially valid. Nevertheless, although on the light of more recent observation the original hypothesis seems to require revisions, the binding change mechanism remains the overall guiding mechanism for ATP synthase, strongly

supported by demonstration of subunit rotation, widely different binding affinities for substrates ATP or ADP at the three catalytic sites, and asymmetric X-ray structures (Senior et al. 2002).
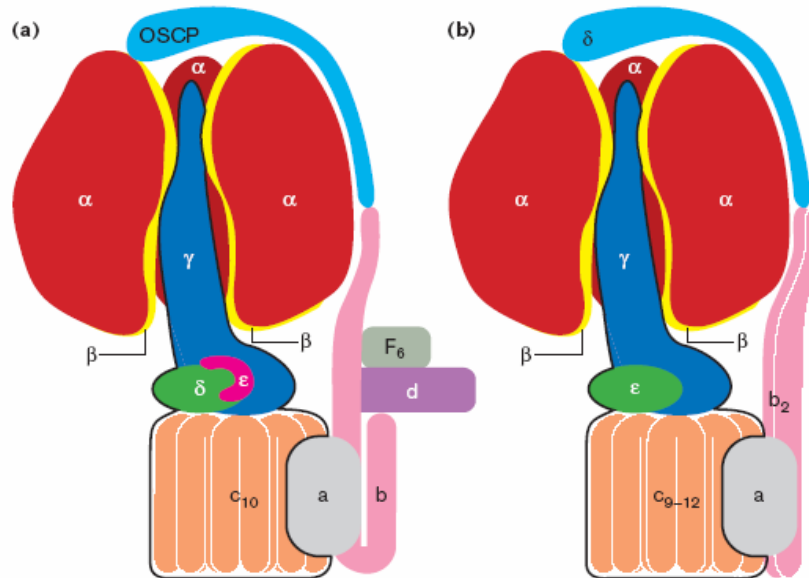
Figure 1.13 Structural model of ATP synthase (F_1F_0) from mitochondria and eubacteria. The model, adapted from Stock et al. (2000), is a summary of the actual knowledge about F_1F_0-ATP synthase obtained combining the model based on EM studies of single particles with the crystal structure of single subunits and the result of biochemical and reconstitution studies. The models elaborated for mitochondria and eubacteria are compared. The overall structure is substantially homologous, however some local differences can be pointed out. The C-ring seems to contain a different number of subunits and also the position of the subunits in the peripheral stalk (b and δ) is slightly different. The structure the ATP synthase from *E.coli* is represented in the figure as a model for the bacterial multi-protein enzyme. Studies on the general structure of ATP synthase from chloroplasts have shown that it is very similar to that of the bacterial enzyme. Again a few difference are evident, special in the "flexible arm", subunit b.

1.5 Working hypothesis

In this work we studied the physiological response of cyanobacterial photosystems to condition of iron deprivation. The object of our interest was the detection of a possible interaction between the iron-induced chlorophyll a-binding protein CP43' and Photosystem II.

1.5.1 *Growth in iron starvation conditions*

Since iron is the fourth most abundant element by weight in the Earth's crust, one would not expect iron stress to be a recurring problem to living organism. However, in aqueous oxic environments Fe^{2+} is quickly oxidized to Fe^{3+}, and, at physiological pH's, Fe^{3+} forms highly insoluble hydroxides. For example, the free Fe^{3+} concentration at pH 7 is only about 10^3 ions per ml (Braun *et al.,* 1990). Since a single bacterial cell *(Escherichia coli)* is estimated to contain about 10^6 iron ions (Archibald, 1983), an actively growing bacterial culture of 10^9 cells ml^{-1} would suffer an incredible deficit of iron if exposed to the soluble iron ions in the environment. Whereas iron is an essential component of electron transport in almost all living organisms, it is furthermore important to phototrophs that require it also to build up a complete photosynthetic apparatus. 22-23 iron atoms are needed for a functional photosynthetic apparatus in cyanobacteria under normal nutrient conditions. The positions of these irons are shown in Fig.1.14: PS II requires 3 irons, the cytochrome b_6f complex has 5 irons, PS I contains 12 irons, and ferredoxin has 2 irons in its single 2Fe-2S centre.

Since the availability of iron in open oceans is sufficiently low to limit photosynthetic activity and phytoplankton growth, aquatic microorganisms have developed a number of responses to cope with iron deficiency. The general observed response is a great improvement of the ability of microbes to scavenge iron and a significant reduction of the cellular demand for it by altering the population of proteins. A number of specific recurring responses have also been seen in the photosynthetic physiology of cyanobacteria. Under extreme iron stress, cyanobacteria show reduced levels of chlorophyll, phycobilisomes, iron-sulfur centres, and other components of the photosynthetic electron transport chain (Sandmann and Malkin, 1983, Sandmann,1985). Iron stress also results in qualitative changes to the light-harvesting structures. Absorption studies on whole cells and phycocyanin-free lamellae display a blue shift of 5-6 nanometers in the main red chlorophyll absorption band (Oquist, 1971, 1974b; Guikema and Sherman, 1983). These spectral shifts are paralleled by the de-repression of an operon tightly regulated by iron. The first gene of this operon, *isiA* codes for a protein that shows significant similarity with the PsbC/CP43 subunit of PSII (therefore the *isiA* gene product is also known as CP43'), whereas the second-open reading frame codes for a

flavodoxin. The function of the latter is to replace ferredoxin in order to reduce the cellular requirements for iron. A number of different hypotheses have been suggested for the former. It has been demonstrated that CP43' can associate with PSI to form a complex consisting of a ring of 18 CP43' molecules around a PSI trimer. This association allows an efficient energy transfer and thus significantly increases the size of the light-harvesting system of PSI (Bibby, Nield and Barber 2001). It has been further shown that CP43' can work as a nonradiative dissipator of light energy, thus protecting PSII from excessive excitation under iron-deficient conditions (Sandström et al., 2001).
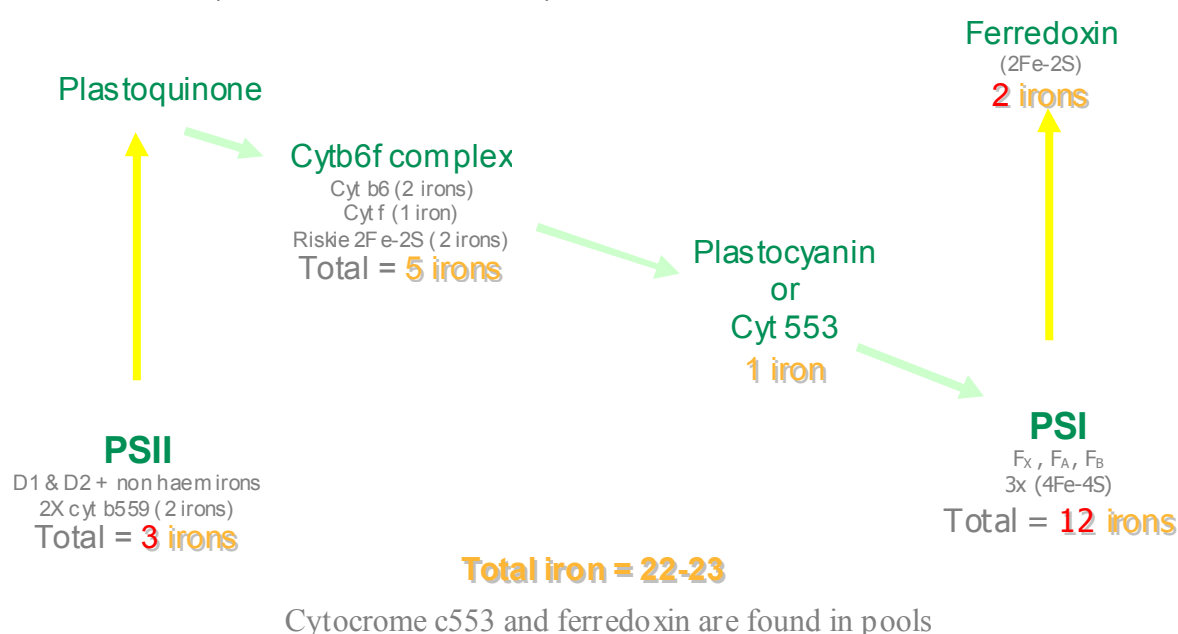
Figure 1.14 Diagrammatic representation of photosynthesis, indicating the location of iron in the complexes involved.

Clearly (as labelled in Fig.1.14) in iron stress condition PSI complex suffers a more dramatic iron starvation than PSII, hence the relative activity of the two photosystems is significantly imbalanced, while the phycobilisomes are not sufficiently concentrated to adjust the influx of energy to the two complexes. At the same time the electron transfer pathway between the two photosystems is also affected by the lowering of Cytb$_6$f complex. The expression of CP43' sets up an extra antenna for PSI and perhaps leads to energy dissipation around PSII, thus compensates for this imbalances in photosynthetic electron transport. Furthermore, since homology searches indicated that CP43' protein sequence shows a great deal of similarity to CP43 and many conserved structural features (Laudenbach and Straus, 1988; Leonhardt and Straus, 1992; Murray et al., 2005) it has also been speculated that it may be capableof replacing CP43 during periods of iron deprivation (Burnap et al. 1993; Straus 1994). There are no evidence at the moment for this hypothesis.

1.5.2 *CP43' iron stress protein*

The gene that encodes CP43', *isiA*, is expressed in depletion of iron levels (Strauss, 1994) although other stress conditions can turn it on, such as high levels of light (Havaux et al., 2005). Transcription of the isiAB operon in normal and iron deprived growth, has been quantitatively analysed by northern blot, normalising data to hybridisation signal obtained from a 16S rRNA probe (Vinneimer et al., 1998). The transcription of the operon is derepressed under iron limiting conditions and, moreover, the monocistronic *isiA* message is found to be more abundant than the dicistronic *isiAB* message. As a result the protein product of isiA gene, CP43', is the most prominent Chl a-protein complex accumulated in the cells in iron-deficiency.

CP43' is a 34 kDa protein. Many features of CP43' protein sequence indicate that it may have analogous structure to CP43, as reviewed by Murray et al. (2005), combining the result of the primary sequences alignment with the structural information derived for PSII. Hydropathy plots (figure 1.15) evidence a correspondence between all the hydrophobic regions of CP43 and CP43', indicating that both probably assume similar membrane spanning structures. In addition, the distribution of histidine residues in the potential membrane spanning regions of CP43' suggest chlorophyll ligand capabilities similar to CP43. A local alignment of the two proteins (not shown) made by Sim software (Huang and Miller 1991) gives a final result of 49.8% identity in 275 residues overlap and above all shows a gap corresponding to the big loop that joins, in CP43, the two helixes V and VI.

The large lumenal domain of CP43 is involved in both the ligation of the Mn_4-Ca cluster of the oxygen-evolving catalytic centre and the docking of the PsbO protein. A motif conserved in all known CP43 sequences (Gly-Gly-Glu-Thr-Met-Arg-Phe-Trp-Asp), is contained in this loop. Part of this motive is a 3_{10} helix localized, in the recent 3.5Å and 3.0 Å X-ray structures (Ferreira et al., 2004; Loll et al., 2005), close to the OEC. The Glu^{354}, contained within the conserved motif, had been suggested, by site-directed mutagenesis experiments (Rosenberg e al. 1999), to play an important role for water oxidation activity and, indeed, shown to be a Mn-ligand by Ferreira et al. (2004). The role of CP43 in binding the PsbO has been suggested from a range of mutational and cross-linking studies (reviewed in Eaton-Rye et al., 2005) and again confirmed by the two available medium resolution X-Ray structures (Ferreira et al., 2004; Loll et al., 2005).

These specific properties of CP43 are related to the water splitting reaction of PSII and are in addition to its functions as a light harvesting protein. Since the loop is not present in CP43' then it functions only as a Chl-binding protein involved in light harvesting and probably also in photoprotection.
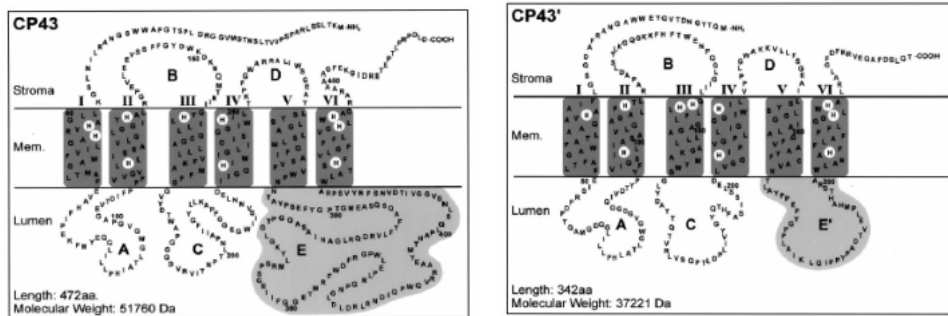
Figure 1.15 Comparison of the folding diagrams of CP43 and CP43' based on the sequences of the PsbC and CP43' proteins of *Synechocystis* 6803 and hydropathy analyses. The predicted amino acid sequences are given with the position of the histidines highlighted. Note that the E-loop joining the 2-transmembrane helices V and VI of CP43 is significantly more extensive than the corresponding loop of CP43' (from Bibby et al., 2001).

1.5.3 *Working hypothesis: a special CP43'-conjugated PS II*

In the light of the significant structural similarity of CP43 and CP43' (section 1.5.2), it is conceivable to suppose that this protein could compete with CP43 during the assembly of PSII reaction centre complexes. Since CP43 is still produced in iron-deficient cells, although probably at lower levels (Leonhardt and Straus, 1993; Burnap et al. 1993), one would expect PSII to accumulate in almost regular amounts and a second form of PSII (CP43'-conjugated PSII), which includes CP43' in the core complex instead of CP43, to eventually exist at the same time. The CP43'-conjugated PSII would most likely represent a small fraction of the total PSII population.

If indeed a stable complex of this type was formed and capable of performing the primary charge separation then the absence of the large lumenal domain will be expected to have essential structural and functional implications.


PSII **CP43'-conjugated PSII**
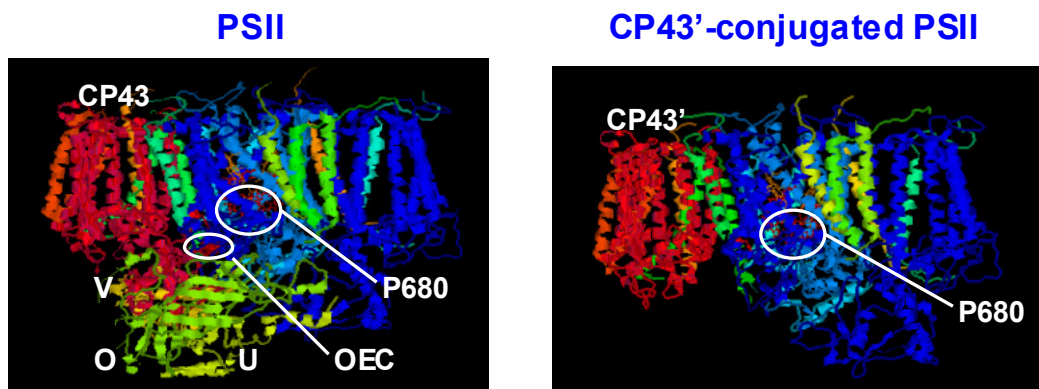
Figure 1.16 Representation of a PS II monomer (left) (Ferreira et al., 2004) and of a hypothetical structure for the CP43' conjugated photosystem, on the framework of the 3.5Å x-ray structure.

In figure 1.16 a hypothetical representation of the CP43'-conjugated PS II is shown (right). The lack of the lumenal loop in CP43' releases a gap close to the OEC. Since the loop is also (as evident in the PS II representation, left) closely associated with the extrinsic proteins, the CP43' conjugated photosystem is unlikely to be able to interact efficiently with the lumenal subunits, therefore even more steric inhibition is removed next to the manganese cluster. The OEC site is thus exposed on the accessible surface of the protein. Furthermore, since both CP43 loop and PsbO subunit are known to coordinate the environment to allow an efficient activity of the OEC, it is very unlikely that the manganese cluster would be associated at all with the hypothetical complex. With the disruption of the oxygen evolving complex, P680 reaction centre becomes accessible for small molecules. Therefore the PS II having CP43' conjugated wouldn't evolve oxygen, but may, however, be able to oxidise other substates.

It has been found that PS II stability and concentration drops when CP43 is deleted or mutated. Core complexes containing only CP47, D1, D2 and $Cytb_{559}$ are purified from this kind of mutants (Rögner et al. 1991; Kuhn and Vermaas 1993). According to this findings, the hypothetical CP43'-conjugated complex, is more likely to be essential, as represented in figure 1.17. Such a photosystem would be comparable with the purple bacterial type-II photosystem.
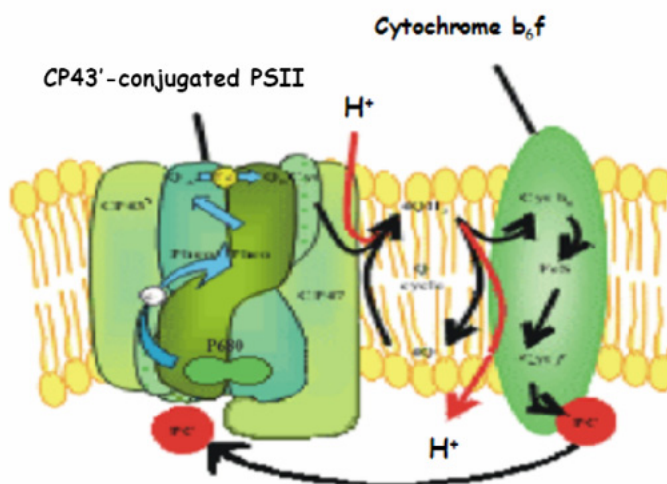
Figure 12 Schematic representation of CP43'-conjugated PSII and cytb6f. The gap on CP43' side is evident, that leaves P680 reaction centre accessible on the donor side, thus allows a cyclic electron transfer via plastocyanin.

The light driven electron transfer reactions across the membrane are performed by the purple bacterial reaction centre with the same mechanism used by PSII: one electron is transferred from the excited special pair first to a pheophytin, then a bound quinone (Q_A) and finally to the acceptor soluble plastoquinone (Q_B). In this type of photosynthetic

organism as in PSII, the double reduced plastoquinone (Q_BH_2) is reoxidised by a cyt bc_1 complex, that transfers back through the membrane the two electrons end two protons. The two protons are released in the periplasm, generating a proton-motive force used for ATP synthesis. However in the case of Photosynthetic purple bacteria, the haem of the soluble cytochrome c_2 cyclec the electrons back to the reaction-centre, from which they had originated. The whole process can be described as a light-driven cyclic electron flow, whose net effect is the generation of a proton gradient across the membrane, that is used for the synthesis of ATP.

In analogy with the purple bacterial type-II photosystem, the hypothetical CP43'-cojugated PSII would perform the primary charge separation, electron would be transfer across the membrane driven by light energy and the oxidised TyrZ• radical would be left accessible for small molecules that can donate an electron. If an electron could be shuttled back from the $cytb_6f$ to TyrZ• by a soluble transporter, a cyclic electron flow would be generated around the CP43'-conjugated PSII, associated with the generation of proton-motive force across the membrane, exactly as in the purple bacterial photosynthesis.

An interesting candidate for the oxidation of TyrZ• could be the soluble plastocyanin available in the lumen. Reduced plastocyanin, whose mid point measured potential is +370mV, is able to transfer one electron to the PS I activated reaction centre. It's generally accepted that the E_m value for the P700/P700$^+$ couple is approximately +500mV whereas the mid point potential of P680/P680$^+$ is estimate to be +1.2V at pH=7. The oxidation of plastocyanin by PS II reaction centre is hence strongly favoured thermodynamically, although it doesn't occur in PS II since P680$^+$ is normally not accessible. In our hypothesis, we speculate that, in iron deprivation, only a small amount of the total PSII is CP43'-conjugated and oxygen-evolving PS II is still abundant in the cell. Active PSII drives the linear electron transfer and reduced plastocyanin is accumulated in the inner water space. If a CP43'-conjugated photosystem is available in the thylakoid membranes, part of the reduced plastocyanin would be oxidised by the accessible P680$^+$ via TyrZ, giving then rise to a cyclic electron flow around the CP43'-conjugated photosystem.

There are experimental evidences in the literature that plastocyanin can act as a donor to PSII, although with a low effivìciency, when the complex is likely to have lost the extrinsic subunits (Arnon and Barber, 1990).

The amount of CP43'-conjugated photosystem that would eventually accumulate in the thylakoid membranes is most likely too small to represent a relevant process in the cell, however, since in iron deprivation there is an imbalance in the activity of the two photosystems, there would be no reason for the cell to suppress by selective pressure a photosystem that works essentially autonomously with production of ATP. Indeed this would help to compensate for a reduction of cyclic electron flow around

PSI due to the relative decrease in the level of this photosystem under iron deficient conditions. It is this rationale which underpins the objective of the work presented here. Namely, is there, under iron limiting conditions, a CP43-conjugated photosystem II like complex which acts as a plastocyanin-plastoquinone oxidoreductase?

1.6 The choice of *Synechocystis* sp PCC 6803 as model organism

In addition to the already mentioned characteristics that make cyanobacteria a favourite model organism for a lot of groups around the world (i.e. the extraordinary similarity of the photosynthetic apparatus in oxyphotobacteria and in higher plants and the possibility of culturing them in strictly controlled conditions). There are other advantages, in particular, *Synechocystis* 6803 presents two important features, found only in a few other cyanobacteria: a naturally occurring genetic transformation system and the ability to grow phototropically in glucose, which is necessary for the propagation of mutant that have one or more important protein deleted or damaged, and thus are incapable of carrying out photosynthesis. This bacterium can integrate foreign DNA into their genomes by homologous recombination, allowing targeted gene replacement. The functional and structural similarity of the two reaction centres in the chloroplast of higher plants and in cyanobacteria, has allowed, in the past, the use of chloroplast genes as hybridization probes to clone the corresponding genes from *Synechocystis 6803*, that encode the homologous proteins. After the determination of the entire genome sequence of *Synechocystis* sp. PCC 6803 in 1996, this model organism has became even more popular, allowing to design *in silico*, with bioinformatic techniques, the genetic manipulations. Using this technique, deletion mutants lacking a specific gene have been created and analyzed for many different genes, giving precious information for the understanding of the biochemistry and the physiology of photosynthesis.

In the work that I present, that is mostly focus on the isolation of PSII from bacteria grown in iron depleted medium, *Synechocystis* has also been preferred to *Synechococcus*, although the latter is a well established source of stable and highly active PSII preparations. *Synechococcus* indeed, even if has been largely used for studies about iron stress, is nevertheless known to produce multiple siderophores (Wilhelm and Trick, 1994) and therefore it's more difficult to induce, in an iron depleted healthy culture, the visible effects of iron starvation on the photosynthetic physiology. Moreover the expression of CP43' protein, whose possible interaction within PSII cores is the object of this investigation, is indeed widely studied in *Synechocystis*, where seems to be highly produced also in response to different signals (Ivanov et al. 2000; Singh and Sherman 2005; Liu et al. 2005; Dühring et al. 2006;).

Chapter 2 – Materials and methods

2.1 Buffers and reagents

All standard solutions buffer and reagents (such as media) were prepared according to previous published protocols (Sambrook et al., 2001) unless specifically stated in the text. Chemicals where purchased from Sigma Chemicals Ltd., BDH Chemicals or Frisons UK Ltd., unless otherwise stated. Nanopure deionized water (NANOpure II-Barnestead) was routinely used for the preparation of solutions.

Culture media was sterilized by autoclaving for at least 45min at 121°C and 103kPa, or for solution that were not thermostable, by filtering through a 0,22μm filter sterilisation unit (Millex GB Millipore).

2.2 Spectrophotometric measurements

All the absorption measurements were recorded at room temperature using a Shimadzu UV-1601 UV-Visible spectrophotometer (Shimadzu Europea).

2.3 Culturing oxyphotobacteria

2.3.1 *Synechocystis PCC 6803 strains*

Cells of a glucose-tolerant strain, dwt, (Williams, 1988) of *Synechocystis* PCC 6803 were used. These cells can be grown photoheterotrophically using cool-white fluorescent lamps and supplementing with glucose, to obtain in a relatively short time a saturate healthy culture. This strain was a gift to this laboratory from Dr. J.K Williams (DuPont, Delaware, USA).

HT-3A strain is a kanamycin resistant, glucose tolerant strain which has been modified to contain a 6x histidine tag on the C-terminus of CP47 (Bricker et al., 1998). The introduction of a His-tag to an integral protein of the core complex of PS II has been used by different groups so far to set up a purification system by affinity chromatography in order to obtain highly active PS II particles. The strain was kindly provided by Dr. T. Bricker, Louisiana University, USA.

Another CP47His-tagged mutant, the ΔCP43-CP47His tagged, was also used in this study. ΔCP43-CP47His tagged is a kanamycin,

chloramphenicol, erithromycin resistant strain in which an his tag has been introduced on the C-terminus of CP47 and the CP43 gene has been deleted. This mutant strain was a kind gift of Mr R. De Vries, Imperial College, UK.

2.3.2 *Propagation of wt glucose tolerant strain, HT-3A and ΔCP43 - CP47His tagged*

Cells were grown in liquid BG11-medium (Allen 1968) supplemented with 5mM N-tris[hydroxymethyl]methyl-2-aminoethanesulfonic acid (TES) pH=8.2 and 5mM glucose. Liquid cultures were grown on a magnetic stirrer with air bubbling as the source of aeration at a light intensity of about 30-50 $\mu E*m^{-2}*s^{-1}$ in a temperature-controlled room (29 °C – 33 °C). The air was prehumidified by bubbling through a solution of 1% copper sulphate and then sterilized by passage through a filter (0,2μm PTFE, Pall Corporation). Routine maintenance of the strains was done on BG11 plates (BG11 with 0.3 % sodium thiosulphate, 10 mM TES pH=8.2 and 1.5 % agar, added separately after autoclaving and cooling to approximately 55°C) in the presence of 5mM glucose. For the maintenance of mutant strains following antibiotics were added to the media at the indicated levels: kanamycin (KAN; 50 μg/ml), chloramphenicol (CAM; 10 or 30 μg/ml) and erotromycin (ERT; 50 μg/ml). The stock plates were restreaked every 2-4 weeks. Prior to inoculation of a liquid culture, cells were restreaked onto fresh BG11 plates containing 5mM glucose and the appropriate antibiotic and used within one week.

2.3.3 *Large scale culturing in standard and iron depleted conditions*

For isolation of PSII particles from cells grown in standard condition a BG11 medium that normally contained ~20μM iron and 5mM glucose (plus eventually the appropriate antibiotics) was used. A few colonies from the fresh plates were used to inoculate 100ml of liquid starter cultures and grown in 250ml sterile flasks (Polystyrene, PD Falkon) until they reached an OD_{750} of 0.9-1.2, that identifies the logarithmic phase of grow of the culture. The initial preculture was then poured in 1000ml of sterile media and grown in vigorous air bubbling again until it reached the exponential phase. 500ml of cells were then transferred to a 20l carboy containing 16-18l of medium, and grown until their optical densities reached 1-1.5 at 750nm, to obtain a saturate culture. This took typically 2-3 days for all the strains used.

For isolation of photosynthetic complexes under iron stress condition, cells were deprived of iron by progressive dilution in BG11-Fe (always added of glucose) to a final concentration of iron in the culture of ~0.4µM. 500ml of the standard +Fe culture were washed in 2000ml of BG11-Fe and grown until the logarithmic phase prior to be inoculated in the 20l carboy. The shift to the blue of the main red peak of chlorophyll was detected and typically found to be at 678-676nm after the first dilution. 2l of iron depleted cells were then transferred into 18l of BG11-Fe and grown for three days to get a final OD_{750} between 0.9-1.3 and the main red peak of chlorophyll at 673nm.

2.3.4 *Estimation of cell concentration of liquid Synechocystis PCC 6803 cultures*

Growth was monitored by spectrophotometric measurement of the optical density at 750 nm (OD_{750}). An OD_{750} of 0,25 corresponds to approximately 10^8 cells*ml^{-1}.

2.4 Growth curves

Cells from a 100ml starting preculture in standard BG11 plus 5mM glucose and the appropriate antibiotics, were diluted in fresh media (either iron containing or not) to a density of ~10^6 cells/ml (OD_{750}=0.0025). The diluted cultures were divided in a suitable number of sterile rack plates for cell culture (VDX plate, Hampton Research) to test different grow conditions. Each rack plate contains 24 wells and was typically used to perform spectrophotometric analysis of four independent samples each day for six days. 0.7 ml of culture was poured in the wells in order to live enough free space for an appropriate aeration; wells were sealed to prevent evaporation during the six days and rack plates were left in the culture room in gentle agitation under temperature and light controlled conditions. Every 12 hours spectral measurements were performed to detect the optical density at 750nm; the position of the main red peak of chlorophyll and the chlorophyll concentration in the cells. Prior to perform the measurements cultures were diluted so that the absorbance at 680nm was kept in the linear range of 0.2-1.0 absorbance unit.

2.5 Preparation of photosynthetic complexes from *Synechocystis* thylakoid membranes

2.5.1 *Preparation of thylakoid membranes*

Cells, grown in a 20L carboy for 4 days to an OD_{750} of 1.4-1.5, were concentrated to 3L using a cell concentrator (Millipore) and then pelleted by centrifugation at 4°C for 15 min at 9000 rpm in a Sorvall GSA rotor. The pellets were washed once with buffer A [50 mM MES-NaOH, pH 6.0, 1.2M betaine monohydrate , 10% glycerol (w/v), 5 mM $CaCl_2$, and 5 mM $MgCl_2$, 1 mM phenylmethanesulfonyl fluoride, 1 mM benzamidine, 1 mM aminocaproic acid] and pelleted again (9000 rpm, Sorvall GSA rotor, 20 min 4°C). The cells were resuspended in the same buffer and adjusted to a final volume of 50 ml. The cells were added to a prechilled Bead-Beater chamber (88 ml) (Bio-spec Products). The chamber was then filled with prechilled glass beads (Sigma Aldrich acid washed, 0.1mm), and the outside jacket was filled with ice. Cells were broken in darkness using 12 pulses of 15 s each, with 5-min cooling intervals. The homogenate was separated from the beads by decantation, and the beads were washed 4-5 times using a total of about 250 ml of buffer A. Unbroken cells and residual beads were removed from the membrane suspension by centrifugation for 5 min at 6000 rpm in a Sorvall GSA rotor. The thylakoid membranes were pelleted by centrifugation at 40000 rpm for 30 min in a Beckman 70Ti rotor. The membrane pellets were then washed in buffer B (buffer A plus 15 mM $CaCl_2$) and pelleted again by centrifugation until the supernatant of soluble proteins (mostly phycobillisomes) was clear. The pelleted thylakoid membranes were resuspended in buffer B at a chlorophyll concentration of 1 mg/ml and were extracted immediately.

2.5.2 *Extraction of thylakoid membranes*

A 10% freshly made solution of *n*-dodecyl β-D-maltoside (Biomol) was added dropwise to the 1 mg of Chl/ml suspension of thylakoid membranes to give a final concentration of 1% in detergent. Extraction proceeded in the dark for 10 min at 4°C with gentle stirring. The suspension was then centrifuged at 40000 rpm in a Beckman 70Ti rotor for 30 min at 4°C.

2.5.3 *Isolation of PSII particles by Affinity Chromatography*

The supernatant was decanted and mixed with the same volume of Ni-NTA superflow affinity resin (Quiagen Inc.) that had been equilibrated with column buffer [buffer B plus 0,03% *n*-dodecyl β-D-maltoside] in a Falkon tube. The solubilized material was incubated with the resin for 1h in the dark at 4°C under gentle agitation. The mix was then poured in to a column of suitable volume and was allowed to pack by gravity. The resin was washed with 20 column volumes of column buffer plus 5mM His, using a peristaltic pump with a flux of 8ml per min and PSII particles were eluted the same way in 10 column volumes in elution buffer [50mM His in column buffer]. All stages of the preparation were performed in green dim light and in the cold room, using pre-chilled equipment. The all preparation was carried out in one day and purified PSII was concentrated to 1mg of chl/ml using Vivaspin 15ml 100KDa cut-off, spinning at 2700rpm in Beckman Allegra. Oxygen evolution was measured from the concentrated solution.

2.5.4 *Isolation of complexes in different oligomeric states by continuous density gradient centrifugation*

Continuous sucrose density gradients were prepared dissolving 0.5M sucrose in gradient mix (50mM MES-NaOH, pH=6.0, 0.5M betaine, 20mM $CaCl_2$, 5mM $MgCl_2$ and 0,03% *n*-dodecyl β-D-maltoside). The centrifuge tubes (Kontron 23.38 swing-out rotor tubes, 25.4mm x 89mm) were filled to approximately 85% of their volume and frozen at −80°C. A continuous, linear sucrose gradient formed on thawing the tubes slowly (usually overnight) at 4°C. 0.5-1 ml of samples at the concentration of 1mg chlorophyll ml^{-1} were load onto the gradients and centrifuged for 18h overnight at 25000rpm in SW28 rotor (Beckman) at 4°C.

Samples loaded for density gradient centrifugation were typically PS II particles eluted from the Ni^{2+} column using histidine, after concentration to approximately 1mg of chl/ml ; or the first concentrated fraction of unbound material, eluted by gravity flow while the column was settling. This latter fraction is greatly enriched in PS I.

2.5.5 *Purification of PSII Core Complexes by Anionic-exchange Column Chromatography*

The supernatant of solubilized membrane proteins was loaded onto a DEAE-Toyopearl 65OS column (1.5 **X** 17 cm, a weak anion-exchanger,

Toso Haas) previously equilibrated with 50-100 mL of equilibration buffer (buffer B + 20 mM MgSO$_4$ + 0.03% *n*-dodecyl β-D-maltoside). The column was then washed with equilibration buffer (50-100 ml) at a flow rate of 6-7 ml/min using an HPLC apparatus (Jasco). Once the red wavelength maximum of the absorbance spectrum of the eluant dropped to 674.5 nm, a 50ml linear gradient from 20 to 30 mM MgSO$_4$ in buffer B' [buffer B added of 0.03% *n*-dodecyl β-D-maltoside] was applied to the column. For samples purified from iron stressed cultures, in which the maximum red peak is registered between 672-674 in all the fractions, the gradient was started to correspond with the drop of the first broad elution peak. In the case of +Fe samples, fractions with chlorophyll absorbance maxima between 673.5 and 674 nm were pooled and immediately concentrated to 5-10 ml with Vivaspin 15ml 100KDa cut-off and then diluted in buffer B' to a final ratio of sample/buffer 1/3 or 1/4. In the chase of –Fe samples, 15 fractions of 4 ml each were pooled together and concentrated to 1mg of chl/ml. Concentrated –Fe samples were then loaded onto continuous sucrose gradient and centrifuged for 18h overnight at 25000rpm in SW28 rotor (Beckman) at 4°,C to get rid of the co-purifying CP43'. The gradient mix was 0,5M betaine 0,6M sucrose in buffer B'. The lower band was collected, washed to dilute the sugar and concentrated to a suitable volume for the next chromatographic step.

2.5.6 *Second column step by anionic exchange chromatography*

PSII particles from plus and minus iron samples obtained by either weak anionic exchange or affinity chromatography were applied to a pre-packed UnoQ column, pre-equilibrated for at least half an hour with buffer B' flowing at a rate of 2-4ml/min. A shallow gradient from 0 to 150mM MgSO$_4$ in buffer B' was performed for 50 min at a flow rate of 2ml/min and all the peaks were collected and analysed by visible-UV spectrometry. Fraction with a peak between 673.5 and 674 were concentrated with the same method as before to 1mg of chl/ml and activity of each fraction was measured and oligomeric state was detected by analytic Size Exclusion Chromatography. After these measurements samples were flash-frozen in liquid nitrogen and stored at –80°C.

Preparation of photosynthetic complexes from
Synechocystis PCC 6803 by anionic exchange chromatography

Coltures of Synechocystis wt glucose tolerant strain

grown to an $OD_{750}=1\text{-}1.5$,

either in iron sufficient or iron depleted medium

centrifuge force →

Cells are concentrated by centrifugation and washed in buffer A to remove any residual BG11

Cells are broken by bead-beater in the cold and dark to release their content in solution

centrifuge force →
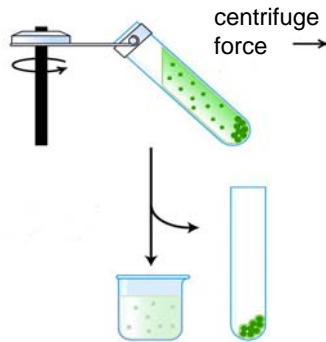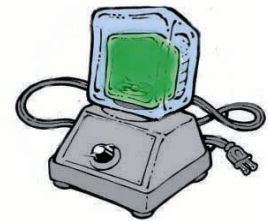
Solubilized membrane proteins are separated passing them through a weak anionic-exchange column by HPLC. The latest fraction, which contains different **aggregates of PSI,** is concentrated and stored at –80°C. Un ulterior fraction peak is collected from –Fe samples, which contains **PSI supercomplex.**

Fractions enriched in PSII are pooled, concentrated and run through a second anionic-exchange column, which cleans the preparation from copurifying proteins and separates monomers from dimers.

Purified PSII particles are then concentrated and used for analysis of the activity by oxygen evolution measurements and of the polypeptide composition by SDS-PAGE and stored at –80°C.

Thylakoid membranes are separated by centrifugation from the soluble protein. Supernatant is largely enriched in **Phycobillisomes.**

Thylakoid membranes are then quickly extracted to release **membrane protein in solution.** Insoluble material is removed by centrifugation.

1 2 3 4 5 6
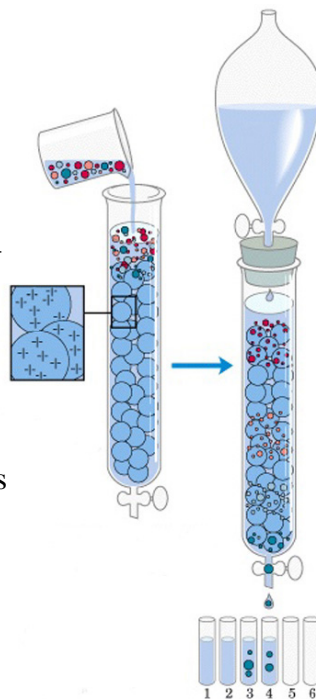
- PSI aggregates, PSI super complex
- PSII
- PSI monomers, small proteins, CP43'
- Carotenoids, CP43', small proteins
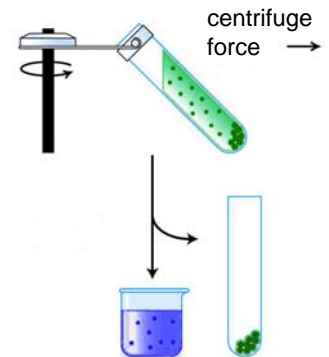
Preparation of photosynthetic complexes from *Synechocystis PCC 6803* by affinity chromatography

**Coltures of Synechocystis wt glucose tolerant strain**

grown to an $OD_{750}=1$-1.5,

either in iron sufficient or iron depleted medium

Centrifuge force →

Cells are concentrated by centrifugation and washed in buffer A to remove any residual BG11

Cells are broken by bead-beater in the cold and dark to release their content in solution

centrifuge force →
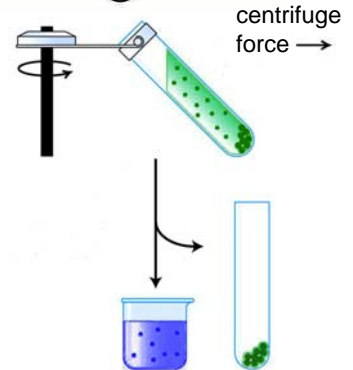
Solubilized membrane proteins are then batched to a Ni^{2+}-sepharose column. While column is settling a highly concentrate fraction of unbound material is collected, largely enriched in **PSI**. **PSII particles** are eluted in 25mM histidine.

PSII particles
histidne
Ni^{2+}-sepharose

Thylakoid membranes are separated by centrifugation from the soluble protein. Supernatant is largely enriched in **Phycobillisomes.**

Thylakoid membranes are then quickly **extracted** to release **membrane protein in solution.** Insoluble material is removed by centrifugation.
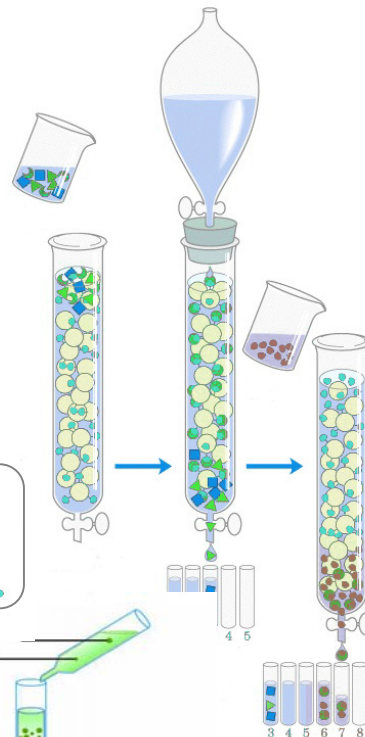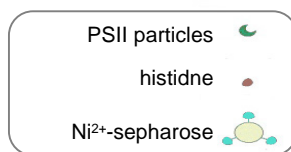
The different bands containing **PSII monomers and dimers** and **PSI trimers, monomers** and eventually **supercomplex** are then concentrated and used for analysis or stored at –80°C..

centrifuge force →
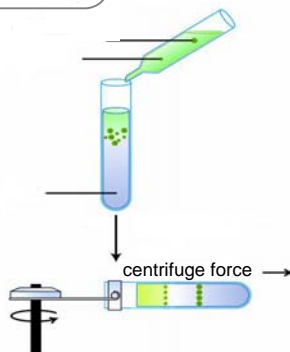
Isolated **PSII** and **PSI** fraction are separately concentrated and loaded on sucrose gradients to separate from each of the protein mixture the typical different oligomeric forms of the photosynthetic complexes

2.6 HPLC size-exclusion chromatography analysis

For HPLC size exclusion analysis a Phenomenex BioSep-SEC-S3000 (600 x 7,8 mm) column was used coupled to an LC-2000*Plus* series liquid chromatography system from Jasco. This column is able to separate a mixture of protein in native condition in a range of molecular weights comprised between 5000 and 700000 Daltons with a linear correlation of 0,977 for the log MW versus K_D plot. The column was equilibrated running through it SEC buffer (20mM MES-NaOH, pH=6.0, 0.5 mannitol, 30mM $CaCl_2$, 10mM $MgCl_2$, and 0,03% *n*-dodecyl β-D-maltoside) for at least half an hour at a flow rate of 1ml/min. Sample were run through the column in the same SEC buffer at a flow rate of 0,5ml/min for 20min for all measurements. Protein retention times were determined by detection of the absorbance at 280nm and 670nm to detect protein and chlorophyll containing fraction respectively. The column was calibrated using preparations of photosynthetic complexes from *T.elongatus.* The molecular weights of this complexes are known and have reported in Zouni et al., 2001 and Jordan et al., 2001. (PSI monomers 356 kDa, PSI trimers 1065kDa, PSII monomers 350 kDa, PSII dimers 700kDa). Identification of the oligomeric state of the isolated photosynthetic complexes was done comparing their elution profile with the retention time of the ones used as standards.
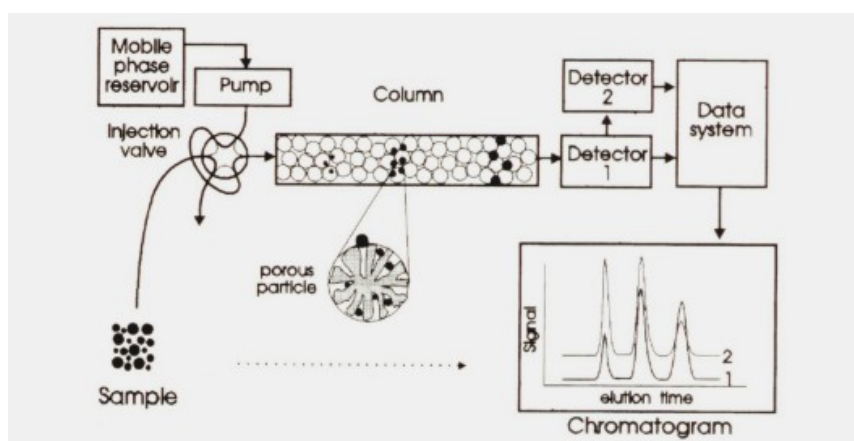
Figure 2.3: Size exclusion chromatography. When a sample is injected into the column, polypeptide are separated according to their hydrodynamic volumes, hence polymer molecules larger than the pores of the packing material cannot enter the pores and are eluted at the interstitial volume. No fraction of the sample can be eluted before the interstitial volume has passed through the column. Small molecules, however, have access to the pores and will therefore elute at the sum of both the interstitial and pore volume.

2.7 Chlorophyll quantification

The chlorophyll a concentration of samples was estimated according to a procedure devised by Lichtenthaler (Lichtenthaler, 1987). 5μl of sample was diluted in 995μl of methanol in an eppendorf tube, vortexed and incubated at room temperature for 1 min. The suspension was then centrifuged at 13000rpm in a microfuge (MSE MicroCentaur) for 5 min to remove insoluble material. The supernatant was used to measure the chlorophyll a concentration according to the equation:

$$(OD_{665,5} - OD_{750}) \times 12,6 \times \text{dilution} = [\text{chl a}] \, \mu g/ml$$

2.8 Polyacrylamide Gel Electrophoresis (PAGE)

2.8.1 D sodium dodecyl sulphate gel electrophoresis (SDS PAGE)

SDS-polyacrylamide gel electrophoresis method was used for analysing protein mixtures qualitatively. Sample to be run were first solubilized diluting 1:1 in buffer containing β-mercaptoethanol and SDS (18.7 mM Tris-HCl pH 6.8, 9% (w/v) SDS, 30% (v/v) glycerol, 15% (v/v) β-mercaptoethanol and bromophenol blue concentrated enough to get a dark blue solution) and incubated in the dark for 60 min at room temperature. The sample were then centrifuged in a microfuge at 14,000xg for 5 min to eliminate unsolubilized components before being loaded into the gel.

Proteins were resolved in 0.75 mm thick, 12,5% or 15% continuous polyacrylamide, 6 M Urea gels (Tables 2.1 and 2.2). Polyacrylamide concentration of the separation gel was dependent for which region the resolution was supposed to be optimised. As a guideline 12.5 % gels were used when the focus was on the 50-30 kDa region and 15 % gel were used to assay PS II preparation for the presence of low molecular weight subunits which was of particular interest. The separating gel was used, with 2.6% C and 40% T, in which the percentage of C and T are defined as:

$$\%T = [(\text{acrylamidev(g)} + \text{bisacrilamide (g)}) / V(ml)] * 100$$
$$\% C = [\text{bisacrilamide (g)}/(\text{acrylamidev(g)} + \text{bisacrilamide (g)})]*100$$

To obtain focused bands it proved crucial to adjust the pH of the separation gel solution to 8.9 just before adding the TEMED and APS. The resolving gel was poured between two clean 12x14 glass plates and gently overlaid with water-saturated isopropanol. Once the gel had polymerised the top was washed with distilled water and the isopropanol replaced with a 5% T stacking gel pH 6.8 (Tables 2.1 and 2.2) to concentrate the negative charged protein-SDS complexes in the sample into a thin band before entering the main separating gel. The SDS-PAGE gels were run in a vertical electrophoresis apparatus for at least two hours using Tris / Glycine running buffer (25 mM Tris; 190 mM Glycine; 0.1 % (w/v) SDS; pH=8.3) at a constant power of 100V.

Table 2.1 Stock solutions for SDS-PAGE

Solutions	Tris (M)	Glycine (M)	pH	SDS % (w/v)	Acrylamide % (w/v)	Bisacrylamide % (w/v)
Separating Gel solution	1	-	8,9	-	-	-
Stacking Gel solution	1	-	6.8	-	-	-
40% T, 2.6% C	-	-	-	-	37,5	1
Running Buffer	0.025	0,19	8.3	0,1	-	-

Table 2.2 Composition of spacer and stacking gels used in SDS-PAGE (for 4 minigels)

Stock solutions	Separating Gel (12,5% T)	Separating Gel (15% T)	Stacking Gel (5% T)
Separating Gel solution	5 ml	5 ml	-
Stacking Gel solution	-	-	0,6 ml
SDS 10 %	0,3 ml	0,3 ml	0,1 ml
Poly acry lamide (30% T, 2.6% C)	7,8 ml	9,375 ml	0.625 ml
Urea (6M final conc.)	10.8 g	10.8 g	-
Distilled Water	to 25 ml	to 25 ml	To 5 ml
Ammonium persulphate 10%	150 µl	150 µl	50 µl
TEMED	25 µl	25 µl	5 µl

After electrophoresis the protein bands were first fixed for 20 min in a 50% (v/v) methanol 25% (v/v) acetic acid solution and then stained. To stain the protein the gel was first incubated in 0.1% (w/v) Coomassie Brilliant Blue (0,05% R-250, 0,05%) in 25% (v/v) isopropanol and 10% (v/v) acetic acid solution under continuous agitation for several hours (usually over night) and then washed using the same solution without Coomassie. Approximate molecular masses of polypeptides were estimated by

correlating the position on the gel of the constituents of the molecular marker solution (BioRad prestained SDS-PAGE standards, low range).

2.9 Western-blotting and immunoblot assay

Following electrophoresis, the gels were washed in transfer buffer (3mM Na_2CO_3, 10mM $NaHCO_3$, 20% (v/v) methanol) and then transferred to 0.2 µm cellulose membranes (Sartorius AG, Germany) (Dunn, 1986) using a Trans-Blot Cell system (Bio-Rad) and setting the power at 50V for 90 min. After transfer the gel was discarded and the membrane blocked against non specific binding of antibodies with TBS (50 mM Tris-HCl pH 7.4, 150 mM NaCl and 0.1% Tween 20) added with 10% semi skimmed milk powder (Marvel) for at least 20 min. Primary antibody, raised in rabbit, was then added to the membrane, at a suitable concentration, in 10-12 ml TBS either for an overnight incubation, at 4-6°C, or 2h at room temperature. The membrane filter was washed six times (5 min each) in TBS before incubation with secondary antibody (anti-rabbit IgG, horseradish peroxidase conjugated, Amersham), at a concentration of 1:3000 in 25 ml TBS. Immunodetection was performed using the ECL chemiluminescence method (Amersham Pharmacia) following the manifacturers instructions.

2.10 Preparation of sample for N-terminal sequencing

Polypeptides separated following a standard procedure for Laemmli SDS-PAGE (as described above) were transferred to a PVDF membrane (Sequi-Blot 0.2 micron PVDF, Bio-Rad). The highly hydrophobic PVDF membrane was pre wetted in 100% methanol for a few seconds, then equilibrated in transfer buffer (10mM MES, pH=6, 20% methanol) for 2-3 min. After the end of the run, the gel was briefly rinsed in mQ water to remove the residual glycine and also equilibrated in transfer buffer. The transfer sandwich was set up and the transfer of protein to the membrane was carried out for 60 minutes at a constant voltage of 50V using the Trans-blot Cell system from Bio-Rad. The PVDF membrane was then washed in mQ water and stained with 0,1% Coomassie Blue R-250 in 40% methanol, 1% acetic acid in gentle agitation for 5min, then quickly destained with a few washes in 50% methanol in mQ water until the background was light blue. PVDF blot was placed on a clean glass gel plate for air dry. When completely dried the band of interest was excised using a scalpel, carefully washed in ethanol, and placed in a microfuge

tube. Band was then washed for 5 times in mQ water, air dried at room temperature and stored at –20°C.

2.11 Oxygen evolution measurements

The activity of photosystem II was assessed by means of oxygen evolution. Samples with a chlorophyll a concentration of 10 μg / ml were assessed for their oxygen evolution rate by use of an oxygen electrode (DW2/2 unit, Hansatech instruments Ltd., Norfolk). Measurements required the use of 2,6 dichlorobenzoquinone (DCBQ, Eastman Kodak Co., New York; final [2 mM] in EtOH), a photosystem II Q_A electron acceptor and $K_3Fe(CN)_6$ (final [1 mM]), a DCBQ oxidising agent. Both reagents were mixed with the sample to a total volume of 1 ml in BG11 for detection in whole cells, in their respective resuspension buffer while assaying broken cells or thylakoids or in oxygen evolution buffer (50mM MES-NaOH, pH=6.5, 20mM $MgCl_2$, 20mMCaCl$_2$, 1mM $NaHCO_3$, 1.2M betaine, 10% (v/v) glycerol) for purified PS II particles and kept in the dark until oxygen evolution had stabilized. After stabilization actinic light illumination at 5000 $\mu E*m^{-2}*s^{-1}$ was applied to the samples and oxygen evolution was recorded. Either red and white light were used. Oxygen evolution rates were calculated in terms of μmol oxygen*mg chl a$^{-1}*h^{-1}$.

Chapter 3 – Results and Discussion

3.1 Growth of cultures of iron-stressed *Synechocystis PCC 6803*, strains HT3A and ΔCP43-CP47his tagged

In order to investigate the possible association of IsiA with the photosynthetic reaction centres, iron stressed cultures of the HT3A and ΔCP43-CP47His tagged strains of *Synechocystis* were grown alongside a non stressed culture of the same respective strains as a control. A few assays have been done in order to delineate the general phenotype of the two different strains in response to iron deprivation.

Figure 3.1 shows growth curves of cultures of *Synechocystis* grown in different iron concentration (section 2.3 and 2.4). The absorption of cell cultures was measured at 750 nm, a wavelength at which there is littele or no absorption by the pigments in the cell. Therefore the apparent absorption at this wavelength is therefore due to scattering of light caused by the cells. As the culture grows the amount of scatter increases.


Growth of Synechocystis 6803 wt and deltaCP43 grown in media containing different iron concentration
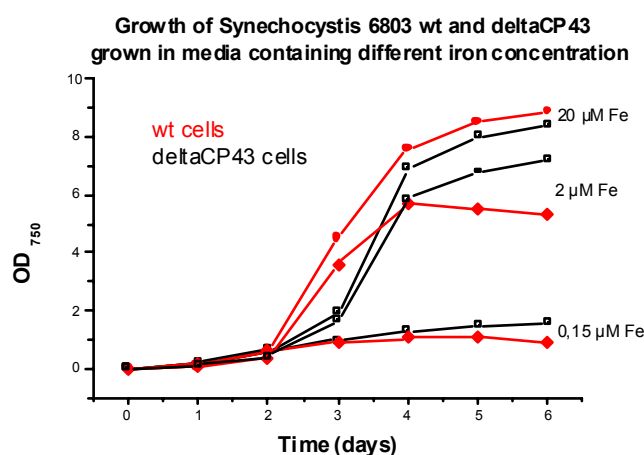
Figure 3.1 Synechocystis PCC 6803 growth curves. Plots of the OD_{750} at room temperature against time for cultures of Synechocystis grown in the presence of 5mM glucose and of different iron concentration in the media.

Figure 3.1 shows that cultures of the mutant cells in which the internal antenna protein of PSII, CP43, has been deleted, grows in the presence of iron and glucose with good growth rates, although they were slightly slower and have smaller maximum density than HT3A cultures grown in standard iron concentration. As the concentration of iron in the media was reduced of 10 times (labelled in the graph as 2µM Fe) and 130 times (lower plot, 0.15µM Fe) the HT3A curves show a clear drop of the maximum density (steady phase) and an anticipate beginning of the decay phase, in which the cultures die. The mutant cultures showed an analogous response to iron deficiency: slower growth and decreased maximum density in comparison to the control culture of the same strain

growth in iron sufficient medium. Surprisingly the detrimental effect of low iron in the ΔCP43-CP47His tagged mutant was slightly less drastic than the that registered for the HT3A cultures. It has been shown that IsiA sets up an extra antenna for PSI when cyanobacteria are deprived of iron (Bibby et al., 2001). We speculated that the CP43-less mutant, who is completely dependent on PSI for photosynthesis, might have benefited from the increased size of the antenna that serves the PSI complex in iron-stress condition, compared to the HT3A.

Chlorophyll concentration in the cells during the different stage of their growth has also been monitored, for cultures of both the two strains grown in 20µM or 0,15µM Fe (Figure 3.2). Consistently with pervious finding (reviewed by Straus, 1994) iron starvation produces a pronounced decrease of the chlorophyll content in the cell, probably by effecting the biosynthesis of chlorophylls as well as that of phycobilins. Here again the effect on the CP43 deletion mutant seems to be less sever.
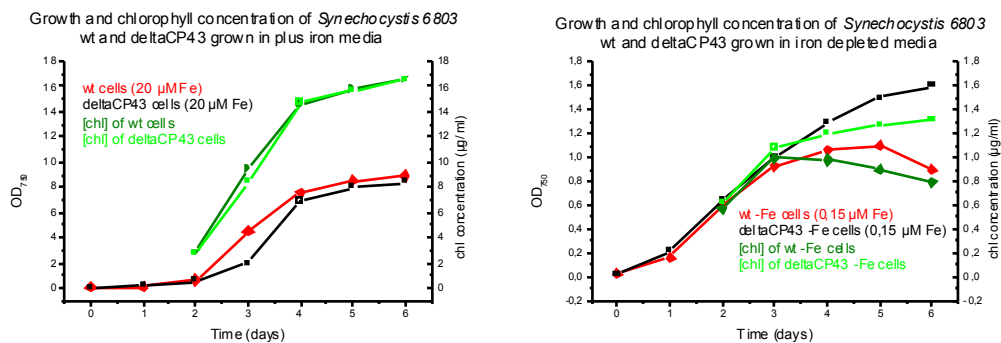

Figure 3.2 Synechocystis PCC 6803 growth curves and cellular chlorophyll concentration. Plots of the OD_{750} at room temperature and chlorophyll concentration in the cells against time for cultures of Synechocystis grown in 5mM glucose in the presence of iron (left) or in iron depleted medium (right). HT3A strain and ΔCP43-CP47His tagged strain are compared.

An analogous comparison of the phenotype in response to iron deprivation has been made between the His tagged strain HT3A and the wt glucose tolerant strain (data not shown). No significant differences have been detected, although in the large scale culturing HT3A cells showed a slightly more pronounced sensitivity to high light, especially when grown in iron depleted media.

In order to confirm that the cells grown in the absence of iron demonstrated the well characterized iron-stress response (Öquist, 1973), the spectral proprieties of the cultures were monitored. The room temperature absorption spectrum of cells grown with an iron concentration below 0,5µM for at least 2 days has a maximal chlorophyll *a* peak that is shifted 10nm to the blue from that of cells grown with iron (Figure 3.3). The result is the same for all the different strains used. This difference in the

spectral characteristics are indicative of the presence in the iron stressed cells of the iron-stress-induced protein IsiA.
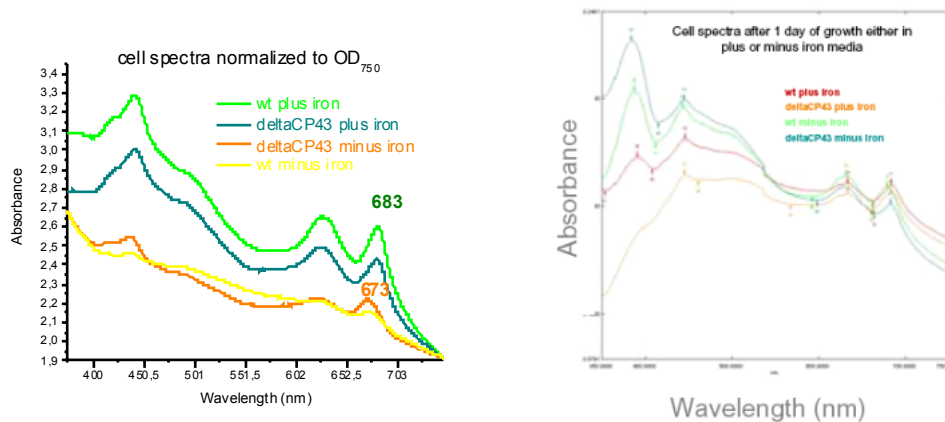

Figure 3.3 Spectral analyses of cells of Synechocystis PCC 6803 grown in the presence and absence of iron. The room temperature optical absorption spectra of cells grown in the absence of iron have a blue shifted maximal chlorophyll a absorption peak. The shift of the peak reaches it's maximum of 10nm in 2 days (plot on the left). An early response (after 1 day) in the region between 300 and 400nm is also registered in our samples (graph on the right). Cells grown in suboptimal concentration of iron have a peak of absorbance in that region. None of the pigment found in cyanobacteria absorb in that region, while heams do. The presence of this peak maybe consistent with the accumulation of an intermedium of the biosynthesis of chlorophylls and phycobilins.

The oxygen evolving capacity of the cells was also determined. A plot of the oxygen evolution in response to different intensities of white light has been done for HT3A cells grown in iron containing medium. A region in which the response could be well approximate to a linear plot has been chosen and those light intensities have been used to detect and compare the oxygen evolving activity of HT3A cells grown in plus and minus iron medium. Results are shown in figure 3.4. The values, has indicated in the graph, have been normalized to the chlorophyll concentration. The absolute value of oxygen evolution registered for minus iron cells is close to 50% the absolute value for the corresponding plus iron samples at the same light intensity, while the slope of the two plots is the same with good approximation (0.21 and 0.20 respectively). A consistent amount of the measured chlorophyll is bound in the minus iron cells to IsiA, therefore, by normalizing to an equal amount of chlorophyll in the samples used for the assay corresponds a smaller amount of PSII in the iron deficient cells. Since the light intensity used is far below the saturating light but is enough to activate the majority of the reaction centres in the sample, the slope should be proportional to the activity of those reaction centres in response to a more intense light. Since the response registered is substantially equal in the two samples, no difference in the oxygen evolving capacity has been evidenced between plus and minus iron cells at this level of sensitivity.

No oxygen evolving activity was registered from the CP43 deletion mutant has expected.
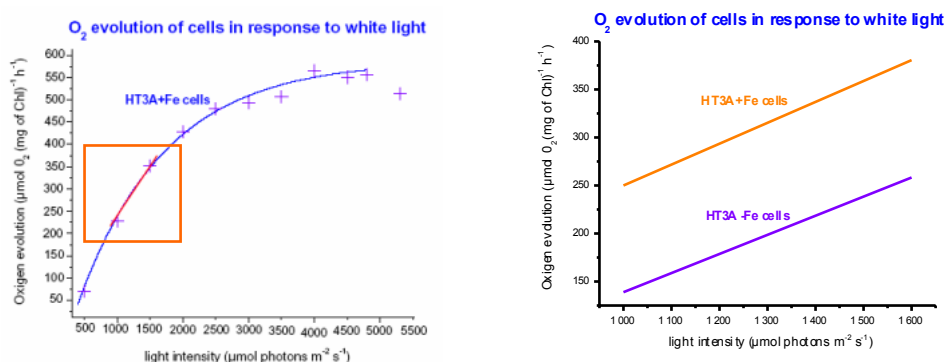

Figure 3.4 Oxygen evolution of *Synechocystis* cells grown in iron containing or iron depleted medium in response to white light. Plot of oxygen evolution (μmol O_2 per mg of chl *a* per hour) against light intensity (μmol photons per m^2 per s) from HT3A plus iron cells, on the left. Comparison of the oxygen evolving activity of HT3A cells grown in the presence or absence of iron in response to light intensity comprised between 1000-1600 μmol photons per m^2 per s, on the right.

3.2 Large scale culturing of *Synechocystis* PCC 6803 strains for protein purification

Cultures of *Synechocystis* PCC 6803 HT3A strain have been grown in 18L carboys for protein purification.

Initially cells were grown in two parallel 18L cultures, one in medium that contained iron in standard concentration and one in BG11 –Fe, inoculated from the same preculture of 2L grown in +Fe BG11. Before starting the purification procedure a spectrum of the cells was taken and the total amount of chlorophyll and the oxygen evolving capacity were measured. These growth condition confirmed the results anticipated by the monitored small scale –Fe cultures (described in the previous paragraph): growth was relatively slow and the maximum OD_{750} reached in the steady phase was far below the one registered from the parallel culture grown in standard iron concentration. Concentration of chlorophyll was also poor as well as the oxygen evolution activity. A summary of these information is given in Table 3.1 and in figure 3.5.

In order to improve the quality of the starting material for our preparations a new strategy was set up to obtain healthier iron-stressed cultures. Procedure is described in section 2.3.3.

General characteristics of the large scale cultures of Synechocystis used for protein purification			
SAMPLES	peak [a]	total chlorofill [b]	oxygen evolution [c]
cells grown in 20µM Fe (18 L)	682-683	30-50	500-600
cells from a 900ml starting culture inoculated directly in iron depleted medium to a final concentration of iron in BG11 of 1µM (18L)	675-676	15-25	250-300
cells grown in a final concentration of 0,4 µM Fe by progressive dilution (as described in materials and methods)	673	30-50	400-550
[a] Maximum in the red region of the spectrum (nm); [b] Milligrams of chlorophyll; [c] Micromoles of O_2 per milligram of chlorophyll per hour			

Table 3.1 Main characteristics of the cultures grown for protein purification. The maximum peak of absorbance in the red region of the spectrum was detected to confirm the expression of IsiA in the iron-stressed cultures prior to purification of the photosynthetic complexes. The total chlorophyll content and the oxygen evolving activity of the starting material was also measured. Cells depleted of iron by progressive dilution in –Fe medium proved to be healthy and to over-express the IsiA protein.


Spectra of cells cultured in large scale for protein purification
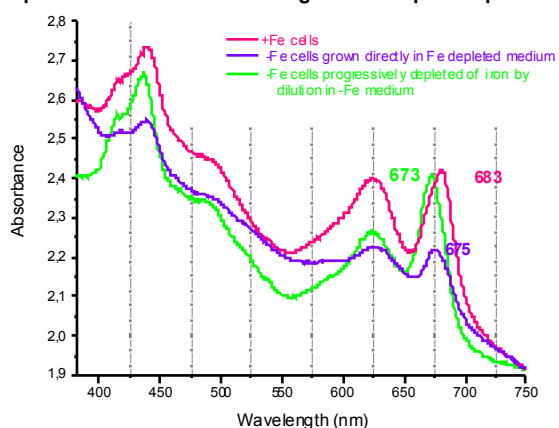
Figure 3.5 Spectra of the cells used for protein purification. Spectra have been normalised to the same OD$_{750}$. As evident form the graph, cells deprived of iron by progressive dilution accumulate a comparable amount of chlorophyll in the cells in respect to the plus iron cultures but show a remarkable decrease in the concentration of phycobilisomes (region of the spectrum between 600 and 650nm). The maximum of the red peak is shifted toward the blue of 10nm in this iron-stressed cultures. Cells inoculated directly in BG11-Fe show on the contrary a lower amount of chlorophyll per cell and a remarkable increase of the signal from carotenoids (region in the spectrum between 500 and 600nm). The maximum of the red peak was also found around 675nm, indicating that IsiA was expressed, but not as much as in the "progressively stressed" cultures.

The results summarised in Table 3.1 and Figure 3.5 indicate that the cells progressively diluted in iron depleted medium until a final concentration of Fe in BG11 of 0,4µM have chlorophyll concentration comparable to that of

the correspondent cells grown in iron containing media and similar rates of oxygen evolution. The registered values are also comparable to previously published chlorophyll contain and rates of oxygen evolution (Tang and Diner, 1994), indicating that both the cultures are photosynthetically active and healthy. Figure 3.5 also indicates that *isiA* gene is highly expressed in the cells, as evident from the shift of 10nm toward the blue of the red peak. Therefore these culturing condition were subsequently used for the purification of the photosynthetic membrane complexes and the study of the possible association of IsiA with PSII.

The same condition of growth that proved to be successfully for the HT3A cells have been subsequently used to grow the ΔCP43-CP47His tagged and dwt glucose tolerant strains.

3.3 Preparation of photosynthetic complexes from *Synechocystis* PCC 6803

3.3.1 Setting up of a first purification protocol for HT3A cells and analysis of the quality of the preparations

The first preparations of photosynthetic complexes were carried on in parallel from cells grown in plus iron media and cells inoculated directly in BG11 –Fe (as described in the previous paragraph). Cells were concentrated in buffer containing 20% glycerol and broken in the dark using a bead beater (30 seconds breakage plus 2 minutes cooling for 10-12 times). Thylakoids were isolated by centrifugation and washed from the soluble proteins. After the extraction, using the mild detergent dodecyl maltoside as described in section 2.5.2, the solubilized material was batch to a Ni^{2+} column. Elutant, collected while the column was setting by gravity flow, was loaded directly onto sucrose gradients to isolate PSI aggregates (monomers and trimers of PSI form +Fe; PSI-CP43' Supercomplex from –Fe). The column was washed until the elutant was clear and PSII particles were eluted in 200mM Histidine.

Results obtained from this preparation are summarised in Table 3.2. Yield is expressed in terms of the total chlorophyll contained in each of the samples. Oxygen evolution activity of each fraction was also recorded.

The fraction of unbound material loaded on to sucrose gradient resulted to be enriched in PSI aggregates as expected. Two bands were found in the plus iron samples. Analytic size exclusion chromatography confirmed that the elution time of the two samples was compatible with the characteristic ones of PSI monomers and PSI trimers (Figure 3.6).

Four bands were found in the sucrose gradient loaded with the minus iron elutant. The lowest and heaviest band was identify as PSI-CP43' Supercomplex by analytic size exclusion chromatography (Figure 3.7).

	SAMPLES	Purification of membrane complexes from Synechocystis 6803 **+Fe**			Purification of membrane complexes from Synechocystis 6803 **-Fe**		
		total chlorofill [a]	oxygen evolution [b]	yeld [c]	total chlorofill [a]	oxygen evolution [b]	yeld [c]
isolation and extraction of thylakoid membranes	harvested cells (18L)	30-50	500-600	100	15-25	250-300	100
	cellular homogenate	20-30	150-200	62	15-20	100-150	87
	thylakoid membranes	20-25	0	56	8-15	0	57
	solubilised thylakoids	10-15	0	31	5-10	0	37
Ni^{2+} column	eluant unbound	5-7	0	15	4-7	0	27
	eluted PS II fraction	0,15-0,18	0	0,4	0,08-0,1	0	0,4
bands collected from sucrose density gradients	PSI trimer/ PSItr-CP43' sc	2-2,5	0	7	sc 3-5	0	20
	PSI monomer	2,5-3	0	5,5	//	//	//
	PSII dimer	0,07-0,09	0	0,2	0,004-0,005	0	0,2
	PSII monomer	0,07-0,09	0	0,2	0,004-0,005	0	0,2

[a] Milligrams of chlorophyll; [b] Micromoles of O_2 per milligram of chlorophyll per hour; [c] Percent of chlorophyll

Table 3.2 Yield and oxygen evolution activity of all the fractions collected during the purifcation of Photosynthetic complexes from *Synechocystis* PCC 6803 HT3A cells, grown in the presents of iron and in iron depleted media.
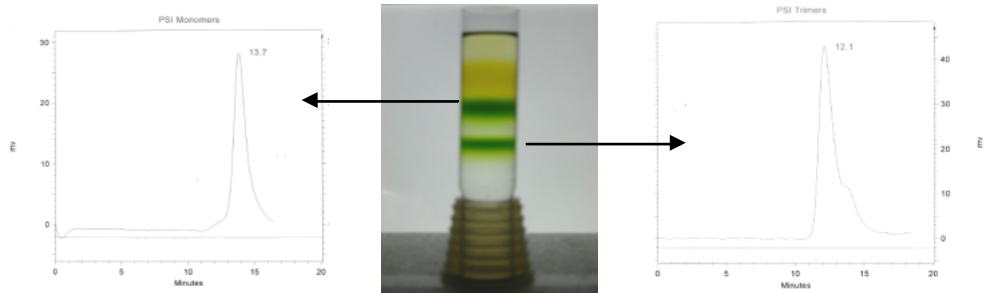
Figure 3.6 Isolation of PSI monomers and trimers from cells grown in media containig iron. Two well separated chlorophyll containing fractions were harvested from the sucrose gradients after the overnight run (section 2.5.4). Bands were analyzed by size exclusion chromatography. The first band contains PSI monomers, while the lower band contains PSI trimers. In the graph obtained from the PSI Trimer fraction a second peak is evident with a retention time comprised between 13.5 and 14min (possibly PSI monomers).
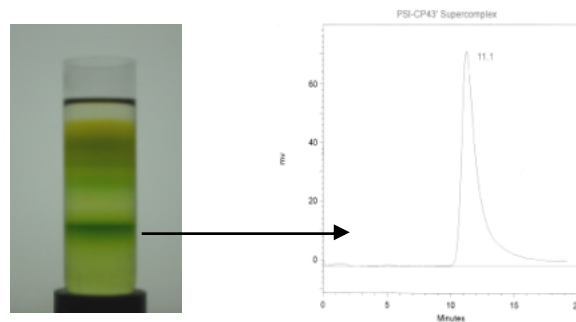

Figure 3.7 Isolation of PSI-CP43' Supercomplex from iron-stressed cells. Four bands were typically separated from the minus iron unbound material. The first two, had a peak at 670 in the red region of the absorption spectra and were found to a be mixture of proteins, largely enriched in free CP43'. The third band was identified by size exclusion chromatography as PSI monomers and the absorption spectra evidenced the presence of copurifying CP43' in this fraction (the characteristic red peak registered for PSI at 679-678nm was shifted to the blue of 5-6nm). The heaviest band was finally identified as PSI-CP43' Supercomplex and analytic size exclusion chromatography is shown in this picture.
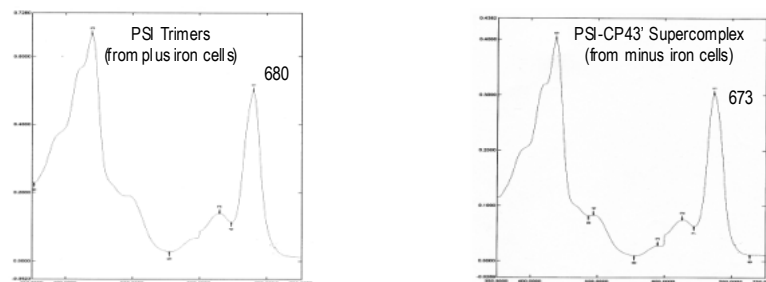
**Figure 3.8 Spectra of the isolated PSI Trimers and PSI-CP43' Supercomplex.** The Supercomplexes consists of PSI Trimers plus an extra antenna ring of 18 subunits of CP43'. The presents of this antenna determines a shift toward the blue of the red peak.

The yield of Photosystem II, which is the membrane complex we were more interested in purifying, to study its possible interaction with IsiA, was

very low and oxygen evolution activity was lost after the cell breakage step. The eluted PSII fractions from plus and minus iron preparations were analysed by size exclusion chromatography and SDS-PAGE, to check for the presence of a PSII population with unusual characteristics in the –Fe samples. Results are shown in Figures 3.9, 3.10 and 3.11. No obvious difference were detected between the plus and minus iron PSII.
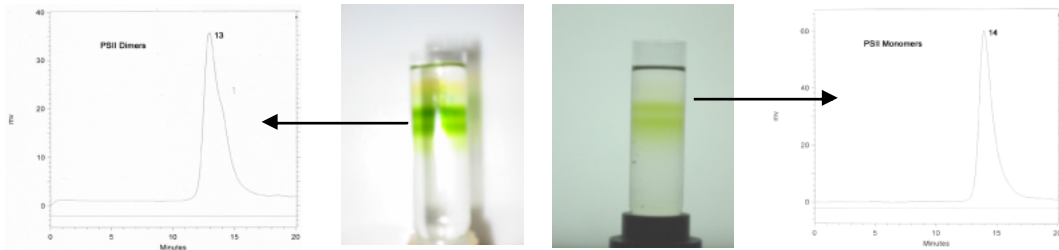

Figure 3.9 Sucrose gradients of the PSII fractions eluted in 200mM His from plus and minus iron preparations. In both plus and minus iron preparations two chlorophyll containing bands, that migrate in the gradient at the same height in the two parallel experiments, were found. Size exclusion chromatography identified the bands as PSII monomers and dimers (respectively the lighter and the heaviest band) in both plus and minus iron gradients without distinction. The results of this first purification don't suggest any evidence of the presence of a special PSII in –Fe samples.
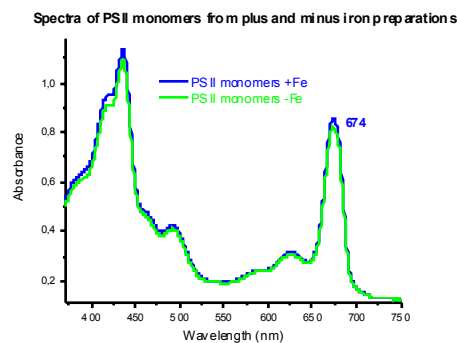

Figure 3.10 Spectra of PSII monomers from plus and minus iron preparations. Red peak is registered in both the spectra at 674nm indicating that there isn't a relevant PSI contamination in the samples. The two spectra, normalized to the same OD_{750} don't show any significant difference. This confirms again that form this first purification no evidence of the presence of a different form of PSII in –Fe samples could be deduced.

SDS-PAGE analysis of the isolated membrane complexes was performed (Figure 3.11). Samples of PSI aggregates were found to contain a number of bands of copurifying proteins, nevertheless PSI-CP43' Supercomplex lane contained an additional band above the 28kDa molecular weight marker which was not presence in the parallel plus iron preparations. Migration of this band in the gel is compatible with what expected for CP43'. The presents of other free proteins in the preparations was not detected in the size exclusion chromatography analysis since the dimension of the pores of the stationary phase and the procedure used were such to give the best resolution for big complexes, whose weight is in the range between 300 and 1000kDa.

More warring was that the PSII samples were degraded (as evident form the smearing in the PSII lanes and the absence of high molecular weight proteins). PSII fractions analysed by immunoblot were found to contain a larger amount of FtsH than the solubilized thylakoids. FtsH is a protease specific for PSII involved in the cycle of repair of photodamaged Photosystem II complexes. As far as we know even other proteases could copurify, as well as other proteins that either unspecifically bind the Ni^{2+} resin or interact with PSII.
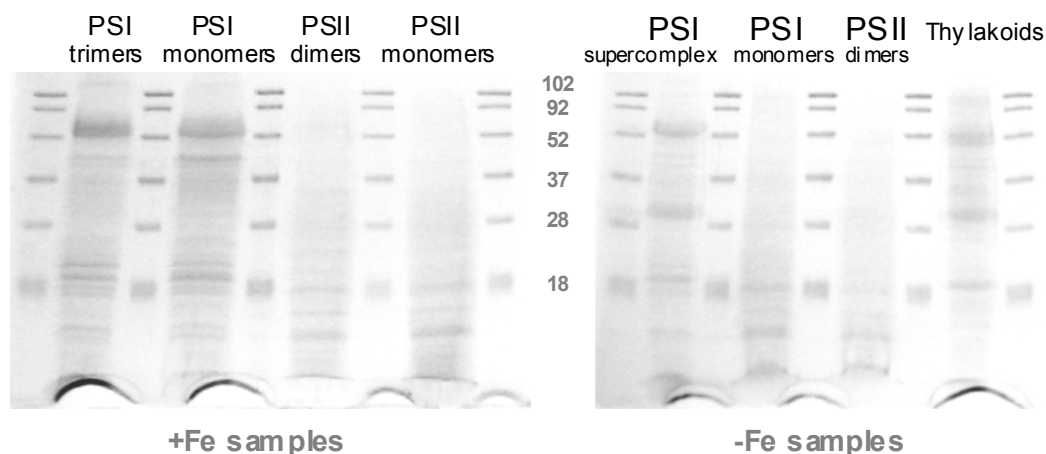
Figure 3.11 SDS-PAGE analysis of the isolated membrane complexes from plus and minus iron cells. In the lanes in which PSI samples have been loaded the heavy band of PsaA-PsaB aggregates is visible on top and a number of aspecific bands of copurifying proteins is also present. An additional band just above the 28kDa marker is found only in the iron-stressed samples (PSI-CP43' Supercomplex and thylakoids) and is presumably CP43'. Lanes in which PSII samples have been loaded show evidences of protein degradation.

As clear from the observations reported in this section the procedure described, which had been used successfully so far to isolate PSI-CP43' Supercomplex particles for Electron Microscopy and Single Particle analysis, needed to be improved for the purpose of this work: the detection of a possible interaction between CP43' and PSII.

First thing was to improve the quality of the –Fe starting material. Healthier iron-stressed cultures were obtained growing the cells as described in section 2.3.3 and the result has been already commented in the previous section (3.2).

To prevent degradation of PSII a mixture of protease inhibitors (1 mM phenylmethanesulfonyl fluoride, 1 mM benzamidine, 1 mM aminocaproic acid) was added to all the buffers and particular care has been taken in carrying on the all purification in dim green light and at 4°C. In order to keep the temperature low during the cell breakage a more mild protocol has been used for the bead beater (method described in section 2.5.1) and another centrifuge step to remove unbroken cells and cell debris has been introduced.

Oxygen evolution activity of the various fraction gives a measure of the amount of PSII in each sample and of the structural and functional integrity of the photosynthetic complex. Oxygen evolution is known to be correlated with the presence of the extrinsic proteins in the purified Photosystem II and therefore can be used as an indirect assay of the subunit composition of the isolated particles. Measurement of the activity was important to monitor the quality of our preparation but also to compare plus and minus iron samples on the structural and functional point of view. In order to preserve the structural integrity of the complex during the preparation 10% glycerol and 1.2M betaine monohydrate have been added to all the buffers (as reported in Debus et al., 2005). Purification of the PSII complex from the extracted thylakoids was performed either using a weak anionic exchange chromatography (starting form wt cells) or by affinity chromatography eluting in a lower concentration of Histidine (50mM). The quality of the two preparations has been compared and will be described in the next section.

Concerning the affinity chromatography system, to improve the purity of the preparation 5mM Histidine has been used during the column wash step to remove the majority of the protein unspecifically bound to the resin prior to elution.

Finally in order to separate subpopulations of PSII particles (monomers, dimers and eventual subcomplexes), free from copurifying proteins (including CP43'), a quicker and more sensitive preparative method has been substituted for the gradient centrifugation: a second chromatographic step using a strong anionic exchange resin.

All these changes led to the elaboration of the final protocol described in Materials and Methods in section 2.5. PSII particles isolated with this new method from plus and minus iron cells could finally be compared and analysed for the presents of CP43' in the pure preparations.

3.3.2 *Results of the improved purification system starting from wt, HT3A and ΔCP43-CP47His tagged cells grown in iron sufficient media*

Table 3.3 summarises the amount, yield and activity of each stage in the preparation of Photosystem II.

A loss of chlorophyll and activity is apparent after the cell breakage step. Efficiency of the cell breakage, made as mild as possible to preserve the activity, is probably relatively poor and also it is possible that a fraction of the thylakoids was spun down together with the cell debris, although the centrifugation step was performed at low speed (section 2.5.1).

Exact quantification of the total amount of PSI was difficult since a consistent fraction of PSI is lost during the column wash step in both the two different preparations. In Table 3.3 the amount of unbound material

(largely enriched in PSI as discussed in section 3.2) is reported for the affinity chromatography purification while the amount of PSI aggregates eluted as latest fraction in 50mM $MgSO_4$ from the DEAE column is indicated for the anionic exchange method. In both cases yield of PSII is poor if compared with the quantity of PSI isolated during the preparation. This difference reflects the normal PSI:PSII ratio characteristic of cells grown in standard conditions (Typically 9:1, Tang and Diner, 1994).

| Purification of PSII from Synechocystis PCC 6803 +Fe				
SAMPLES	total chlorophyll [a]	oxygen evolution [b]	yield [c]	
harvested cells (18L)	30-40	500-550	100	
concentrated cells in washing buffer	30-35	500-550	92	
broken cells	20-25	250-300	65	
thylakoids	20	300-400	57	
solubilized thylakoids	15-20	300-400	50	
elutant unbound	6-8	0 (control)	20	affinity chromatography
eluted PS II particles	1,5-2	1500	5	
PS II particles after II column step	1-1,5	0	3,5	
PSI aggregates	4,5-5	0 (control)	15	anionic exchange chromatography
PS II fractions (after I column step)	1,5-1,8	600-800	4,7	
PS II particles after II column step	1-1,5	0	3,5	
elutant unbound	6-8	0 (control)	20	deltaCP43 by affinity chromatography
eluted PS II particles	0,5-0,6	0	1,6	
PS II particles after II column step	0,2-0,3	0	0,7	
[a] Milligrams of chlorophyll; [b] Micromoles of O_2 per milligram of chlorophyll per hour; [c] Percent of chlorophyll				

Table 3.3 Summary of preparation of photosynthetic complexes from *Synechocystis* PCC 6803 strains dwt, HT3A and ΔCP43-CP47his tagged, grown in the presents of iron. Values recorded for the thylakoid isolation (first 4 lanes) are average values for which we didn't record any significant difference between the dwt and HT3A strains. The total chlorophyll at each stage had also comparable values in the preparation from CP43-less mutant cells, while no oxygen evolving activity was registered at any stage from this strain.

Oxygen evolution activity is not lost in the extraction of membrane proteins from thylakoid membranes, indicating that there isn't oversolubilisation of the complexes. No O_2 evolution activity is detectable in the preparation in the PSI enriched fractions, indicating that separation of the complexes is

good in the case of the anionic exchange chromatography and that the majority of the active PSII binds to the Ni^{2+} resin in the case of affinity chromatography. The increase of the rate of O_2 evolution through the isolation procedure is coincident with PSII purification.

No activity has been detected from the isolated CP47-RC from the ΔCP43-CP47His tagged mutant. Yield, in terms of total chlorophyll content of the PSII enriched fraction from this mutant cells, was higher than expected, comparing with previously published data (10% of the wt PSII amount, Rögner et al., 1991). The purification procedure used in our work was completely different from the cited publication. Sample isolated after the first affinity chromatography step contained a relevant amount of free CP47 that bound to the Ni^{2+} column. The second chromatographic step was needed to isolate the complete CP47-RC complex. The obtained yield after this second step was 20% of that obtained from the HT3A cells.

In order to monitor the various steps during the preparation the spectral proprieties of the fractions were analysed (Figure 3.12). During the preparation, starting from whole cells toward extracted thylakoids the relative ratio between the red peak of chlorophyll *a* and the OD_{750} (light scatter from lipid membranes) increases. The maximal of the red peak shifts from 683nm, characteristic of healthy cells, to 679nm, which is the typical peak of PSI, the most abundant photosynthetic complex found in the cells. In the room temperature absorption spectra of the cellular homogenate the presence of phycobilisomes, which have an absorbance peak at 620nm, is evident. In the isolated and washed thylakoid membranes the absorbance due to the extrinsic water-soluble phycobillisomes is drastically reduced.
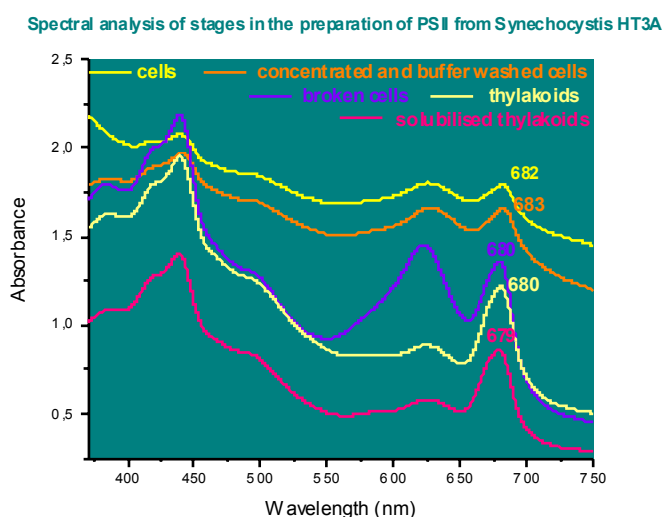
Figure 3.12 Spectral analysis of stages in the preparation PSII from cultures of Synechocystis PCC 6803 grown in iron containing media. Data are reported for HT3A samples as an example but might be referred to any of the thee strains used, since we didn't evidenced at this stage any relevant difference.

3.3.3 Isolation of PSII particles by Affinity Chromatography

By employing the His-tag on the C-terminus of CP47, one of the internal antenna proteins of PSII, then, if mild conditions have been employed during the extraction of proteins from the isolated thylakoid membranes, only complete PSII core complexes should bind to the Ni^{2+}-NTA sepharose resin. All the other complexes should not bind or at least should be removed during the wash with 5mM His.

An SDS-PAGE analysis of all the fractions has been performed to check the actual purification of PSII during our preparation (Figure 3.13, gel on the left). The polypeptide profile shows that the PSII enriched fraction is essentially free of polypeptides from the PSI core complex, which are clearly visible in the thylakoids and in the fraction that did not bind to the column. PSII lane is largely enriched in the bands characteristic of PSII core complex subunits, visible in the region between the 52 and 28kDa standards. Cytocrome$_{550}$ band (subunit V) is also visible below the 28kDa marker. A few other bands are also visible in the isolated PSII fraction. Resolution of this gel (12.5% polyacrylamide) was not enough to assign three of those bands as small molecular weight subunits of PSII and the rest as copurifying proteins.

In order to check for the presence of the extrinsic and small subunits, the isolated PSII particles prepared from *Synechocystis* have also been compared to an extremely pure preparation of Photosystem II cores from *Thermosynechococcus elongatus,* from which 3D crystals had been obtained and used for diffraction analysis. A 15% polyacrylamide gel has been run and results are shown in figure 3.13. All the subunits visible in the control preparation are also present in our PSII fraction from *Synechocystis*, although in some cases in different stoichiometric amounts. The results indicates anyway that the majority of the complexes in our preparation are intact.
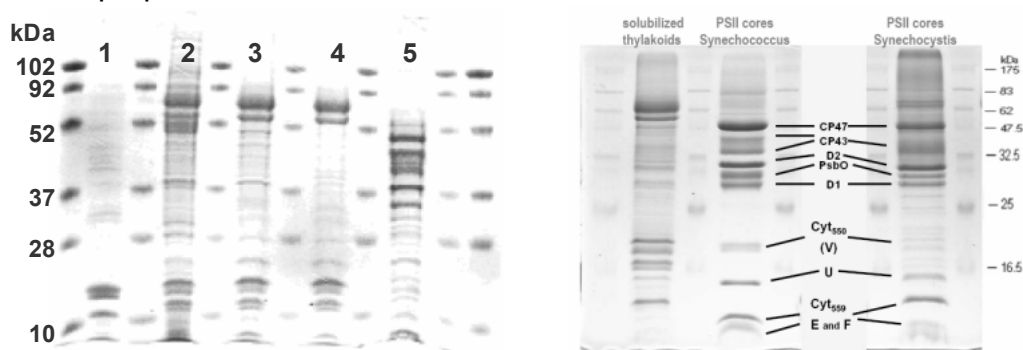

Figure 3.13 SDS-PAGE of the different fractions collected during PSII preparation. A 12.5% polyacrylamide gel is shown on the left of this figure. In lane 1 a whole cell extract has been loaded, thylakoid membranes and solubilized thylakoids have been loaded respectively in lane 2 and 3, the unbound fraction is in lane 4, while the PSII enriched fraction is in lane 5. Lane 5 is clearly enriched in PSII core subunits and PSI bands are not visible. A few unspecific bands are also visible indicating that the preparation is not pure. A 15% polyacrylamide gel is shown on the right, in which a *T. elongatus* preparation has been also loaded as a control. All the subunits visible in the control

preparation have been identify in our *Synechocystis* preparation as well, indicating that the majority of the purified complexes is intact. Here again the presets of unspecific band is even more evident.

A spectroscopic analysis of the PSII preparation has been also performed. The room temperature absorption spectra (Figure 3.14) show a steady tincrease of the chlorophyll level toward OD_{750} ratio between solubilized thylakoids and isolated PSI and PSII enriched fractions. PSII red peak is registered at 674nm while, in the solubilized thylakoids fraction the predominant signal is that of PSI and peak is registered at 679nm. This is a clear indication of PSII purification. Signal in the region in which there is absorption of phycobilisomes is lower in the PSII spectrum than in the unbound fraction's one, indicating that there isn't copurification of phycobiliproteins in our isolated PSII particles.
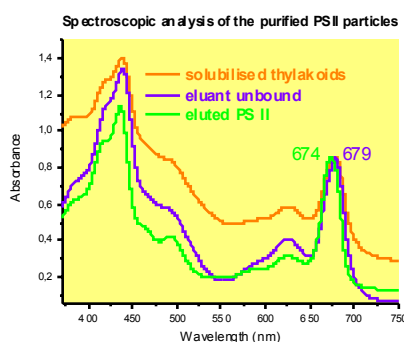

Figure 3.14 Comparison between the room temperature absorption spectra of the isolated PSII particles and of the extracted thylakoids and PSI enriched fraction.

Samples of isolated PSII particles were assessed for the presence of cytochromes. Cyt b_{559} and Cyt c_{550} content were detected using the reduced-minus-oxidized difference spectrum performed in Buffer B (section 2.5) at 50 μg of chl/ml, 1 mM $K_3Fe(CN)_6$ ± 2 mM sodium dithionite (Cramer et al., 1986). We were able to detect a signal from both cytochromes and estimation of cyt c_{550} content indicates that at least 20% of it it's lost during the preparation when compared with data published in Lakshmi et al., 2002. The result is anyway consistent with what observed already from the comparison with the *T. elongatus* preparation in the SDS-PAGE analysis (Figure 3.13).
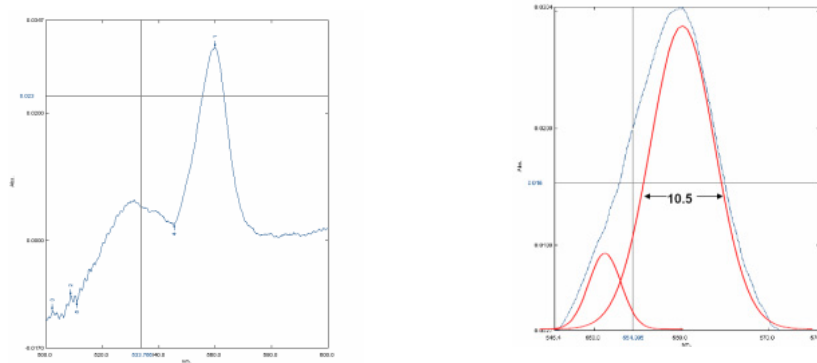
Figure 3.15 Reduced-minus-oxidized optical difference spectrum of the His-tagged *Synechocystis* PCC 6803 PS II core complex (chlorophyll concentration 50 μg/ml). On the left, reduced minus oxidized difference absorbance spectra of cytochromes c_{550} and b_{559} in preparations of PS II core complexes from *Synechocystis*. On the right, the spectrum is modelled as linear combination of two Gaussian peaks (red plots): a cyt c_{550} peak centred at 551 nm and a cyt b_{559} peak centred at 559 nm with FWHM of 10.5nm (as reported in Lakshmi et al., 2002). The experimentally measured composite optical spectrum modelled as the sum of two individual Gaussian peaks is shown in blue. An additional linear baseline correction has been applied to the fit that consists of a straight line connecting the spectral values at 540 and 570nm and the two wings of the experimental spectrum above and below these cutoff values. The peak that we assigned as cyt c_{550} contribution is approximately 20% lower than the value published by Brudvig and coworkers (Lakshmi et al., 2002) for an His tag preparation from *Synechocystis*. The result is anyway consistent with the approximate concentration deducible from the comparison of the *Thermosynechococcus* and *Synechocystis* lanes in the SDS-PAGE (Figure 3.13).

PSII particles isolated by affinity chromatography were also analysed for the oligomeric composition by size exclusion chromatography. We registered the characteristic peaks of monomers and dimers in the samples (Figure 3.16, left side).

PSII enriched fraction were finally loaded onto a UnoQ column for a second chromatographic step. Two early fractions were collected from the anionic exchange chromatography according to the absorption signal at 430nm, which is characteristic of chlorophyll containing samples (elution profile is shown in Figure 3.16, right side). Two collected fractions were identified as monomers (early peak) and dimers (late peak) by size exclusion chromatography (data not shown).
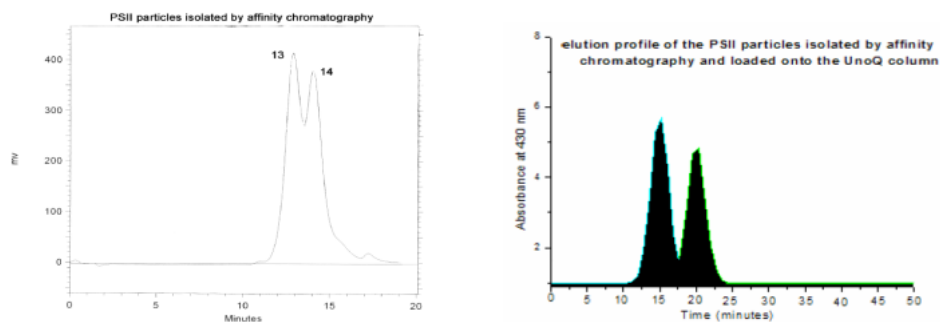

Figure 3.16 Size exclusion chromatography of the PSII particles isolated by affinity chromatography (left) and elution profile of the same sample run through an anionic exchange column (right).

The oxygen evolution activity was measured for the two PSII fractions collected after the second chromatographic step was performed. No activity could be registered from any of them. The most likely reason for that is the loss of the extrinsic protein after this step as evident from the SDS-PAGE shown in Figure 3.25.

A number of papers was published in the past few years in which affinity chromatography is used to obtain highly active PSII preparations from different strains of *Synechocystis* with a tag of histidines on CP47. In our hands the preparation gave pretty intact and active PSII complexes but we could always detect the presence of copurifying proteins in the samples after applying our procedure. Nevertheless our observation is that this kind of preparation can be a really interesting tool for the isolation of PSII enriched fractions from cells that normally contain a relatively small amount of PSII compared to cells grown in standard conditions (i.e. iron-stressed cells; mutants in which the mutation of one or more PSII subunits affect either the stability or the assembly of the complex). This technique of isolation of PSII particles is really sensitive indeed. In the more common preparation of PSII from wt cells by weak anionic exchange chromatography (Tang and Diner, 1994) detection of the red peak of absorption is crucial for the setting up of the salt gradient and for obtaining a good separation of the membrane complexes (PSI and PSII). In all the cases in which concentration of PSII is too low to register its signal during the chromatographic run, the isolation of the PSII fraction is in general not successfully. In those cases affinity chromatography might possibly be the best way.

The introduction of the second chromatographic step, although it did bring about the loss of the extrinsic proteins and therefore of the activity, was a useful way to separate different populations of PSII core complexes (i.e. monomers and dimers) and achieve a clean preparation. This method was used to look for the presence of a subpopulation of PSII form minus iron samples in which CP43 could have been replaced by CP43'.

Purification using a weak anionic exchange column was also applied, first to preparations isolated from plus iron cells and then from iron-stressed cells, in order to check for a possible interaction of CP43' with PSII in a second preparation, in case the subpopulation we were looking for could have been lost at a point during the process of PSII isolation by affinity chromatography.

3.3.4 *Purification of PSII Core Complexes by Anionic-exchange Column Chromatography*

Weak anion-exchange column chromatography was used for purifying the PSII core complex. The weak anion-exchange resin (DEAE) permits the use of low salt concentrations to elute PSII core complexes from the column, thus allowing to preserve the activity of oxygen evolution.

Figure 3.17 shows the elution profile, using DEAE-Toyopearl 650S, of a dodecyl maltoside extract of thylakoid membranes. The wash with the equilibration buffer is a pink-orange colour and shows very little absorbance in the red wavelength region of the visible spectrum. It is likely to contain carotenoids and a small amount of free chlorophyll. The first peak eluted by the equilibration buffer wash is a mixture of proteins in which the most abundant chlorophyll binding complex is PSI, showing an absorbance maximum around 679 nm. Components eluted by the 20-30 mM linear $MgSO_4$ gradient show a small peak in the elution profile. Those fractions with absorbance maxima between 673.5 and 674nm were active in oxygen evolution, and were pooled and concentrated. The major component eluted at 50mM $MgSO_4$ shows an absorption peak at 679nm and contains aggregates of PSI core complexes. The yield of purified PSII core complexes is approximately 4.7% of the total starting chlorophyll in the cells (Table 3.3).
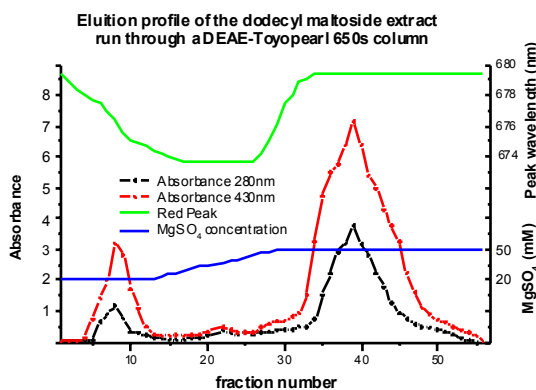

Figure 3.17 Elution profile of the dodecyl maltoside extract on a DEAE-Toyopearl65Os column. Absorbance is measured at the red absorption maximum (red line) and at 280 nm (black line). Also indicated is the MgSO, concentration (blue) and the wavelength at the red absorption maximum of the elutant (light green).

The preparation was checked for the presence of the PSII core complex subunits by immunoblot detection with the antibodies available in the laboratory (Figure 3.18). The presence of the core subunits has been confirmed. The two cytochrome b_{559} binding subunits were also detected in the PSII preparation. SDS-PAGE of the preparation is shown in Figure 3.20 in comparison with the fraction collected after the second chromatographic step.
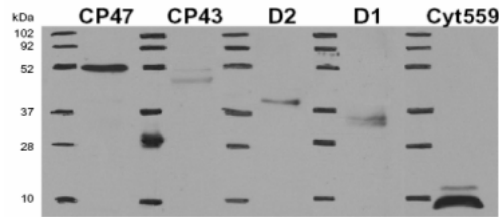
Figure 3.18 Immunoblot analysis of PSII preparation by anionic-exchange chromatography, from wt cells grown in iron sufficient medium.

Room temperature absorption spectrum of the purified PSII core complexes has been taken. The chlorophyll *a* absorption peak is registered at 674nm. A small absorption peak at 545nm is also registered which may be ascribed to pheophytin a, while no signal is evident from phycobilisomes in the region between 600 and 650nm. The reduced minus oxidized spectrum in the region between 500 and 600nm has also been registered from the sample to detect the cytochromes signal. Cytochrome b_{559} peak is evident and its normalised absorption value resulted to be coherent with previously published data (Tang and Diner, 1994). The presence of the cytochrome b_{559} in the preparation was also evident from the immunoblot detection of subunit E and F (Figure 3.18). The signal of cyt c_{550} hasn't been calculate from the spectral analysis, but the band characteristic of V subunit is visible in the SDS-PAGE (Figure 3.20) in the lane in which PSII particles isolated by weak anionic exchange chromatography had been loaded. The band becomes weaker in the samples subjected to the second chromatographic step.

The spectroscopic analysis of our preparation substantially reproduces the results published so far for this kind of preparation by Tang and Diner (1994).
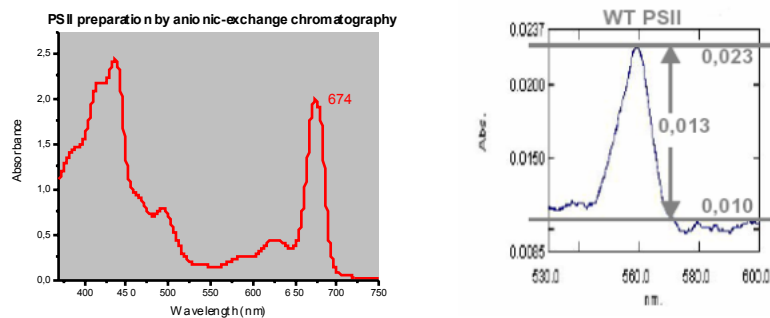

Figure 3.19 Absorbance spectrum on the left and dithionite-reduced minus ferricyanide-oxidized difference spectrum on the right. In the room temperature absorption spectrum of the purified PSII the red chlorophyll *a* peak is observed at 674nm, the typical value reported in literature for PSII core complexes (Tang and Diner, 1994). A small absorption peak near 545nm, ascribed to pheophytin a, is also evident. No significant signal from phycobilisomes (absorbance between 600 and 650nm) is recorded in this spectrum, indicating that they've been removed during the purification. A measure of the cytochrome signal in the region between 500 and 600nm has been performed and is shown on the right in his figure. 15 µg of chlorophyll of the PSII sample in 1ml of buffer B (section 2.5) have been used for the assay. A peak was registered at 559nm with a normalised absorption value of 0,013. The measured value is in the range with that measured form

Tang and Diner in an analogous preparation of PSII cores. The result is also in agreement with the detection of E and F subunits in the western blot of the isolated PSII particles (Figure 3.18).

As described before for the PSII particles isolated by affinity chromatography, the PSII enriched fraction collected from the DEAE column has been loaded onto a second anionic exchange column (section 2.5.6). Three fractions were separated using this second chromatographic run according to the absorption at 430nm. An SDS-PAGE of all the fractions has been run (Figure 3.20). In the gel the first lane shows the sample collected after the first chromatography while in the second, third and forth lane the three fraction separated by the second chromatography have been loaded according to their elution order.

PSII fraction after the first column step contains a number of unspecific bands. The dimensions of the column used for the chromatography were different from the ones indicated in the Tang and Diner protocol, according to which we set up our preparation. This difference in the dimension of the stationary phase may have effect the resolution of the chromatography. Nevertheless two clean fractions of PSII cores (lane 3 and 4 in the SDS-PAGE) were eluted after the second chromatographic step, in which a loss of the extrinsic subunits is evident. The loss of the extrinsic proteins in the majority of the PSII cores is observed after the run through the UnoQ both in the affinity chromatography and in the anionic exchange chromatography preparation.
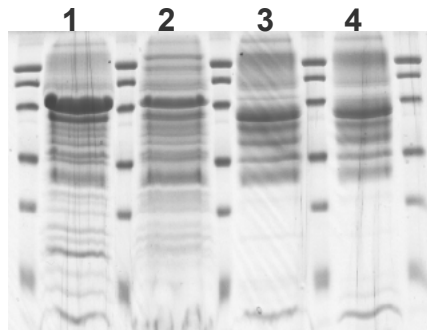

Figure 3.20 SDS-PAGE analysis of the PSII enriched fractions collected during the anionic-exchange chromatography preparation. In the first lane the isolated PSII particles obtained after the first chromatographic step were loaded. Lane 2, 3, 4 show respectively the first, second and third fraction separated by the second chromatography. In the first lane PSII core complex subunits are visible and a few bands may be tentatively assigned as extrinsic proteins of PSII complex. A number of copurifying protein is also visible. In the first fraction eluted from the UnoQ column the preparation is still not pure and the band tentatively assigned as extrinsic protein are lost. In the last two lanes (3 and 4) the preparation is pretty pure but the extrinsics are lost in the majority of the complexes. No oxygen evolution activity is indeed registered from this samples.

3.3.5 *Purification of CP47 Reaction Centres by Affinity Chromatography from ΔCP43-CP47His tagged cells*

In order to see if a different form of Photosystem II, in which CP43' replaces CP43, might assembly and accumulate in the cells we decided to

set up a preparation from a mutant strain of *Synechocystis* in which CP43 gene had been deleted. If this complex existed in iron-stressed cells we might expected it to be more concentrated in the CP43 less mutant grown in iron depleted medium. The preparation has been performed and analysed from ΔCP43-CP47His tagged cells grown in standard conditions and the same procedure has then been repeated using iron-stressed cells. The fraction of chlorophyll binding proteins that bound to the Ni^{2+} resin was eluted in 50mM His, as in the HT3A preparation and analysed.

Analytic size exclusion chromatography was performed and we obtained one peak after 14.7minuts (Figure 3.21, left). The retention time measured for PSII monomers was 14minutes. We inferred that this profile was compatible with a sub-complex of PSII like CP47-Reaction Centre.

A room temperature absorption spectra was taken and the peak in the red was registered at 675nm (Figure 3.21, right). The spectrum looked pretty much similar to that of purified PSII looking at the relative ratio of absorbance values registered for the red and the blue peak of chlorophyll. The red peak, however, shifted 1nm toward the red. This datum differs from the observation that the red peak of chlorophyll of the purified CP47-RC is shifted toward the blue of 0,5-1nm reported in Rögner et al., 1991, but results consistent with the value published in Szabò et al., 2001. The small peak of pheophytin is well visible in the CP47-RC spectrum. This signal was indeed expected to be more evident than that registered for complete PSII cores, since the pheophytin to chlorophyll ratio should be higher in the absence of the chlorophyll molecules bound to CP43.
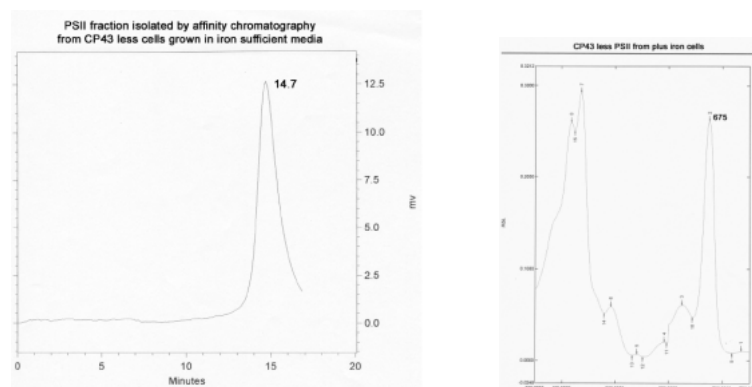

Figure 3.21 Analysis of the fraction isolated by affinity chromatography from the ΔCP43-CP47His tagged cells grown in iron containing media. On the left the result of the analytic size exclusion chromatography is shown. Only one population of particles is found, whose dimensions are consistent whit those of a PSII subcomplex, that we assigned as CP47-RC. On the right the room temperature absorption spectra of the sample is shown. The maxima of the chlorophyll *a* absorbance in the red region is registered at 675nm. The peak of pheophytin is also visible at 545nm.

The fraction isolated by affinity chromatography was loaded onto the UnoQ column for the second chromatographic step. Only one peak with a significant absorbance at 430nm was eluted, whose retention time in the size exclusion chromatography resulted to be again 14.7minutes (data not

shown). An SDS-PAGE of the two samples is shown in picture 3.22. CP47, D1, D2, PsbE and PsbF bands are visible in both the gels. The copurifying proteins present in the sample isolated by affinity chromatography are removed after the second chromatographic step.
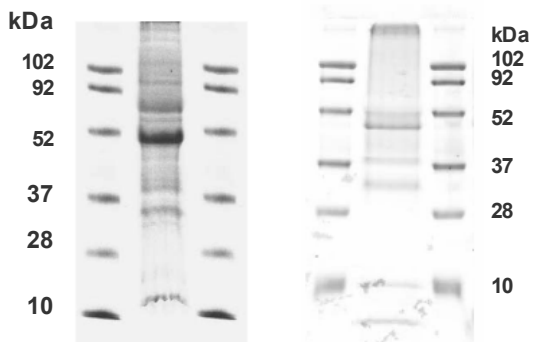

Figure 3.22 SDS-PAGE of the CP47-RC isolated by affinity chromatography (left) and after the run through a second column (right).

3.3.6 *Isolation of PSII complexes from iron stressed cells*

The PSII preparation described in the previous paragraphs have been repeated using iron-stressed cells. Results have been analysed in order to underline eventual differences in the characteristic of the purified PSII complexes. A table that summarises the activity of oxygen evolution and the yield expressed as chlorophyll content of the samples at the various stages of the preparation is reported (Table 3.4).

Oxygen evolution activity is in general lower than that registered from plus iron samples during all the stages from whole cells to solubilized thylakoids. As already observed a comparison is made difficult by the different distribution of chlorophyll between the chlorophyll binding proteins found in the cells grown in different conditions. Lower values of activity were anyway expected from iron-stressed cells, since the ratio of PSII to chlorophyll is much lower in those cells. A drop of the activity after the cell breakage is visible also in this samples and it is even more pronounced since less mild condition had to be apply to iron-stressed cells to obtain an efficient breakage. This was consistent with the observation that iron stress condition produce changes in the ultrastructure of cyanobacteria and membrane become in general thicker (Sherman and Sherman, 1983). We observed that obtaining a good quality preparation from minus iron cells was in general more difficult. Therefore reaching a compromise between efficiency and preservation of the activity during the cell breakage was crucial for all the three strains used. In addition, concerning the wild type strain, all the fractions collected during the first chromatographic step had a peak between 672 and 674nm. This characteristic made it particularly difficult for setting up of the salt gradient at the right timing during the run and therefore effected the separation of the photosynthetic complexes. A significant concentration of PSI or CP43' in the PSII

enriched fraction caused a lower PSII to chlorophyll ratio in the sample and therefore a lower value of activity, which is normalized to the chlorophyll concentration. The values that we registered for the oxygen-evolving activity in different preparation from the same kind of cells were significantly different, ranging from 0 to the same top value registered from the corresponding plus iron preparations. We didn't noticed any other difference between the active and non active PSII particles isolated from iron-stressed cells a part from the presence or absence of the extrinsic proteins. As a conclusion we can't say that oxygen evolution measurements on the purified PSII spotted any significant difference between the minus and plus iron complexes or evidenced the presence of a subpopulation of PSII complexes in iron-stressed cells with a different activity.

Purification of PS II Core Complexes from *Synechocystis 6803* -Fe			
SAMPLES	**total chlorophyll** [a]	**oxygen evolution** [b]	**yield** [c]
harvested cells (18L)	30-40	400-550	100
concentrated cells in washing buffer	30-35	400-550	92
broken cells	20-25	100-170	65
thylakoids	15-20	190-250	50
solubilized thylakoids	10-15	180-200	36
PSI aggregates	4-4,5	0 (control)	12
PS II fractions (after I column step)	0,7-1,1	0-1200	2,7
PS II partides after II column step	0,5-0,9	0	2
elutant unbound	6-8	0 (control)	20
eluted PS II partides	1-1,6	0-800	3,3
PS II partdes after II column step	0,5-0,7	0	1,7
elutant unbound	//	//	//
eluted PS II partides	0,5-0,6	0	1,6
PS II partdes after II column step	0,2-0,3	0	0,7
[a] Milligrams of chlorophyll; [b] Micromoles of O_2 per milligram of chlorophyll per hour; [c] Percent of chlorophyll			

Side labels spanning groups: anionic exchange chromatography (PSI aggregates / PS II fractions / PS II partides); affinity chromatography (elutant unbound / eluted PS II partides / PS II partdes); deltaCP43 by affinity chromatography (elutant unbound / eluted PS II partides / PS II partdes).

Table 3.4 Summary of preparation of photosynthetic complexes from *Synechocystis* PCC 6803 strains dwt, HT3A and ΔCP43-CP47his tagged, grown in suboptimal iron concentration. As for the plus iron preparations the values recorded for the thylakoid isolation (first 4 lanes) are average values for which we didn't record any significant difference between the dwt and HT3A strains. The total chlorophyll at each stage had also comparable values in the preparation from CP43-less mutant cells, while no oxygen evolving activity was registered at any stage from this strain.

The yield of PSII purified by affinity chromatography is approximately 2/3 of that obtained from the correspondent plus iron preparation and reflects the decrease of PSII concentration in the iron-stressed cells (Ivanov et al., 2000). The yield of PSII fractions purified from the ΔCP43-CP47His tagged cells was the same from plus and minus iron cultures, indicating that no significant stabilization of the complex is introduced by the growth in iron deprivation.

Spectral analysis of the PSII particles isolated from iron-stressed HT3A and dwt cells after the first and second chromatographic step is shown in picture 3.23. The spectra of PSII fractions isolated by affinity chromatography and PSII monomers eluted after the run through the UnoQ column almost superpose, indicating that there isn't any significant copurification of chlorophyll binding proteins during the first step. A different profile was obtained from the dwt samples after the first chromatographic step, in which the absorbance value registered for the peak in the blue is higher than that characteristic of PSII and the peak in the red region is shifted toward the blue of 1,5-2nm. This was a clear indication of CP43' copurification. The signal of CP43' is not evident any longer after the second chromatographic step.


Room temperature absorption spectra of PSII particles isolated from iron-stressed cells

Legend:
- HT3 I^{st} column Ni^{2+}
- HT3 IInd column UnoQ
- wt I^{st} column DEAE
- wt IInd column UnoQ
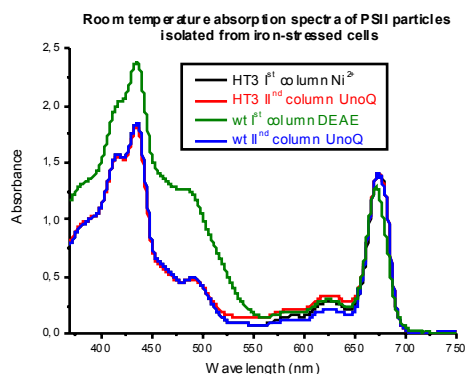
Figure 3.23 Comparison of the spectra of PSII enriched fractions obtained from iron-stressed HT3A and dwt cells after the first and the second chromatographic step. No copurification of CP43' is evident in the samples purified by affinity chromatography, while CP43' signal is registered in the PSII particles isolated by anionic-exchange chromatography but disappears after the second column step.

The PSII fraction collected after the first chromatography was analysed for the oligomeric composition by size exclusion chromatography. Two peaks have been eluted with a retention time of 13 an 14minutes respectively, which correspond to dimer and monomers as already observed in the plus iron preparation. The proportion of dimers in the graph shown (Figure 3.24, left) is relatively high indicating that there wasn't oversolubilization of the thylakoids. The peak of monomers is quite sharp and no signal from an eventual smaller complex is registered.
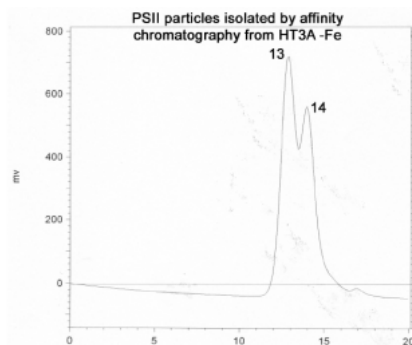
Figure 3.24 Size exclusion chromatography of the PSII particles isolated by affinity chromatography from iron-stressed HT3A cells. The peaks of PSII dimers and monomers are detected. No evidence was found for the presence of a subpopulation of PSII with a different elution time. Data were confirmed by the elution profile of the second chromatographic step, in which only two fractions of PSII particles were separated.

Sample isolated by affinity chromatography were run through the second anionic exchange column and two peaks were eluted according to the absorption at 430nm.The peaks have been identify as monomers and dimers by size exclusion chromatography (data not shown). The profile of the preparation from minus iron cells resulted from this first analysis the same as that recorded from plus iron cells. No evidence for a subpopulation of PSII with different characteristics was found.

Samples obtained from plus and minus iron preparations were loaded on a 15% polyacrylamide gel for an SDS-PAGE analysis of the subunit composition. Result is shown in picture 3.25. Dimers and monomers obtained after the second chromatographic step from minus and plus iron cells were loaded on to the gel. In all of them the 5 bands of PSII core complex proteins as well as those of the cytochrome b_{559} subunits are visible. An additional band just above the 28kDa marker is visible at very low concentration in both the minus iron samples. No alteration of the stoichiometry of CP43 is evident. Further analysis was needed to determine whether that band could be identify as CP43', nevertheless from this result there was no suggestion that the protein could actually interact within the core complex, replacing CP43, rather than interact with PSII as an non radiative energy dissipator, for example, as suggested in Sandström et al., 2001. The hypothesis of a copurification even after the second chromatographic step can't be excluded, although it seems less likely since the core complexes eluted from the UnoQ column look pure at this level of sensitivity.
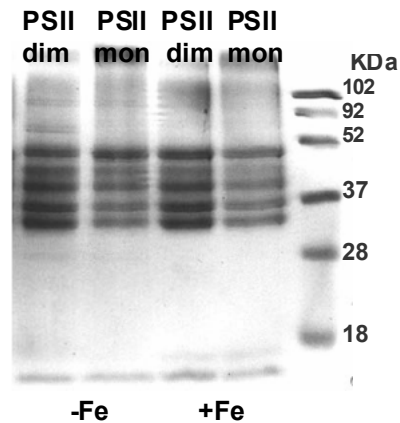
Figure 3.25 SDS-PAGE analysis of the PSII cores purified with a two step chromatography from minus and plus iron HT3A cultures. Dimers and monomers of PSII cores were loaded on the 15% polyacrylamide gel. In the first two lanes (minus iron samples) an extra band is barely visible just above the 28kDa marker. Stoikiometry of CP43 looks the same in the different samples.

Affinity chromatography preparation was performed also from the ΔCP43-CP47His tagged iron-stressed cultures. The profile of the preparation was almost identical to that recorded from the correspondent plus iron cells. Only one peak was detected by size exclusion chromatography of the CP43-less PSII isolated by affinity chromatography with a retention time of 14.7 minutes. Only one fraction was eluted from the UnoQ column. Again the retention time of the purified complex recorded by analytic size exclusion chromatography was 14.7 minutes (Figure 3.26, left). Spectral analysis of the samples after the first and second chromatographic step was performed and the maximum of chlorophyll *a* absorption in the red region of the visible-UV spectra was found at 675nm in both of them (Figure 3.26, right).
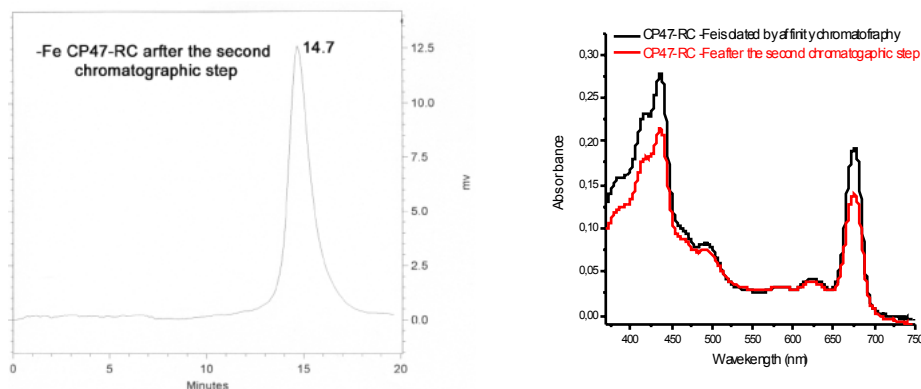

Figure 3.26 Size exclusion chromatography of the –Fe CP47-RC isolated by two step chromatography (left). Comparison of the room temperature absorption spectra of the sample after the first and the second column purification (right). Both the analysis reproduced the same results obtained from the parallel plus iron preparation. The comparison of the spectra before and after the run through the UnoQ column confirmed, as noticed for the HT3A preparation, that there isn't significant copurification of CP43' in the samples isolated by affinity chromatography.

The result obtained from this preparation was of particular interest. We proved that in standard growth condition a stable complex assembly in the absence of CP43 (as published already in Rogner et al., 1991) and

accumulate in the cells with a concentration which is at least 20% of the usual PSII concentration. In cultures deprived of iron an homogeneous fraction of PSII particles is isolated, with the same molecular weight (estimated by size exclusion chromatography, Figure 3.26) and almost the same polypeptide composition (SDS-PAGE Figure 3.29) as the one isolated from plus iron cells. As already mentioned the yield of purified CP43-less PSII complexes was the same in the two parallel purifications. We can conclude that with the isolation procedure used no evidence could be found for the association of CP43' within PSII core complex even in the absence of CP43.

Anionic exchange chromatography preparation was performed to isolate PSII complexes from dwt iron-stressed cells. The elution profile recorded was different from that obtained from the correspondent plus iron preparation (Figure 3.27). The initial wash contained a significant level of carotenoids. The first eluted peak was a mixture of proteins that was enriched in PSI complexes but also consisted of a significant amount of CP43'. When the value of absorbance at 430nm of this first peak dropped, the gradient was started and all the fractions collected during the running of the salt gradient were pooled as PSII enriched fraction. Two more peaks were eluted from the column and both of them was identify by size exclusion chromatography as PSI-CP43' Supercomplex.
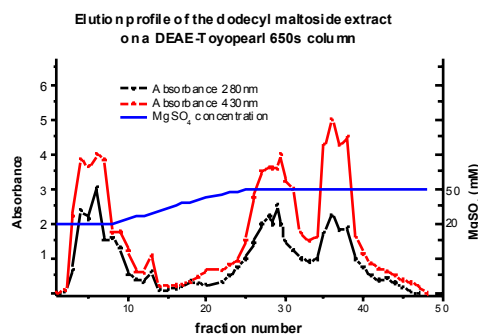
Figure 3.27 Elution profile of the solubilized thylakoids isolated from minus iron wt cells on the DEAE column.

Since the spectra evidenced that the isolated PSII fraction contained a significant amount of CP43', the sample was concentrated, loaded onto thawed sucrose gradients (0,6M sucrose, 0,5M betaine) and run for 20 hours at 30.000rpm using a Beckman SW40 rotor. This procedure allowed us to separate the copurifying CP43' from the PSII complexes. The higher sucrose concentration used improved the separation of CP43' from PSII while PSII monomers and dimers were found to migrate as one band. As evident from the data shown in Figure 3.28, the amount of CP43' in the sample was almost equivalent to that of PSII particles. The lower band, whose absorbance peak was registered at 674nm was then loaded onto the UnoQ column for

the second chromatographic step.
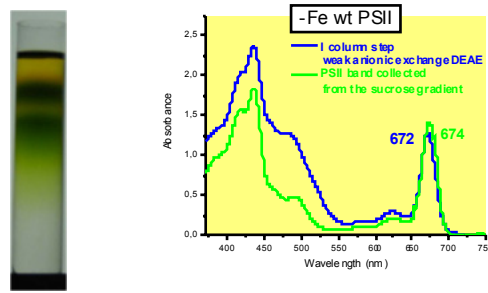
Figure 3.28 Sucrose gradient of the PSII enriched fraction eluted from the anionic-exchange column (left) and spectral analysis of the sample before and after the separation by gradient centrifugation (right). Two bands have been separated by gradient centrifugation (left). The lower band has been identify by room temperature absorption spectroscopy as PSII. In the fraction collected after the gradient centrifugation CP43' contribution is no longer visible.

As for the complementary plus iron preparation three peaks were separated by the second chromatographic step. All the fractions had a red chlorophyll *a* peak between 673.5 and 674nm.

The three fractions were checked by SDS-PAGE for the subunit composition. A detail of the 15% polyacrylamide gel is shown in Figure 3.29. In the first lane the PSII fraction isolated by two step chromatography from iron-stressed ΔCP43-CP47His tagged cells has been loaded, second, third and forth lane show the three PSII fractions isolated after the run through the UnoQ column from the –Fe wt cells, while in the last one (labelled as 5) a sample of plus iron wt PSII has been loaded as a control. During the process of purification of wt –Fe PSII, PsbO subunit is lost. The band of the 33kDa subunit is not found in the three wt –Fe samples, while is present in really low concentration in the ΔCP43 –Fe lane and is visible, although not well separated in the wt +Fe PSII. A band with a weak signal that migrate just below the D1 subunit is visible in all the samples. A second protein found again in low concentration is present in all the minus iron samples while is not visible in the control. The band runs below D1 and the unidentified protein and is present in all the three fractions of wt –Fe PSII in small amounts and in the ΔCP43 –Fe sample in even smaller concentration.
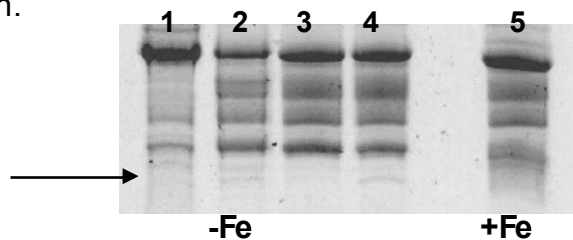
Figure 3.29 SDS-PAGE of the –Fe PSII particles isolated from dwt and ΔCP43-CP47His tagged cells. In the first lane the CP43-less –Fe PSII has been loaded, the three fractions of wt –Fe PSII have been loaded in lanes 2-3-4 following the order of elution from the UnoQ column. Lane 5 shows a +Fe wt PSII sample. A band that migrates below D1 and un unknown protein is visible in all the minus iron samples. The signal is really weak, indicating that the protein is found in the samples in small amounts.

Using this preparation no significant differences have been found out between the plus and minus iron samples concerning the number and the characteristics of the isolated PSII fractions. No subpopulation of PSII have been isolated which presented different detectable characteristics from the iron stressed cells of any of the strains used. But, in all the iron stressed cells, an extra band was found in the SDS-PAGE analysis of the minus iron PSII fractions, which is not visible in the correspondent plus iron samples.

In this case, as observed already for the affinity chromatography preparations, the extra band is unlikely to just copurify while it is rather likely to interact with the complex. Since the band was detected in all the three fractions separated by the second anionic exchange column it seems unlikely that an eventual PSII in which CP43' replaces CP43 copurifies with all the different fractions as it is not separated during the chromatography. It seems instead more reasonable that the protein can interact somehow with the purified PSII complexes in different oligomeric state. To actually check whether the extra band could be reasonable assigned as CP43', one of the fractions of wt –Fe PSII was loaded in the same gel as the –Fe thylakoids, the purified PSI-CP43' Supercomplex (latest peak in the first chromatographic step) and the CP43' enriched fraction (first band on the sucrose gradient). The extra band was found to migrate in the same position as the CP43' protein (Figure 3.30).
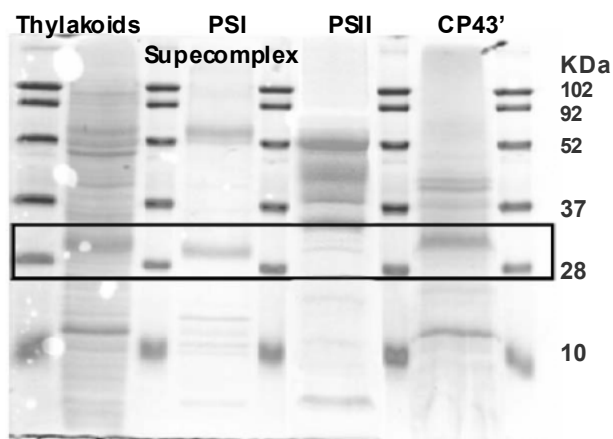

Figure 3.30 SDS-PAGE of the –Fe wt samples. In the thylakoids lane and in lanes in which PSI-CP43' Supercomplex and CP43' enriched fraction have been run (respectively first, second and fourth from the left), CP43' band is visible and migrates above the 28kDa marker. In the wt –Fe PSII sample (lane 3) the extra band is found in the same position.

The antibody against CP43' available in the laboratory has been tested on a western blot of thylakoids isolated from plus and minus iron cultures of dwt cells (Figure 3.31). A signal was detected in both of them between the 28kDa and the 10kDa standards. The result was not consistent with the identification of the CP43' protein, which should be found between the 37 and 28kDa standards (as shown in the various gels) and in far larger amount (if not exclusively) in the –Fe thylakoids.
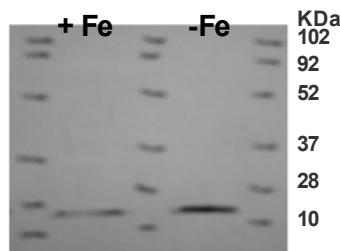
Figure 3.31 Immonoblot on plus and minus Fe thylakoids to test an antibody for CP43'. The molecular weight of the band identified by the antibody doesn't correspond to that expected for CP43' and doesn't reproduce the pattern of expression detected by SDS-PAGE analysis of the plus and minus iron thylakoids.

To identify the interesting band individuated in the −Fe PSII fractions, an SDS-PAGE of one of samples that contained the "extra band" was run, the proteins were blotted on a PVDF membrane and the isolated protein was sent for N-terminal sequencing. At the moment we haven't received any feed back yet from the sequencing service.

3.4 BPSI-CP43' SupercomplexB

As a by-product of the weak anionic exchange chromatography performed to purify −Fe PSII particles, two peaks were eluted, as already mentioned, that could be identify as PSI-CP43' Supercomplex. A fraction of chlorophyll binding proteins was found to be still bound to the column after the wash with 50mM $MgSO_4$. This remaining fraction was eluted using 100mM $MgSO_4$ and analysed. The fraction collected was identified as PSI-CP43' Supercomplex by size exclusion chromatography and, as it is visible in the graph reported in Figure 3.32, on the left, the peak at 11.1 minutes is really sharp, indicating that the population of protein complexes is very homogeneous. An SDS-PAGE analysis of the isolated PSI-CP43' Supercomplexes was performed and confirmed that the sample was pure and no unspecific bands could be detected.
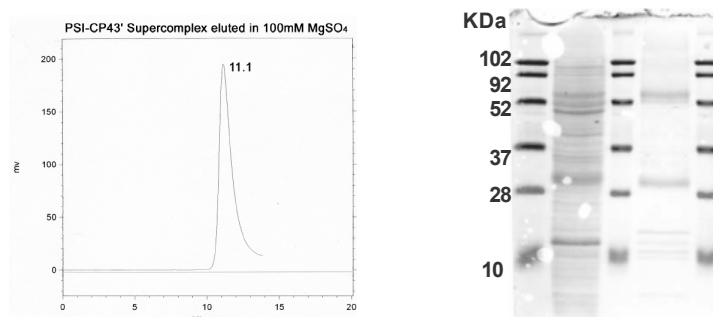
Figure 3.32 Size exclusion chromatography profile (left) and SDS-PAGE analysis (right) of the PSI-CP43' Supecomplex isolated by weak anionic-exchange chromatography.

The application of this procedure for the purification of PSI-CP43' Supercomplex produced a significant improvement in the quality of the

samples in comparison with what obtained from the isolation by density gradient centrifugation (described in section 3.3.1). The purification by column chromatography is also much quicker than the isolation by sucrose gradient centrifugation and therefore helps preserving the integrity of the complexes during the preparation. Samples isolated by weak anionic exchange chromatography are now used in Professor Barber's Group for conducting crystallization trials of the Supercomplex.

Chapter 4 – Conclusions

This project was driven by the hypothesis that under conditions which stimulate the expression of the *isiA* gene, particularly low Fe, the resulting CP43' protein could assemble with other PSII proteins to form a CP43'-conjugated PSII like complex. Such a complex, it was hypothesised, would have a modified donor side and would not evolve O_2 but rather could receive electrons from a donor such as reduced plastocyanin. In this way a light driven cyclic electron flow around the PSII-like reaction centre could occur providing a means of generating a proton gradient for ATP synthesis. Such a cycle would be analogous to that which occurs in the type-II reaction centres of purple photosynthetic bacteria.

However comparing the data collected from the preparations of Photosystem II from standard and iron-stressed cultures, no evidence was found of the presence, in the iron stressed cells, of a PS II complex that incorporates CP43' within the reaction centre.

The hypothesis of a possible function of CP43' not only as extra antenna for PSI in iron stress condition, but also as energy dissipator in connection with PSII, has been supported by the works of Sandstrom et al., 2001 and Ihalainen et al., 2005. According to this interpretations CP43' should be involved in the photoprotection of PSII and serve, in different situation of oxidative stress, the function of non radiative energy dissipator. On the light of this evidences the detection of a possible interaction between CP43' and PSII complexes could be reasonable. A number of different methods could be used for that aim, that could reveal more sensitive than the isolation of photosynthetic complexes in the detection of protein-protein interactions.

The purpose of this work, instead, was that of specifically detected if CP43' could functionally replace CP43 in the assembly of a complex that most likely would have been accessible for small molecules on the donor side of the reaction centre and therefore work in a way similar to that of the purple bacterial reaction centre. The isolation of an heterogeneous population of PSII by affinity chromatography and the subsequent detection and separation of eventual subpopulations that could be analysed for structural and functional characteristics, seemed the more suitable way to carry on our experiment. Affinity chromatography has been used recently in our laboratory to isolate PSII complexes from cells in which point mutations in the loop of CP43 dramatically effect the stability of the complex, that therefore is found in the cells in extremely low concentrations. The technique was successful in isolationing various PSII subcomplexes which are estimated to represent in the cell, in some cases, less of the 1% of the total chlorophyll content. This approach is therefore sensitive enough to reveal the presence of complexes that contain CP47, and are present in low concentration. We expected that if the hypothetic

CP43'-conjugated PSII was present in the PSII fraction isolated by affinity chromatography, it should have been spotted by the size exclusion chromatography or the second anionic- exchange chromatography as a separate peak, although with a very weak signal. Since no evidences have been collected in that sense we concluded that it is probably not possible to assembly a complex stable enough to perform the primary charge separation, in which CP43' replaces CP43.

An important assumption of our hypothesis was that CP43' is actually similar enough to CP43 to be able to interact with the PSII reaction centre subunits and assembly a complex. The docking site between two proteins is in general really optimised through the evolution by complementary selective pressure. This is specially important for highly specialised complexes, which usually consist of a significant number of subunits, to preserve the structural stability and the functionality. Although a number of evidences supported the hypothesis that the two proteins assume the same folding, probably the characteristics of CP43' protein surface in the positions important for the structural assembly of the complex don't permit an efficient interaction of the protein with D1 and the other PSII subunits.
It is interesting to note that the similarity of 40% between the aminoacidic sequences of the two proteins corresponds to a poor similarity of the nucleotidic sequences of the corresponding genes. The result of a simple blast between the two nucleotidic sequences is shown in Figure 3.33. No significant similarity was found, indicating that either the gene duplicated from long enough to accumulate a high number of silent mutations or that, more likely, the two proteins don't have a direct common ancestor and are therefore analogous rather than homologous. The two proteins might have evolved the same fold and similar properties so as to function as chlorophyll binding antenna. In both the hypothesis, provided that the association with PSII is not the function of CP43', there shouldn't have been any selective pressure on the aminoacids potentially involved in the docking to D1. The resolution of the structure of CP43', which is just inferred by homology modelling at the moment, might provide an important insight to solving this issue.

BLAST 2 SEQUENCES RESULTS VERSION BLASTN 2.2.12 [Aug-07-2005]

Match: 1   Mismatch: -2   gap open: 5   gap extension: 2
x_dropoff: 50   expect: 1.00000 wordsize: 9   Filter ☑   [Align]

| **Sequence 1** | gi 16329170 | Synechocystis sp. PCC 6803, complete genome | **Length** 1029 |
| **Sequence 2** | gi 340699 | Synechocystis sp. (strain 6803) chlorophyll a-binding protein (psbC) gene, complete cds | **Length** 3047 |

No significant similarity was found

Figure 3.33. Result of a Blast of the nucleotidic sequences of CP43 and CP43'.

Appendice 1 Riassunto in italiano dell'elaborato di tesi presentato in lingua inglese

1.1 Introduzione

Poiché il ferro è il quarto elemento per abbondanza presente sulla crosta terrestre è abbastanza sorprendente constatare che, al contrario, la biodisponibilità di questo metallo costituisca in genere un fattore limitante per la crescita di una parte della biosfera: i microrganismi acquatici. Il Fe^{2+} viene rapidamente ossidato a Fe^{3+} in acqua e la scarsa solubilità del Fe^{3+} a pH fisiologici risulta nella formazione di precipitati e nella drastica riduzione della concentrazione di ioni assimilabili dalla cellula. Se il ferro riveste una importanza essenziale per il corretto svolgimento di processi metabolici fondamentali, quali la respirazione cellulare, che sono comuni a tutti gli organismi, ancora più rilevante diviene il suo ruolo nella crescita degli organismi fotosintetizzanti, che ne necessitano anche per la sintesi ed il funzionamento dell'apparato di trasporto elettronico guidato dalla luce. Nel lavoro di ricerca presentato in questa relazione ci siamo occupati della risposta fisiologica dell'apparato fotosintetico dei cianobatteri alla crescita in concentrazioni subottimali di ferro, che sembra essere una condizione più naturale di quella utilizzata normalmente per la coltura in laboratorio.

Un numero di specifiche risposte fisiologiche delle cellule batteriche alla deprivazione di ferro è noto ed è ampiamente descritto in letteratura (Strauss, 2004). Fra queste, notevole rilievo riveste nei cianobatteri la sintesi di una proteina, CP43', capace di legare clorofilla, la cui funzione principale è la formazione di un sistema antenna intorno al Fotosistema I (PSI) in forma trimerica (Bibby et al.,2001). Ulteriori ruoli funzionali sono stati proposti per questa proteina, quali la protezione del Fotosistema II (PSII) in situazioni in cui l'afflusso di energia al sistema supera la capacità di utilizzo o dissipazione (Sandström et al., 2001). L'analisi della sequenza primaria di CP43' ha messo in evidenza una rilevante similarità con la sequenza di CP43 (PsbC), una delle due antenne interne del PS II, da cui infatti deriva il nome (Laudenbach e Straus, 1988; Leonhardt e Straus, 1992; Murray et al., 2005). La distribuzione dei residui idrofobici suggerisce che le due proteine assumano la stessa struttura terziaria, caratterizzata da 6 eliche transmembrana. La distribuzione dei residui di istidina risulta inoltre analoga e pertanto compatibile con l'ipotesi che le due proteine leghino le molecole di clorofilla in posizioni corrispondenti. Proprio in accordo con queste osservazioni è stato ipotizzato in passato

che CP43', la cui concentrazione diviene particolarmente elevata in condizioni di stress da ferro, possa sostituire, almeno in parte, CP43 nell'assemblaggio del Fotosistema II (Burnap et al. 1993; Straus 1994). Questa ipotesi non era mai stata comprovata almeno fino ad ora.

Dal nostro punto di vista, poiché la sequenza aminoacidica delle due proteine presenta, non solo una percentuale di similarità superiore al 40%, ma anche un numero rilevante di residui identici uniformemente distribuito, l'ipotesi di una possibile interazione di CP43' con le proteine del core del PS II, con cui normalmente CP43 interagisce, sembrava ragionevole.

La più rilevante differenza fra le due proteine è l'assenza, in CP43', del loop che in CP43 congiunge l'elica V e VI. L'ampio loop, presente in CP43 (circa 132 residui) sporge sul lato lumenale della membrana. Dati ottenuti da mutagenesi mirata di residui del dominio lumenale (Rosenberg e al. 1999) e confermati dalle recenti strutture a media risoluzione ottenute dalla diffrazione ai raggi X di cristalli di PS II di *T. elongatus* (Ferreira et al., 2004; Loll et al., 2005), provano che questo dominio svolge una funzione fondamentale per l'attività di evoluzione di ossigeno svolta dal complesso. La presenza di questo extradominio sembra pertanto essere legata alla specifica funzione di CP43 nel processo di ossidazione dell'acqua, mentre il fold a 6 eliche transmembrana è un motivo ricorrente in un gruppo di proteine (PsbC, PsbB, PsaA, PsaB, CP43', PcbA, PcbB) che svolgono la funzione di antenna per i fotosistemi, per le quali si ipotizza una origine evolutiva comune (Murray et al., 2005; Chen et al., 2005).

Alla luce di queste considerazioni, se CP43' fosse sufficientemente simile a CP43 da interagire efficacemente con le altre subunità del core del PS II e assemblare un complesso funzionale, è evidente che il sito donatore dell'ipotetico CP43'-conjugated PSII risulterebbe alterato rispetto a quello del PSII.

In seguito alla separazione di carica indotta dall'energia luminosa, $P680^+$ viene ri-ridotto nel PSII utilizzando elettroni forniti dall'acqua attraverso il ciclo di Kok. L'ossidazione dell'acqua, catalizzata dal cluster calcio-manganese, avviene in una nicchia del complesso proteico essenzialmente formata dai domini lumenali delle due proteine intrinseche D1 (PsbA) e CP43 (PsbC) e dalla proteina estrinseca PsbO (De Las Rivas e Barber, 2004). La presenza di questo intorno proteico, responsabile per l'efficacia dell'evento catalitico, costituisce un ingombro sterico che rende P680 inaccessibile sul lato donatore.

L'assenza del loop lumenale nell'ipotetico CP43'-conjugated PSII comporterebbe molto verosimilmente la perdita di PsbO, che si lega al core del PSII interagendo proprio con i loop di CP43 e D1, così come

quella delle altre due piccole proteine estrinseche presenti sul lato lumenale (PsbV e PsbU). Il complesso non sarebbe in grado, di conseguenza, di legare in modo stabile il cluster calcio-manganese. Il sito donatore dell'ipotetico complesso sarebbe di conseguenza accessibile a piccole molecole in grado di trasferire un elettrone al centro di reazione P680. In questo senso il fotosistema che verrebbe a formarsi avrebbe le stesse caratteristiche strutturali del fotosistema dei proteobatteri.

Il fotosistema di tipo secondo dei proteobatteri ha struttura e funzionamento analoghi a quelli del PSII degli organismi evolventi ossigeno, ma non è in grado di catalizzare l'idrolisi dell'acqua. Il complesso di cui i proteobatteri dispongono non ha subunità proteiche sul lato donatore, che risulta pertanto normalmente accessibile. In seguito a ciascun evento fotochimico primario un elettrone viene trasferito sul lato opposto della membrana attraverso la catena di trasporto elettronico e plastochinone in forma ridotta viene accumulato (QH_2). Gli elettroni vengono trasportati indietro attraverso la membrana da un complesso proteico di tipo cyt bc_1 e trasferirti di nuovo al centro di reazione, da cui erano originati, per via di un citocromo solubile (cyt c_2). Il risultato è un flusso ciclico di elettroni attorno al centro di reazione alimentato dalla luce, a cui è associata la formazione di un gradiente protonico transmembrana e di conseguenza la produzione di ATP per accoppiamento chemiosmotico.

Se un trasportatore solubile, la cui riduzione è alimentata dall'attività del CP43-conjugated PSII, fosse in grado di agire come donatore di elettroni per la clorofilla eccitata del centro di reazione P680, un flusso ciclico di elettroni, del tutto analogo a quello appena descritto per il fotosistema proteobatterico, avrebbe luogo intorno all'ipotetico fotosistema. Un interessante candidato in grado di assolvere questo compito potrebbe essere la plastocianina. La plastocianina ridotta ha un potenziale medio misurato di +370mV, che le consente di donare un elettrone alla clorofilla eccitata $P700^+$ del centro di reazione del PSI (E_m +500mV). Poiché il potenziale della coppia $P680/P680^+$ del PSII è di +1.2V, la plastocianina è termodinamicamente in grado di ridurre anche il centro di reazione del PSII, sebbene questo normalmente non avvenga a causa dell'impedimento sterico intorno al sito donatore. Evidenze sperimentali di ossidazione diretta della plastocianina da parte di subcomplessi di PSII sono riportate in letteratura (Arnon e Barber, 1990). Plastocianina in forma ridotta è inoltre verosimilmente disponibile in cianobatteri cresciuti in stress da ferro, in quanto, in queste cellule, la presenza di PSII attivo ed in grado di evolvere ossigeno è misurabile, sebbene risulti in concentrazioni ridotte, e si registra anche attività del PSI (Ivanov et al., 2000).

L'ipotesi alla base del nostro lavoro sperimentale può essere pertanto riassunta nel seguente modo: se CP43', che è espressa ad alti livelli in carenza di ferro, è in grado di associarsi con le proteine del core del PSII e dar luogo ad un complesso stabile, il risultante fotosistema potrebbe avere caratteristiche strutturali e funzionali simili a quelle del fotosistema protobatterico e dar luogo ad un flusso ciclico di elettroni, plastocianina mediato, con risultante produzione netta di ATP.

Il lavoro sperimentale svolto aveva il proposito di verificare se un complesso tipo PSII in cui CP43' fosse presente in sostituzione di CP43 fosse presente in cianobatteri cresciuti in concentrazioni subottimali di ferro.
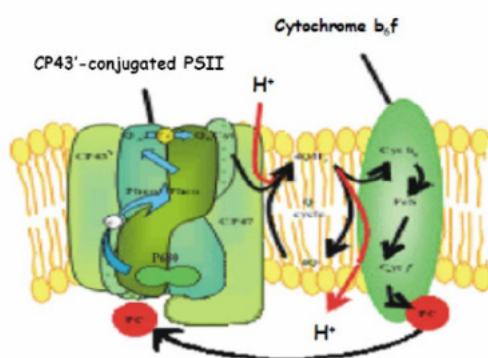

Figura 1 Rappresentazione schematica dell'ipotetico CP43'-conjugated PSII e del suo funzionamento.

1.2 Strategia sperimentale

Al fine di verificare se un fotosistema di tipo PSII, in cui CP43' sostituisce CP43, fosse presente in cianobatteri in stress da ferro, abbiamo deciso di isolare e comparare campioni di PSII ottenuti da colture di *Synechocystis* cresciute in condizioni standard e a basse concentrazioni di ferro.

Diverse strategie sono state utilizzate per la coltura dei batteri e alcune analisi sono state effettuate per verificare che si registrasse la risposta attesa, quando le cellule venivano trasferite in terreno privo di ferro, e che tuttavia le colture fossero vitali.

Il PSII è stato purificato utilizzando due diverse strategie: cromatografia di affinità e cromatografia a scambio anionico. La composizione oligomerica dei risultanti campioni è stata analizzata e una seconda cromatografia a scambio anionico è stata applicata, in entrambi i casi, per separare le sottopopolazioni di Fotosistema II. I complessi così purificati sono stati analizzati tramite SDS-PAGE per definirne la composizione in termini di subunità e l'attività di evoluzione di ossigeno è stata misurata nei vari campioni. I risultati ottenuti dalle colture parallele più e meno ferro, sono

stati comparati per controllare se fosse presente, esclusivamente nelle cellule in stress da ferro, una ulteriore sottopopolazione di PS II.

Al fine di mettere in evidenza la presenza di un complesso stabile del tipo ipotizzato, nell'eventualità che questo si trovasse nella cellula a basse concentrazioni, le stesse preparazioni sono state effettuate da un mutante di *Synechocystis* in cui il gene codificante per CP43 era stata deleto.

1.3 Risultati

1.3.1 *Purificazione del PS II da culture di Synechocystis PCC 6803*

Una prospetto riassuntivo dei risultati ottenuti dall'applicazione della procedura di purificazione del PSII alle diverse colture di *Synechocystis* utilizzate in questo lavoro sperimentale è presentato in Tabella 1.

La resa della purificazione è espressa in termini di contenuto totale di clorofilla in ciascuno dei campioni, mentre l'integrità, l'attività e la concentrazione del Fotosistema II durante i vari passaggi del processo di purificazione sono state monitorate misurando l'evoluzione di ossigeno in risposta alla luce. L'attività di evoluzione di ossigeno misurata nelle cellule e nei tilacoidi in stress da ferro risulta in ogni caso minore di quella registrata nei campioni di controllo. A questo stadio della preparazione ad un valore più basso di attività corrisponde una minor concentrazione di PS II nel campione esaminato, normalizzato rispetto al contenuto di clorofilla. Nelle cellule in stress da ferro infatti la più abbondante proteina capace di legare clorofilla è CP43'. Ne risulta di conseguenza che, comparando un campione meno ferro con il suo controllo, ad una pari concentrazione di clorofilla, corrisponderà una diversa concentrazione di PSII. Dai campioni di PSII purificati da colture in stress da ferro, valori di attività che variavano da zero fino a quelli registrati per le migliori preparazioni +Fe sono stati misurati. Questo risultato sembra essere dipendente principalmente dalla qualità della preparazione, più che da una risposta del complesso fotosintetico alla carenza di ferro. L'unica differenza che è stato possibile rilevare infatti fra le diverse preparazioni, a cui valori così variabili di attività sono stati associati, è sembrata essere la maggiore o minore integrità e purezza del complesso. In tutte le preparazioni in ogni caso si nota una totale perdita di attività dopo il secondo passaggio cromatografico, associata alla perdita delle proteine estrinseche (analizzata tramite SDS-PAGE). Nessuna attività si regista in alcuno dei passaggi della preparazione da cellule ΔCP43-CP47His tagged. E' interessante notare che la resa della preparazione nel caso del mutante di delezione per CP43 è identica nei campioni cresciuti in stress da ferro e nei controlli. Sembra pertanto che nessuna stabilizzazione del complesso purificato sia stata introdotta dall'espressione di CP43'.

CAMPIONI	Purificazione del PS II da *Synechocystis* 6803 **+Fe**			Purificazione del PS II da *Synechocystis* 6803 **-Fe**		
	totale clorofilla [a]	Evoluzione di ossigeno [b]	resa [c]	totale clorofilla [a]	Evoluzione di ossigeno [b]	resa [c]
Coltura cellulare (18L)	30-40	500-550	100	30-40	400-550	100
Cellule risospese in washing buffer	30-35	500-550	92	30-35	400-550	92
Omogenato cellulare	20-25	250-300	65	20-25	100-170	65
Tilacoidi	20	300-400	57	15-20	190-250	50
Tilacoidi dopo la solubilizzazione	15-20	300-400	50	10-15	180-200	36
Cromatografia a scambio ionico — Oligomeri di PSI	6-8	0 (control)	20	4-4,5	0 (control)	12
Frazione contenente PS II (I cromatografia)	1,5-2	1500	5	0,7-1,1	0-1200	2,7
Sottopopolazioni di PS II (II cromatografia)	1-1,5	0	3,5	0,5-0,9	0	2
Cromatografia per affinità — eluente	4,5-5	0 (control)	15	6-8	0 (control)	20
Frazione contenente PS II (I cromatografia)	1,5-1,8	600-800	4,7	1-1,6	0-800	3,3
Sottopopolazioni di PS II (II cromatografia)	1-1,5	0	3,5	0,5-0,7	0	1,7
cromatografia per affinità da mutanti deltaCP43 — eluente	6-8	0 (control)	20	//	//	//
Frazione contenente PS II (I cromatografia)	0,5-0,6	0	1,6	0,5-0,6	0	1,6
Sottopopolazioni di PS II (II cromatografia)	0,2-0,3	0	0,7	0,2-0,3	0	0,7

[a] Milligrammi di clorofilla; [b] Micromoli di O_2 per milligrammo di clorofilla all'ora; [c] Percentuale di clorofilla

Tabella 1 Riassunto della purificazione di complessi fotosintetici da *Synechocystis* PCC 6803 strains dwt, HT3A e ΔCP43-CP47His tagged, cresciuti in concentrazioni standard di ferro e in stress da ferro. I valori riportati per la preparazione delle membrane tilacoidali (prime 4 righe) rappresentano valori medi, per i quali nessuna rilevante differenza è stata registrata fra le colture dwt e HT3A. Analoghi valori sono stati registrati per le colture del mutante di delezione per CP43, con l'unica variante che l'attività di evoluzione di ossigeno era pari zero in tutti gli stadi della preparazione.

Dall'analisi dei campioni purificati sono stati ottenuti i seguenti dati:

- Dalla purificazione per mezzo di cromatografia di affinità si sono ottenuti complessi per la maggior parte integri, e di conseguenza attivi. Non si è però riuscita ad evitare la copurificazione di un numero di altre proteine, fra le quali in ogni caso non compare CP43', nel caso dei campioni in stress da ferro. Dal primo passaggio cromatografico si ottengono complessi in stato dimerico e monomerico. La seconda cromatografia separa i due diversi stati oligomerici. Nessuna differenza è stata rilevata fra campioni –Fe e controlli, che presentano analogo profilo in cromatografia ad esclusione molecolare e stesso profilo di eluizione durante il secondo passaggio cromatografico. E' rilevante però notare che l'analisi tramite SDS-PAGE (Figura 2) della composizione proteica delle due frazioni ottenute dopo questa seconda cromatografia, mette in evidenza la presenza di una banda nei campioni meno ferro, che non è visibile nei controlli, e che è rilevabile sia nei monomeri che nei dimeri. La banda migra in posizione compatibile con quella attesa per CP43' e l'ipotesi di copurificazione a questo stadio sembra abbastanza improbabile.
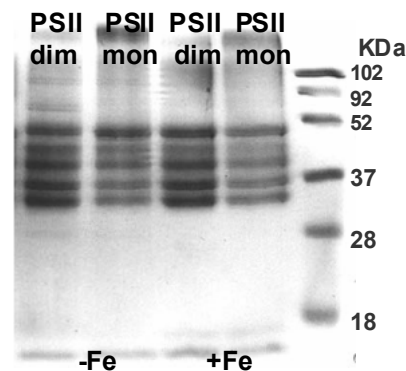

Figura 2. SDS-PAGE delle due frazioni ottenute da campioni più e meno ferro a seguito del secondo passaggio cromatografico ed identificate tramite cromatografia ad esclusione molecolare come dimeri e monomeri.

- L'applicazione della stessa procedura di purificazione ha permesso di isolare, da cellule ΔCP43-CP47His tagged una popolazione mista composta dalla sola proteina CP47 e da complessi contenenti CP47, D_1, D_2, PsbE e PsbF (CP47-RC). Il secondo passaggio cromatografico ha consentito di isolare una frazione omogenea di CP47-RC. Anche in questo caso si sono ottenuti per i campioni più e meno ferro stessi profili di eluizione sia nell'analisi tramite cromatografia a esclusione molecolare sia nel secondo passaggio di purificazione tramite cromatografia a scambio anionico. Anche in questi campioni la presenza di una ulteriore banda (Figura 3) è stata rilevata in SDS-PAGE nei complessi meno ferro, che non è invece visibile nei controlli.

- Dalle particelle di PSII isolate tramite cromatografia a scambio ionico da colture cresciute in presenza di ferro si sono ottenute 3 subpopolazioni a seguito del secondo passaggio cromatografico. Per ragioni legate alla lunghezza della procedura lo stato oligomerico di ciascuna frazione non è mai stato analizzato. Nell'analoga preparazione da colture in stress da ferro una significativa copurificazione di CP43' con la frazione contenente PSII era evidente dopo la prima cromatografia e pertanto si è deciso di inserire un ulteriore passaggio di centrifugazione in gradiente prima di applicare i campioni alla seconda colonna a scambio anionico. I campioni di PSII così isolati hanno comunque dato luogo a tre picchi di assorbimento a 280 e 430nm esattamente come il controllo. Anche in questo caso, dopo il secondo passaggio cromatografico, una banda delle dimensioni di CP43' è presente in tutte le frazioni –Fe (Figura 3). Considerando la procedura utilizzata l'ipotesi di una semplice copurificazione della proteina risulta ancora meno probabile.
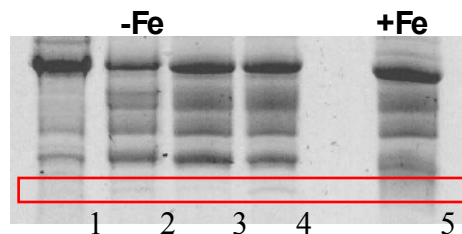

Figura 3. SDS-PAGE delle particelle di PSII isolate utilizzando due passaggi cromatografici da cellule ΔCP43-CP47His tagged (1) e wt (2; 3; 4). Nell'ultima lane (5) è stato caricato un controllo +Fe wt. Nei campioni –Fe una banda molto debole (individuata dal un rettangolo rosso in figura) è presente. La banda non è visibile nel controllo wt.
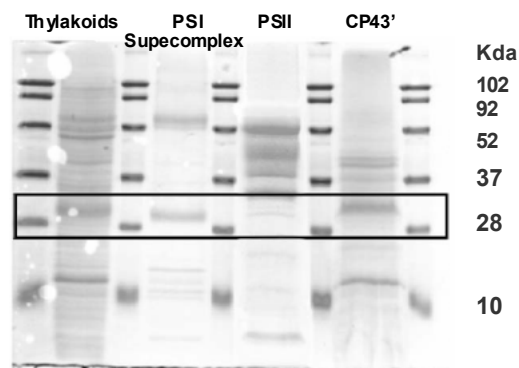

Figura 4. SDS-PAGE dei campioni ottenuti da colture cresciute in stress da ferro. Il rettangolo individua una banda presente in tutti i campioni verosimilmente identificabile come CP43'. La proteina sembra essere presente, sebbene in minor concentrazione anche nella lane dove è stato caricato il PSII ottenuto da cellule wt –Fe dopo due passaggi cromatografici.

1.3.2 *Purificazione del Supercomplesso PSI-CP43'*

Il sistema utilizzato per isolare frazioni contenenti PSII da cellule wt cresciute a basse concentrazioni di ferro è risultato utile anche per la purificazione di un ulteriore complesso di particolare interesse: il Supercomplesso PSI-CP43'. Il Supercomplesso è costituito da trimeri di Fotosistema I, circondati da una extra antenna di 18 subunità di CP43', che si assembla esclusivamente in condizioni di stress da ferro.

Durante la corsa cromatografica (descritta nel capitolo "Materials and Methods" al paragrafo 2.5), dalla colonna a scambio ionico debole due frazioni venivano eluite in 50mM $MgSO_4$ che risultavano identificabili con il complesso in questione. Utilizzando un ulteriore volume di buffer B' contenente 100mM $MgSO_4$ una terza frazione è stata eluita, con picchi di assorbimento a 280nm e 430nm (indicativi di proteine in grado di legare clorofilla). L'analisi tramite cromatografia ad esclusione molecolare e tramite SDS-PAGE di quest'ultima frazione ha permesso di identificare il campione ancora come Supercomplesso PSI-CP43' ed ha inoltre messo in evidenza che, almeno a questo livello di sensibilità, le particelle isolate sono omogenee dal punto di vista della struttura quaternaria e nessuna evidenza è stata trovata della copurificazione di eventuali altre proteine con quella di interesse. Questo sistema di purificazione è utilizzato al momento nel gruppo del Professor Barber per l'allestimento di prove di cristallizzazione del Supercomplesso.
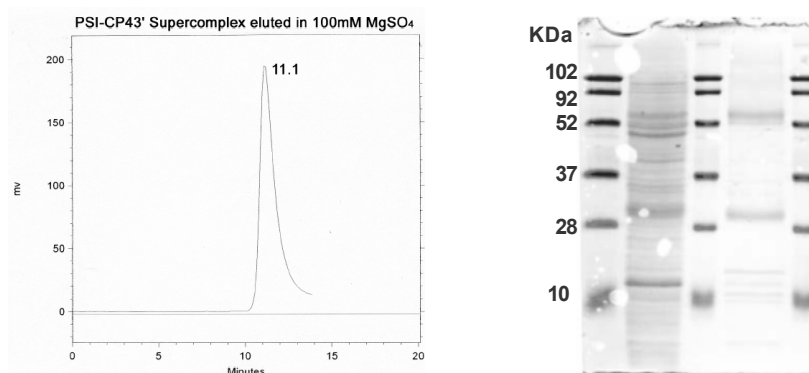

Figure 1. Cromatografia ad esclusione molecolare (sinistra) e SDS-PAGE (destra) della frazione eluita dalla colonna DEAE in 100mM $MgSO_4$ durante la separazione di complessi fotosintetici da colture di *Synechocystis* **in stress da ferro.** Il picco molto netto, sulla sinistra, è indicativo di una popolazione di complessi proteici omogenea dal punto di vista delle dimensioni e della forma. Sulla destra, le bande caratteristiche delle subunità del PSI più quella identificabile con CP43' sono chiaramente visibili, mentre nessuna altra proteina sembra essere presente a questo livello di risoluzione.

1.4 Conclusioni

Utilizzando la procedura decritta non è stato possibile rilevare la presenza di alcuna ulteriore subpopolazione di PSII in cellule cresciute in stress da ferro, che presentasse dimensioni o profilo di eluizione distinti rispetto a quelli dei complessi presenti anche nel controllo.

E' stata tuttavia osservata in tutte le frazioni contenenti PSII purificate da colture –Fe, la presenza di una proteina, verosimilmente identificabile con CP43', che non appare nei rispettivi campioni di controllo +Fe. Per identificare la banda caratteristica dei campioni –Fe si è scelto di far sequenziare la proteina separata in SDS-PAGE e trasferita su PVDF. Al momento della stesura di questa relazione non abbiamo ancora ricevuto l'informazione richiesta dall'Università di Leads dove il servizio è stato commissionato.

Poiché l'ipotesi di una semplice copurificazione dopo l'applicazione di due passaggi cromatografici e, nel caso dei preparati wt, anche di un ulteriore centrifugazione in gradiente di densità, sembra alquanto inverosimile, riteniamo che si debba piuttosto ipotizzare che la proteina sia in grado di interagire in qualche modo con il PSII.

Se la proteina in questione è in effetti CP43' è difficile sostenere che possa essere presente nel core in sostituzione di CP43. La formazione di un complesso contenente CP43' infatti, come esposto nell'introduzione, comporterebbe alterazioni strutturali rilevabili. Esistono evidenze che CP43' sia coinvolta nella dissipazione di energia in forma non radiativa in casi in cui l'afflusso di energia al PSII non è bilanciato da una altrettanto rapida ossidazione del pool dei plastochinoni (Sandstrom et al., 2001; Ihalainen et al., 2005). Alla luce di queste evidenze è ragionevole ipotizzare che alcune copie della proteina, presente in abbondanza nella cellula, si trovino ad interagire con il Fotosistema II con funzione di fotoprotezione e che queste vengano purificate insieme al PSII isolato in diverse forme oligomeriche.

Si osserva in generale che quando due o più proteine sono coinvolte nella formazione di un complesso, i residui chiave, che si trovano all'interfaccia fra le varie subunità, risultano strettamente conservati o evidenziano coevoluzione. Poichè la funzione principale per cui CP43' è stata selezionata e quella di assemblare un complesso antenna in grado di trasmettere energia al PSI (Bibby et al., 2001) è perfettamente possibile che, se anche si assuma che CP43' e CP43 siano omologhe, CP43' non sia in grado di interagire efficacemente con D_1 e le altre subunità del PSII e pertanto non si abbia formazione di un complesso sufficientemente stabile in presenza di CP43'.

References

Abrahams, J.P., Leslie, A.G., Lutter, R., Walker, J.E. (1994) Structure at 2.8 A resolution of F1-ATPase from bovine heart mitochondria. Nature 370(6491):621-8.

Allen, J.P., Feher, G., Yeates, T.O., Komiya, H., Rees, D.C. (1988) Structure of the reaction center from Rhodobacter sphaeroides R-26: protein-cofactor (quinones and Fe2+) interactions. *Proc. Natl. Acad. Sci. U.S.A.* 85(22):8487-91.

Allen, M. M. (1968) Simple conditions for growth of unicellular blue-green algae on plates. J. Phycol. 4: 1-4.

Arnon, D. I. (1995) Divergent pathways of photosynthetic electron transfer: The autonomous oxygenic and anoxygenic photosystem s. *Photosynth Res* 46: 47-71.

Arnon, D. I. and Barber, J. (1990) Photoreduction of NADP+ by isolated reaction centers of photosystem II: requirement for plastocyanin. Proc Natl Acad Sci U S A. 87(15):5930-4.

Aspinwall, C.L., Sarcina, M., Mullineaux, C.W. (2004) Phycobilisome Mobility in the Cyanobacterium Synechococcus sp. PCC7942 is Influenced by the Trimerisation of Photosystem I. *Photosynth Res.* 79:179-87.

Barbato R, Friso G, Rigoni F, Dalla Vecchia F, Giacometti GM. Structural changes and lateral redistribution of photosystem II during donor side photoinhibition of thylakoids. *J Cell Biol.* 119(2):325-35.

Barber, J. (2003) Photosystem II: The engine of life. *Biophys. Quart. Revs.* 36: 71-89.

Barber, J. (2004) Towards a full understanding of water splitting in photosynthesis. Int. *J. Photoenergy* 6: 43-51.

Barber, J. (2004) Water, water everywhere, and its remarkable chemistry. *BBA-Bioenerg.* 1655: 123-132.

Barber, J. and Archer, M.D. (2001) P680, the primary electron donor of photosystem II. *J Photochem Photobiol A* 142: 97-106.

Barber, J. et al. (1997) *Physiol. Plantarum.* 100:817-827.

Barber, J., Ferreira, K., Maghlaoui, K. and Iwata, S. (2004). Structure of the oxygen evolving centre of photosystem II with mechanistic implications. *PhotoChem. Chem. Phys.* 6: 4737-4742.

Barter, L. M. C., Durrant, J. R. and Klug, D. R. (2003) A quantitative structure–function relationship for the Photosystem II reaction center: Supermolecular behavior in natural photosynthesis. *PNAS* 100: 946–951

Barter, L. M. C., Durrant, J. R., Klug, D. R. (2003) A quantitative structure-function relationship for the Photosystem II reaction center: supermolecular behavior in natural photosynthesis. *PNAS .* 100(3):946-51.

Bibby, T. S., Nield, J., and Barber, J. (2001). Three-dimensional model and characterization of the iron stress-induced CP43'-photosystem I supercomplex isolated from the cyanobacterium Synechocystis PCC 6803. *J. Biol. Chem.* 276, 43246-43252.

Bibby, T. S., Nieldm, J. and Barber, J. (2001). Iron deficiency induces the formation of an antenna ring around trimeric photosystem I in cyanobacteria. *Nature* 412, 743-745.

Blankenship R.E. (1992) Origin and early evolution of photosynthesis. *Photosynth Res.* 33:91-111.

Boekema, E. J. et al. (1995). Supramolecular structure of the photosystem II complex from green plants and cyanobacteria. *Proc. Natl. Acad. Sci.* 92: 175-179.

Boyer, P.D. (1989) A perspective of the binding change mechanism for ATP synthesis. *FASEB J.* 3(10):2164-78.

Boyer, P.D. (1993) The binding change mechanism for ATP synthase--some probabilities and possibilities. *Biochim Biophys Acta* 1140(3):215-50.

Bricker, T. M., Morvant, J., Marsi, N., Sutton, H. M. and Frankel, L. K. (1998). Isolation of a highly active photosystem II preparation from Synechocystis 6803 using a histidine-tagged mutant of CP47. *Biochim. Biophis. Acta* 1409: 50-57.

Bricker, T.M. and Frankel, L.K. (2002) The structure and function of CP47 and CP43 in photosystem II. *Photosynth. Res.* 72:131–46.

Britt, R.D, Peloquin, J.M., Campbell, K.A. (2000) Pulsed and parallel-polarization EPR characterization of the photosystem II oxygen-evolving complex. *Annu. Rev. Biophys. Biomol.*

Capaldi, R.A., Schulenberg, B. (2000) The epsilon subunit of bacterial and chloroplast F(1)F(0) ATPases. Structure, arrangement, and role of the epsilon subunit in energy coupling within the complex. *Biochim Biophys Acta*.1458(2-3):263-9.

Chen, M. and Bibby, T. S. (2005) Photosynthetic apparatus of antenna-reaction centres supercomplexes in oxyphotobacteria: insight through significance of Pcb/IsiA proteins. *Photosynthesis Research* 86: 165–173.

Cramer, W. A., Theg, S. M. and Widger, W. R. (1986) On the structure and function of cytochrome b-559. *Photosynth. Res.* 10: 393–403.

Danielsson R., Albertsson P.A., Mamedov F., Styring S. (2004) Quantification of photosystem I and II in different parts of the thylakoid membrane from spinach. *Biochim Biophys Acta* 1608(1):53-61.

Debus,R J., Stickler, M. A., Walker, L. M. and Hillier, W. (2005) No evidence from FTIR difference spectroscopy that aspartate-170 of the D1 polypeptide ligates a manganese ion that undergoes oxidation during the S0 to S1, S1 to S2, or S2 to S3 transitions in photosystem II. *Biochemistry* 44(5):1367-74.

Deisenhofer, J., Miki, K., Huber, R. and Michel, H. (1985) Structure of the protein subunits in the photosynthetic reaction centre of Rhodopseudomonas viridis at 3Å resolution. *Nature* 318: 618-623.

Deisenhofer. J. and Michel, H. (1989) Nobel lecture. The photosynthetic reaction centre from the purple bacterium Rhodopseudomonas viridis. *EMBO J.* 8:2149–70.

Diner, B.A. and Rappaport, F. (2002) Structure, dynamics, and energetics of the primary photochemistry of photosystem II of oxygenic photosynthesis. *Annu. Rev. Plant Biol.* 53:551–80.

Diner, B.A., Schlodder, E., Nixon, P.J., Coleman, W.J., Rappaport, F., Lavergne, J., Vermaas, W.F., Chisholm, D.A. (2001) Site-directed mutations at D1-His198 and D2-His197 of photosystem II in Synechocystis PCC 6803: sites of primary charge separation and cation and triplet stabilization. *Biochemistry* 40(31):9265-81.

Dmitriev, O.Y., Jones, P.C., Fillingame, R.H. (1999) Structure of the subunit c oligomer in the F1Fo ATP synthase: model derived from solution structure of the monomer and cross-linking in the native enzyme. *PNAS* 96(14):7785-90.

Dühring, U., Axmann, I. M., Hess, W. R. and Wilde A. (2006) An internal antisense RNA regulates expression of the hotosynthesis gene isiA. *PNAS* 103, 18: 7054-7058.

Duncan, J., Bibby, T., Tanaka, A. and Barber, J. (2003). Exploring the ability of chlorophyll b to bind to the CP43' protein induced under iron deprivation in a mutant of Synechocystis PCC 6803 containing the cao gene. *FEBS Letters* 541: 171-175.

Durrant JR, Klug DR, Kwa SL, van Grondelle R, Porter G, Dekker JP. (1995) A multimer model for P680, the primary electron donor of photosystem II. *PNAS* . 92(11):4798-802.

Ferreira, K. N., Iverson, T. M., Maghlaoui, K., Barber, J. and Iwata, S. (2004) Architecture of the photosynthetic oxygen-evolving center. *Science* 303 1831-1838.

Girvin, M.E., Rastogi, V.K., Abildgaard, F., Markley, J.L., Fillingame, R.H. (1998) Solution structure of the transmembrane H+-transporting subunit c of the F1F0 ATP synthase. *Biochemistry.* 37(25):8817-24.

Glazer, A.N. (1985) Light harvesting by phycobilisomes. *Annu Rev Biophys Biophys Chem.* 14:47-77.

Glazer, A.N. (1989) Light guides. Directional energy transfer in a photosynthetic antenna. *J Biol Chem* 264:1-4.
Golbeck, J. H. (1999) A comparative analysis of the spin state distribution of in vitro and in vivo mutants of PsaC. *Photosynth. Res.* 61: 107-144.

Guergova-Kuras, M., Boudreaux, B., Joliot, A., Joliot, P. & Redding, K. (2001) Evidence for two active branches for electron transfer in Photosystem I. *Proc. Natl Acad. Sci. USA* 98: 4437-4442.

Haag, E., Eaton-Rye, J. J., Renger, G. and Vermaas, W. F. J. (1993). Functionally important domains of the large hydrophilic loop of CP47 as probed by oligonucleotide-directed mutagenesis in Synechocystis sp. PCC 6803. *Biochemistry* 32: 4444-4454.

Harauz, G., Boekema, E. and Van Hell, M. (1998). Statistycal Immage Analysis of Electron Micrographs of Ribosomal Subunits. *Methods in Enzimology* 164: 35-48

Hastings G., Kleinherenbrink F.A., Lin S.and Blankenship R.E. (1994) Time-resolved fluorescence and absorption spectroscopy of photosystem I. *Biochemistry* 33(11):3185-92.

Havaux, M., Guedeney, G., Hagemann, M., Yeremenko, N., Matthijs, H. C. P., Jeanjean, R. (2005). The chlorophyll.binding protein IsiA is inducible by high light and protects the cyanobacteria Synechocystis PCC6803 from photooxidative stress. *FEBS Letters* 559: 2289-2293.

Hihara, Y., Sonoike, K., and Ikeuchi, M. (1998). A Novel Gene, pmgA, Specifically Regulates Photosystem Stoichiometry in the Cyanobacterium Synechocystis Species PCC 6803 in Response to High Light. *Plant Physiol.* 117: 1205–1216.

Huang X. and Miller W. (1991). A Time-Efficient, Linear-Space Local Similarity Algorithm. *Adv. in Applied Mathematics*. 12: 337-357.

Hangarter, R. and Ort, D. R. (1985) Cooperation among electron-transfer complexes in ATP synthesis in chloroplasts. Eur J Biochem. 149(3):503-10.

Huang, F. , Fulda, S., Hagemann, M. and Norling B. (2006) Proteomic screening of salt-stress-induced changes in plasma membranes of Synechocystis sp. strain PCC 6803 *Proteomics* 6: 910–920

Huber, R. (1989) Nobel lecture. A structural basis of light energy and electron transfer in biology. *EMBO J.* 8(8):2125-47.

Ihalainen, J. A. et al , (2005). Aggregates of the Chlorophyll-Binding Protein IsiA (CP43') Dissipate Energy in Cyanobacteria. *Biochemistry* 44: 10846-10853.

Ivanov, A.G., Park, Y.-I., Miskiewicz, E., Raven, J.A., Huner, N.P.A., Öquist, G. (2000) Iron stress restricts photosynthetic intersystem electron transport in Synechococcus sp. PCC 7942. *FEBS Letters* 485:173-177

Iwata, S., Barber, J. (2004). Structure of photosystem II and molecular architecture of the oxygen-evolving centre. *Curr Opin Struct Biol.* 14: 447-453.

Dekker, J.P., van Grondelle, R. (2000) Primary charge separation in Photosystem II. *Photosynth Res.* 63(3):195-208.

Jeanjean, R., Zuther, E., Yeremenko, N., Havaux, M., Matthijs, H. C.P., Hagemann, M. (2003). A photosystem 1 psaFJ-null mutant of the cyanobacterium Synechocystis PCC 6803 expresses the isiAB operon under iron replete conditions. *FEBS Letters* 549: 52-56.

Jiang, W., Fillingame, R.H. (1998) Interacting helical faces of subunits a and c in the F1Fo ATP synthase of Escherichia coli defined by disulfide cross-linking. *PNAS* 95(12):6607-12.

Joliot, P. & Joliot, A. (1999) In vivo analysis of the electron transfer within photosystem I: are the two phylloquinones involved? *Biochemistry* 38:11130-11136.

Jordan, P., Fromme, P., Witt, H. T., Klukas, O., Saenger, W. And Krauss, N. (2001). Three-dimensional structure of cyanobacterial photosystem I at 2.5 Å resolution. *Nature* 441: 909-917.

Kamiya, N. and Shen, J. R. (2003) Crystal structure of oxygen-evolving photosystem II from Thermosynechococcus vulcanus at 3.7Å resolution. *Proc. Natl Acad. Sci. USA* 100: 98-103.

Karrasch, S., Walker, J.E. (1999) Novel features in the structure of bovine ATP synthase. *J Mol Biol.* 290:379-84.

Kashino, Y., Lauber, W. M., Carroll, J. A., Wang, Q., Whitmarsh, J., Satoh, K. and Pakrasi, H. B. (2002). Proteomic Analysis of a Highly Active Photosystem II Preparation from the Cyanobacterium Synechocystis sp. PCC 6803 Reveals the Presence of Novel Polypeptides. *Biochemistry* 41(25):8004-8012

Kern, J., Loll, B., Lqneberg, C., Di Fiore, D., Biesiadka, J., Irrgang, K.-D., Zouni, A. (2005) Purification, characterisation and crystallisation of photosystem II from Thermosynechococcus elongatus cultivated in a new type of photobioreactor. Biochim. et Biophys. Acta 1706: 147–157.

Kirilovsky, D. and Ohad, I. (1986) Functional assembly in vitro of phycobilisomes with isolated photosystem II particles of eukaryotic chloroplasts. *J Biol Chem.* 261(26):12317-23.

Klein, M.P., Sauer, K. and Yachandra, V.K. (1993) Perspectives on the structure of the photosynthetic oxygen-evolving manganese complex and its relation to the Kok cycle. *Photosynth. Res.* 38:265–77.

Kouril, R., Arteni, A.A., Lax, J., Yeremenko, N., D'Haen, S., Rögner, M., Matthijs, H. C., Dekker, J. P., Boekema, E. J. (2005) Structure and functional role of supercomplexes of IsiA and Photosystem I in cyanobacterial photosynthesis. *FEBS Lett.* 579 (15): 3253-7.

Kruip J.,Chitnis P.R.,Lagoutte B.,Rogner M., Boekema E.J. (1997) Structural organization of the major subunits in cyanobacterial photosystem 1. Localization of subunits PsaC, -D, -E, -F, and -J. *J Biol Chem.* 272:17061-9.

Kühlbrandt, W. (2003) Dual approach to a light problem. *Nature* 426:399-400.

Kurisu, G., Zhang, H., Smith, J. L., Cramer W. A. (2003) Structure of the Cytochrome b6f Complex of Oxygenic Photosynthesis: Tuning the Cavity. *Science* 302:1009-1014.

Lake J.A., Clark M.W., Henderson E., Fay S.P., Oakes M., Scheinman A., Thornber J.P., Mah R.A. (1985) Eubacteria, halobacteria, and the origin of photosynthesis: the photocytes. *PNAS* 82(11):3716-20.

Lakshmi, K. V., Reifler, M. J., Chisholm, D. A., Wang, J. Y., Diner, B. A. and Brudvig, G. W. (2002) Correlation of the cytochrome c_{550} content of cyanobacterial Photosystem II with the EPR properties of the oxygen-evolving complex. *Photosynthesis Research* 72: 175–189.

Lancaster, C. R. D., Bibikova, M. V., Sabatino, P., Oesterhelt, D. & Michel, H. (2000) Structural basis of the drastically increased initial electron transfer rate in the reaction center from a Rhodopseudomonas viridis mutant described at 2.00-AÊ resolution. *J. Biol. Chem.* 275: 39364-39368.

Latifi, A., Jeanjean, R., Lemeille, S., Havaux, M. and Zhang, C. (2005) Iron Starvation Leads to Oxidative Stress in Anabaena sp. Strain PCC 7120 *Journ. of Bacteriol.* 187 (18): 6596–6598.

Leonhardt, K. and Straus, N.A. (1994). Photosystem II genes isiA, psbDI and PsbC in Anabaena sp. PCC 7120: cloning, sequencing and the trascriptional regulation in iron-stressed and iron-repleted cells. *Plant. Mol. Biol.* 24: 63-73.

Leslie, A. G. W. and Walker, J. E. (2000) Structural model of F1-ATPase and the implications for rotary catalysis. *Philos Trans R Soc Lond B Biol Sci.* 355(1396):465-71.

Li, H., Singh, A. K, McIntyre, L. M. and Sherman L. A. (2004). Differential Gene Expression in Response to Hydrogen Peroxide and the Putative PerR Regulon of *Synechocystis* sp. Strain PCC 6803. *Juorn. Of Bacteriol.* 186: 3331–3345.

Lichtenthaler, H. K. (1987). Chlorophylls and carotenoids, the pigments of photosynthetic biomembranes. In *Methods in Enziomology*, R. Douce and L. Packer, eds.(New York, Academic press inc), pp. 350-382.

Liu, X., Zhao, J. and Wu Q. (2006) Biogenesis of Chlorophyll-Binding Proteins under Iron Stress in Synechocystis sp. PCC 6803. *Biochemistry (Moscow)* 71 (1): S101-S104.

MacColl R. (1998) Cyanobacterial phycobilisomes. *J Struct Biol.* 124(2-3):311-34.

Margulis L. Archaeal-eubacterial mergers in the origin of Eukarya: phylogenetic classification of life (1996) *PNAS* 93(3):1071-6.

Maxson P., Sauer K., Zhou J.H., Bryant D.A., Glazer A.N.(1989) Spectroscopic studies of cyanobacterial phycobilisomes lacking core polypeptides. Biochim Biophys Acta. 977(1):40-51.

Miller M.J., Oldenburg M., Fillingame R.H. (1990) The essential carboxyl group in subunit c of the F_1F_0 ATP synthase can be moved and H(+)-translocating function retained. *PNAS* 87(13):4900-4.

Mitchell, P. (1961) Coupling of phosphorylation to electron and hydrogen transfer by a chemi-osmotic type of mechanism.. *Nature* 191:144-148.

Mitchell, P. (1966) Chemiosmotic coupling in oxidative and photosynthetic phosphorylation. *Biol Rev Camb Philos Soc.* 41(3):445-502.

Morais, F., Kuhn, K., Stewart, D.H., Barber, J., Brudvig, G.W. and Nixon, P.J. (2001) Photosynthetic water oxidation in cytochrome b559 mutants containing a disrupted heme-binding pocket. *J. Biol. Chem.* 276:31986–93.

Mulkidjanian, A.Y., Cherepanov, D. A., Heberle, J. and Junge, W. (2005) Proton transfer dynamics at membrane/water interface and mechanism of biological energy conversion. Biochemistry (Mosc). 70(2):251-6.

Murray, J. W., Duncan, J. and Barber, J. (2006) CP43-like chlorophyll binding proteins: structural and evolutionary implications. *Trends in Plant Science* 11(3):152-8.

Nakamoto, R.K. (1999)<Molecular Features of Energy Coupling in the F(0)F(1) ATP Synthase. *News Physiol Sci.* 14:40-46.

Nelson, N. and Yocum, C. F. (2006) Structure and Function of Photosystems I and II. *Annu. Rev. Plant Biol.* 2006. 57:521–65.

Nitschke W., Rutherford A.W. (1991) Photosynthetic reaction centres: variations on a common structural theme? *Trends Biochem Sci.* 16(7):241-5.

Nogi, T. and Miki, K.(2001).Structural Basis of Bacterial Photosynthetic Reaction Centers. *J. Biochem.* 130: 319-329.

Ogilvie, I., Aggeler, R., Capaldi, R.A. (1997) Cross-linking of the delta subunit to one of the three alpha subunits has no effect on functioning, as expected if delta is a part of the stator that links the F1 and F0 parts of the Escherichia coli ATP synthase. *J Biol Chem.* 272(26):16652-6.

Peloquin, J.M., Campbell, K.A., Randall, D.W., Evanchik, M.A., Pecoraro, V.L., et al. (2000) Mn-55 ENDOR of the S2 state multiline EPR signal of photosystem II: Implications on the structure of the tetranuclear Mn cluster. *J. Am. Chem. Soc.* 122:10926–42.

Prasil, O., Kolber, Z., Berry, J. A., and Falkowski, P. G. (1996) Cyclic electron flow around Photosystem II *in vivo. Photosynth Res* 48:395-410.

Rakhimberdieva M.G., Boichenko V.A., Karapetyan N.V., Stadnichuk I.N. (2001) Interaction of phycobilisomes with photosystem II dimers and photosystem I monomers and trimers in the cyanobacterium Spirulina platensis. *Biochemistry* 40(51):15780-8.

Rögner, M., Chisholm, D. A. and Diner, B. A. (1991) Site-Directed mutagenesis of the psbC gene of Photosystem II: isolation and functional characterization of CP43-less Photosystem II Core Complexes. *Biochemistry* 30:5387-5395.

Rosing, J. and Slater, E. C. (1972) The value of G degrees for the hydrolysis of ATP. Biochim Biophys Acta. 267(2):275-90.

Rutherford A.W. How close is the analogy between the reaction centre of photosystem II and that of purple bacteria? (1986) *Biochem Soc Trans.* 14(1):15-7.

Sambrook, J. and Russell, D. W. (2001) Molecular Cloning: A Laboratory Manual. *Cold Spring Harbor Laboratory; 3rd edition.*

Sandström, S., Park, Y., Öquist, G. and Gustafsson, P. (2001) CP43', the IsiA Gene Product, Functions as an Excitation Energy Dissipator in the Cyanobacterium Synechococcus sp. PCC7942. *Photochem. and Photobiol* 74: 431-437.

Schubert WD, Klukas O, Saenger W, Witt HT, Fromme P, Krauss N. (1998) A common ancestor for oxygenic and anoxygenic photosynthetic systems: a comparison based on the structural model of photosystem I. *J Mol Biol.* 280(2):297-314.

Senior AE. (1988) ATP synthesis by oxidative phosphorylation. *Physiol Rev* 68(1):177-231.

Senior, A. E., Nadanaciva, S., Weber, J. (2002) The molecular mechanism of ATP synthesis by F1F0-ATP synthase. *Biochimica et Biophysica Acta* 1553: 188-211.

Shen G., Boussiba S., Vermaas W.F. (1993) Synechocystis sp PCC 6803 strains lacking photosystem I and phycobilisome function. *Plant Cell.* 5(12):1853-63.

Shutova, T., Irrgang, K.D., Shubin, V., Klimov, V.V., Renger, G. (1997) Analysis of pH-induced structural changes of the isolated extrinsic 33 kilodalton protein of photosystem II. *Biochemistry* 36:6350–58.

Singh, A. K. and Sherman, L. A. (2006) Iron-independent dynamics of IsiAproduction during the transition to stationary phase in the cyanobacterium Synechocystissp.PCC6803. *FEMS Microbiol. Lett.* 256:159–164.

Singh, A.K., McIntyre, L.M. and Sherman, L.A.(2003) Microarray analysis of the genome-wide response to iron deficiency and iron reconstitution in the cyanobacterium *Synechocystis* sp. PCC 6803, *Plant Physiol.* 132 :1825–1839.

Stewart, D. H., Brudvig, G. W. (1998) Cytochrome b559 of photosystem II. *Biochimica et Biophysica Acta* 1367: 63-87.

Stiller J.W., Hall B.D. (1997) The origin of red algae: implications for plastid evolution. *PNAS* 94(9):4520-5.

Stock, D., Gibbons, C., Arechaga, I., Leslie, A. G. W. and Walker, J. E. (2000) The rotary mechanism of ATP synthase. *Current Opinion in Structural Biology* 10: 672–679.

Stock, D., Leslie, A.G., Walker, J.E. (1999) Molecular architecture of the rotary motor in ATP synthase. *Science* 286(5445):1700-5.

Straus, N. A. (1994) Iron Deprivation: Physiology and Gene Regulation. In "The molecular biology of Cyanobacteria", D. A. Bryant, ed. The Netherlands, Kluwer Academic Publishers, pp. 731-750.

Stroebel, D., Choquet, Y., Popot, J.-L. and Picot, D. (2003) An atypical haem in the cytochrome b(6)f complex. *Nature* 426: 413–418.

Sun, J. et al. Oxidizing side of the cyanobacterial photosystem I. (1999) Evidence for interaction between the electron donor proteins and a lumenal surface helix of the PsaB subunit. *J. Biol. Chem.* 274, 19048-19054.

Szabò, I., Rigoni, F., Bianchetti, M., Carbonera, D., Pierantoni, F., Seraglia, R., Segalla, A. and Giacometti, G. M. (2001) Isolation and characterization of photosystem II subcomplexes from cyanobacteria lacking photosystem I. Eur. J. Biochem. 268: 5129-5134.

Tang, X. S. and Diner B. A. (1994) Biochemical and spectroscopic characterization of a new oxygen-evolving photosystem II core complex from the cyanobacterium Synechocystis PCC 6803. *Biochemistry* 33(15):4594-603.

Trick C.G., Wilhelm S.W., Brown C.M. (1995) Alterations in cell pigmentation, protein expression, and photosynthetic capacity of the cyanobacterium Oscillatoria tenuis grown under low iron conditions. *Can J Microbiol.* 41(12):1117-23.

Trost J.T., Blankenship R.E. Isolation of a photoactive photosynthetic reaction center-core antenna complex from Heliobacillus mobilis. (1989) *Biochemistry* 28(26):9898-904.

Trost J.T., Brune D.C., Blankenship R.E. (1992) Protein sequences and redox titrations indicate that the electron acceptors in reaction centers from heliobacteria are similar to Photosystem I. *Photosynth Res.* 32:11-22.

Tsukihara T., Kobayashi M., Nakamura M., Katsube Y., Fukuyama K., Hase T., Wada K., Matsubara H. (1982) Structure-function relationship of [2Fe-2S] ferredoxins and design of a model molecule. *Biosystems* 15:243-57.

Vasil'ev S, Brudvig GW, Bruce D. (2003) The X-ray structure of photosystem II reveals a novel electron transport pathway between P680, cytochrome b559 and the energyquenching cation, ChlZ+. *FEBS Lett.* 543:159–63.

Watanabe, T., Kobayashi, M., Hongu, A., Nakazato, M. & Hiyama, T. (1985) Evidence that a chlorophyll a' dimer constitutes the photochemical reaction centre 1 (P700) in photosynthetic apparatus. FEBS Lett. 235: 252-256.

Wilhelm, S. W. and Trick, C. G. (1994) Iron-limited growth of cyanobacteria: multiple siderophore production is a common response. *Limnol Oceanogr* 39:1979-1984.

Wilkens, S. (2000) F1F0-ATP synthase-stalking mind and imagination. J *Bioenerg Biomembr.* 32(4):333-9.

Wilkens, S., Rodgers, A., Ogilvie, I., Capaldi, R.A. (1997) Structure and arrangement of the delta subunit in the E. coli ATP synthase (ECF1F0). *Biophys Chem.* 68(1-3):95-102.

Williams, J. G. K. (1998) Construction of specific mutations in Photosystem II photosynthetic reaction center by genetic engineering methods in *Synechocystis 6803.* *Meth. Enzimol.* 167:766-778.

Williams, R. J. (1961) Possible functions of chains of catalysts. *J Theor Biol.* 1:1-17.

Williams, R. J. (1961) The multifarious couplings of energy transduction. Biochim Biophys Acta. 505(1):1-44.

Woese C.R. (1987) Bacterial evolution. *Microbiol Rev.* 51(2):221-71.

Woese C.R., Kandler O., Wheelis M.L. (1990)Towards a natural system of organisms: proposal for the domains Archaea, Bacteria, and Eucarya. *PNAS* . 87(12):4576-9.

Yousef , N., Pistorius, E. K. and Michel, K. P. (2003). Comparative analysis of idiA and isiA transcription under iron starvation and oxidative stress in Synechococcus elongatus PCC 7942 wild-type and selected mutants. *Arch. Microbiol*.180 : 471–483.

Zhao, J., Li, N., Warren, P. V., Golbeck, J. H. & Bryant, D. A. (1992) Site-directed conversion of a cysteine to aspartate leads to the assembly of a [3Fe-4S] cluster in PsaC of photosystem I. The photoreduction of F_A is independent of F_B. *Biochemistry* 31: 5093-5099.

Zouni, A., Witt, H. T., Kern, J., Fromme, P., Krauss, N., Saenger, W. And Orth, P. (2001) Crystal structure of Photosystem II from *Synechococcus elongatus* at 3.8 Å resolution. *Nature 409* : 739–743.

Acknowledgements